CRANFIELD UNIVERSITY

James Peter Tucker

A Whole Life Assessment of Extruded Double Base Rocket Propellants.

Department of Engineering and Applied Science

PhD
Academic Year: 2009 - 2012

Supervisor: Dr P.P.Gill

July 2012

CRANFIELD UNIVERSITY

Department of Engineering and Applied Science

PhD

Academic Year 2009- 2012

James Peter Tucker

A Whole Life Assessment of Extruded Double Base Rocket Propellants.

Supervisor: Dr P.P.Gill

July 2012

This thesis is submitted in partial fulfilment of the requirements for the degree of PhD

KEY RESULTS:

- The reworking stages of extruded double base propellant manufacture are crucial to the homogenisation of the propellant.
- Dynamic mechanical measurements did not detect changes in mechanical properties between samples of extruded double base propellant that were un aged, and those which had undergone an accelerated ageing program which simulated up to 8 years of storage at 25°C.
- A novel method for analysing the concentration of stabiliser in solution using ultra violet-visible (UV-Vis) spectroscopy was developed.

KEY WORDS

Nitrocellulose, mechanical properties, double base rocket propellant, ageing, glass transition temperature.

ABSTRACT

The manufacturing process for solventless extruded double base propellants involves a number of rolling and reworking stages. Throughout these processes a decrease in weight average molecular weight was observed, this was attributed to denitration. Differential scanning calorimetery data indicated that the reworking stages of extruded double base propellant manufacture were crucial to the homogenisation of the propellant mixture.

To determine the homogeneity of the final extruded product, a sample was analysed across its diameter. No variations in stabiliser concentration, molecular weight, or Vickers hardness were detected.

An accelerated thermal ageing trial simulating up to 8 years of ageing at 25°C was carried out to evaluate the storage characteristics. Reductions in stabiliser concentration, number average molecular weight, weight average molecular weight and polydispersity compared with un-aged samples were observed. The glass transition temperature measured using differential scanning calorimetery decreased by ~3°C. The decrease was attributed to the initial denitration reducing the energy of bond rotation and shortening the polymer chains, both factors reducing the energy required for movement. Modulus values determined from dynamic mechanical analysis temperature scanning experiments, did not detect significant variation between un-aged and aged samples. Though it was considered that variations would be likely if a more extensive ageing program was completed.

In order to evaluate propellant behaviour at very high and low frequencies, time temperature superposition (TTS) and creep testing were carried out. The TTS technique superpositioned data well, allowing future investigation of high frequency propellant properties. Creep testing was considered to be an appropriate approach, though the equipment available was not optimised for such testing.

This thesis is concerned with understanding how propellants are manufactured from nitrocellulose, nitroglycerine and other constituents. It is also about how the propellants decompose during long periods of time in storage, and how these changes can be measured using thermal and mechanical methods.

It is about how the physical, chemical and thermal properties of the propellant composition change throughout the manufacture. This is relevant as it could be used to develop more efficient manufacturing processes, allow operators to adjust processes to tailor product properties or be used to re-design manufacturing to compensate for a different starting material.

The thesis also considers how and why the properties of the product change over the course of years of storage. A specific focus on whether changes in mechanical and thermal properties occur, and if so how they can be detected.

The thesis is structured into 10 chapters.

Chapter 1 ‘Introductory background’ summarises and discusses the synthesis, structure and stabilisation of nitrocellulose. It introduces the grain shapes that propellants can be formed into and the reasons for these.

Chapter 2 ‘Analytical techniques’ gives a brief theoretical background to the technique of dynamic mechanical analysis, detailing how samples are investigated and the properties that are determined. The chapter also explains how and why the dynamic mechanical analysis results have been interpreted mathematically.

Chapter 3 ‘Literature review’ is a discussion of relevant work that has been published. It forms the basis from which this research builds.

The following five chapters discuss the experimental work carried out. Each chapter investigates a separate area, following the life cycle of a propellant.

Chapter 9 ‘Thesis outcomes’ discusses the overall conclusions of the thesis, drawing together the work described in the experimental chapters. The chapter

discusses how the findings could be useful and highlights further work that could be completed.

Table 0-1 Compositions of propellants used in this thesis

Propellant	Composition % mass	Analysis performed
Single base gun I	Nitrocellulose unknown % Diphenylamine 1% Graphite (coating)	High performance liquid chromatography
Single base gun II	Nitrocellulose unknown % Diphenylamine 1% Graphite (coating)	High performance liquid chromatography Ultraviolet-visible spectroscopy
Double base rocket I	Nitrocellulose +CDA 53.9-58.4% Nitroglycerine 21.6% Ethylcentralite 0.9-1.4% Potassium nitrate 2.9% Triacetin 18.9%	High performance liquid chromatography Gel permeation chromatography Dynamic mechanical analysis Microhardness (Vickers) Differential scanning calorimetery
Double base rocket II	Nitrocellulose 5-57% Nitroglycerine 19-46% 2,Nitrodiphenylamine 1-8% Copper oxide CuO 0-3%	High performance liquid chromatography Gel permeation chromatography Dynamic mechanical analysis Differential scanning calorimetery X-ray diffraction UV-visible spectroscopy
Triple base gun I	Nitrocellulose 16% Nitroglycerine 16% Nitroguanidine 55% Ethylcentralite, plasticiser, burn rate modifier 13%	High performance liquid chromatography
Triple base gun II	Nitrocellulose 28.9-32.1% Nitroglycerine 29.7-31.3% Nitroguanidine 33-35% Ethylcentralite 2% Dibutyl phthalate 2.7-3.3% Graphite (coating)	High performance liquid chromatography

ACKNOWLEDGEMENTS

I would like to acknowledge the following people and organisations for their support throughout the PhD process:

- Dr Philip P Gill, Dr John M Bellerby and Dr Mike Williams – my project supervisors and thesis committee, for their guidance and encouragement throughout the duration of the project.

- Dr Nathalie Mai and Mr Anjum N Aghi - for advice and guidance on the use of the chromatographic equipment.

- Chemring Energetics and Dr John Hand – for sponsorship, propellant samples and guidance.

- Dr M Paquet – for permission to reproduce images from his work (Figure 4-1)

- Dr P Gabbott – for permission to reproduce images from his work (Figure 2-2)

DECLARATION

The work presented in this thesis is that of the student unless referenced to another source.

TABLE OF CONTENTS

LIST OF FIGURES

LIST OF TABLES

LIST OF EQUATIONS

GLOSSARY

DMA	Dynamic mechanical analysis
(2N)DPA	(2 nitro) Diphenylamine
DTA	Differential thermal analysis
DSC	Differential scanning calorimetery
Ea	Activation energy
E^*	Complex modulus
E^i	Storage modulus
E^{ii}	Loss modulus
EC	Ethylcentralite
HPLC	High performance liquid chromatography
j	Geometry constant (DMA)
Mn	Number average molecular weight
Mw	Weight average molecular weight
NC	Nitrocellulose
NG	Nitroglycerine
Std dev	Standard deviation
T_g	Glass transition
T_α	Alpha transition
T_β	Beta transition
T_γ	Gamma
TGA	Thermal gravimetric analysis
UV-vis	Ultra violet visible spectroscopy
δ	Loss angle
ε	Dynamic strain
σ	Dynamic stress
ω	Frequency

CONFERENCE PAPERS

Assessment of propellant stabiliser extraction methods. **J.Tucker, P.P.Gill, N.Mai, J.Hand.** Karlsruhe : 41st International Conference of ICT, 2010.

Effect of manufacturing processes on nitrocellulose in extruded double base propellant. **J.Tucker, P.P.Gill, N.Mai, J.Hand.** Karlshruhe : 41st International Conference of ICT, 2010.

Assessment of factors effecting stabiliser extraction from nitrocellulose based propellants. **J.Tucker, P.P.Gill, J.Hand.** Pardubise : New Trends in Research of Energetic Materials, 2011

DEDICATION

I dedicate this work to my family and friends, as their support and encouragement has made this work possible.

1 INTRODUCTORY BACKGROUND

1.1 Double base Propellant

Double base propellants consist of nitrocellulose (NC) and an energetic plasticiser, commonly nitroglycerine (NG). A number of other chemicals are often added in small concentrations to adjust the mechanical, thermal and ballistic properties. Stabilisers are also added to extend the chemical safe life of the propellants.

1.2 Nitrocellulose

1.2.1 Sources of Cellulose

Cellulose is a naturally occurring polymer found in plants. It is formed by condensation reactions between glucose molecules, with all of the condensation reactions occurring on the 1 and 4 positions of the glucose ring, as shown in Figure 1-2. This leads to long polymer chain strands that are completely un-branched. Intramolecular bonding forms between the polymer strands. The strands form highly organised fibrils which contain both amorphous and crystalline regions.

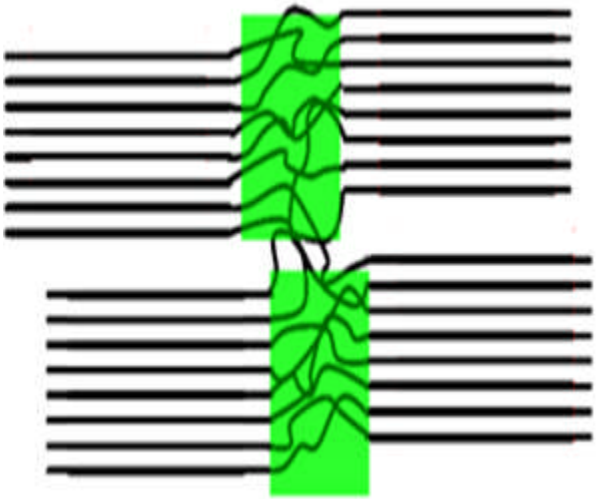

Figure 1-1 Amorphous and crystalline structure of cellulose (1)

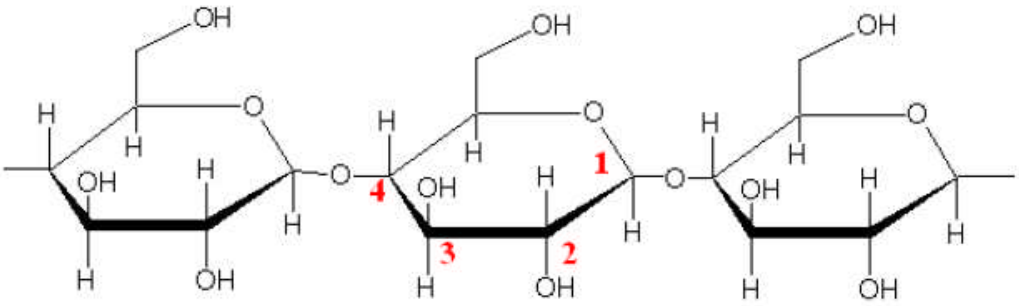

Figure 1-2 Cellulose polymer chain containing 3 glucose units

Cellulose can be obtained from a number of sources, most commonly wood pulp and cotton. Cotton is often considered the superior source of cellulose, because the wood source has a lower cellulose content. The wood contains higher concentrations of other substances such as Lignin and Pentosans (Appendix A) (2). Cellulose sourced from cotton typically has ~50% longer polymer chains than that sourced from wood (3), though variation due to climatic conditions will occur. It has been reported that the cotton linters are easier to nitrate and that the products are more consistent and reproducible, due to the lower concentration of impurities (3), Additional information about sources of cellulose in (Appendix A).

1.2.2 Synthesis of nitrocellulose

Cellulose is most commonly nitrated using a mixture of sulphuric and nitric acid (2), (Appendix B), the nitration process is technically an O-nitration process, as the nitrate bonds to the oxygen as shown in (2). As a result of the intramolecular bonds holding the long polymer chains in their fibrous structure, cellulose does not dissolve in the nitration mixture. This makes it difficult for the nitration mixture to reach and react with the functional groups of the cellulose. During nitration the reagents are mechanically mixed. This process breaks down some of the regular structure and intermolecular bonding, leading to formation of amorphous regions, this is the initial stage in a process of gelatinisation. The incorporation step also could cause chain scission. The length of the polymer chains and the distribution of chain lengths, has an effect upon the overall mechanical properties of the propellant grain. The chain length or degree of

polymerisation may vary from a couple of hundred to a couple of thousand monomer units, shorter chains may act to plasticise the polymer (2).
In Figure 1-2 the nitrocellulose molecule is illustrated with three nitrate groups, however the degree of nitration can vary. The tri-nitrated species can only practically be obtained in a lab, however it is not necessary to nitrate to this degree in order to obtain a propellant grade product. As the nitrocellulose is a polymer, the degree of nitration is an average of the degrees of nitration within the monomer units. The nitration level is most commonly expressed as a percentage of the total molecular weight (of an average monomer) denoted as Wt%N, the nitration and corresponding oxygen balance of a range of types of nitrocellulose and nitroglycerine are given in Table 1-1.

Table 1-1 Nitrogen content and Oxygen balance of nitrocellulose and nitroglycerine (2)

Degree of substitution	Nitrogen content (Wt%N)	Oxygen balance (Ω)
Mono-nitrocellulose	6.67	-73.39
Di-nitrocellulose	11.12	-44.35
Lower limit for propellant	12.50	-35.16
Upper limit for propellant	13.40	-29.17
Tri-nitrocellulose	14.14	-24.24
Nitroglycerine	18.50	-3.5

The level of nitration and oxygen balance affect the energy stored in the propellant, the burning rate and the flame temperature during burning. It can also have an influence on the solubility and the mechanical properties as it influences the mechanical properties. Additives can be included in the propellant composition to adjust the burning temperature, mass burning rate and stability.

1.3 The decomposition mechanism and stabilisation process of nitrocellulose

1.3.1 Chemical decomposition reactions

The chemical decomposition reactions of nitrate esters fall into two categories; denitration and chain scission. The hydrolysis of nitrate esters is shown by equation (1-1) (Appendix B) .The hydrolysis process is catalysed in the presence of acid and base. Acid conditions can lead to the cleavage of the nitrate group *via* equation (1-2),(Appendix B). In basic conditions the cleavage of the nitrate group can occur *via* one of three reactions; reaction (1-3) represents a SN2 nuceophilic substitution leading to the formation of alcohol and nitrate, this is basically the reverse of the nitration process (Appendix B). Reaction (1-4) is an E2 elimination of the β-hydrogen leading to the formation of alkene and nitrate (Appendix B).

$$H_2O + RONO_2 \rightarrow ROH + HNO_3 \quad \textbf{(1-1)}$$

$$H^+ + RCH_2ONO_2 \rightarrow RCH_2OH + NO_2^+ \quad \textbf{(1-2)}$$

$$HO^- + RCH_2CH_2ONO_2 \rightarrow H_2O + RCH = CH_2 + NO_3^- \quad \textbf{(1-3)}$$

$$HO^- + RCH_2ONO_2 \rightarrow H_2O + RCOH + NO_2^- \quad \textbf{(1-4)}$$

$$HO^- + RONO_2 \rightarrow ROH + NO_3^- \quad \textbf{(1-5)}$$

Finally reaction (1-5) represents an elimination of the α-hydrogen Eco2 forming a carbonyl (Appendix B) (4). As the ester bond connecting the nitrate group to the hydrocarbon back bone is very weak, the auto catalytic nature of the decomposition reactions represents a very serious stability issue for nitrate esters. These chemical decomposition reactions cause denitration. Chain scission shortens the polymer chains and occurs *via* a hydrolysis mechanism, this is likely to weaken and soften the structure. Denitration reduces the energy

content of the propellant, because the energetic nitrate groups are replaced by hydroxyl groups. The nitrate groups are involved in the intermolecular bonding, so their loss also leads to changes in the structure, the hydroxyl groups that form in their place are also capable of forming the intermolecular hydrogen bonds, and have an influence on the solubility and the mechanical properties.

It is known that in propellants containing NG, the small NG molecules can migrate through the structure to the surface and evaporate. This can be considered as a physical ageing process. As NG is an energetic plasticiser its concentration effects both the energy content and the mechanical properties.

Table 1-2 Bond strengths (5)

Chemical bond	Average bond dissociation enthalpy kJ/mol
Nitrate ester	167
Carbon-Carbon	342
Carbon-Hydrogen	416
Carbon-Oxygen	343
Nitrogen-Oxygen (nitro group)	305
Carbon (aromatic)-Nitrogen (nitro group)	295

1.3.2 Stabilising propellants

Stabilisers increase the chemical safe life of a propellant by reacting with the nitrate groups released from the nitrocellulose (6), this prevents the nitrate causing further chemical decomposition. Stabilisers added to double base propellant must be able to react with the decomposition products from hydrolysis and thermolysis, (Appendix B), to prevent an auto catalytic decomposition occurring. Another important criteria for a good stabiliser is that it and its derivatives do not react with the. It is also useful if stabiliser decomposition products have a stabilising effect

Ethylcentralite (EC) also known as Carbamite, is a good example of this, it is an effective long term stabiliser which is compatable with nitrate esters (7). The derivatives of the stabiliser also have a stabilising effect.

The stabiliser, N-methyl 4-nitroaniline (pNMA) is also compatible with nitrate esters however unlike ethylcentralite, its derivatives unfortunately do not have any stabilising effect (7).

Diphenylamine (DPA) is a good stabiliser as the derivatives are also effective stabilisers. It is often considered that DPA is too basic for use with propellant containing high concentrations of nitroglycerine. Typically rocket propellant use the less basic 2-nitrodiphenylamine (2N-DPA) as a stabiliser.

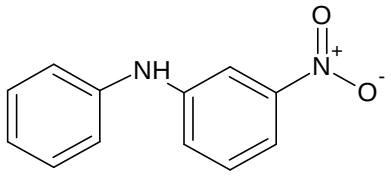

Figure 1-3 2-Nitrodiphenylamine

1.3.3 Geometries of rocket propellant grain

Propellants are manufactured into grains, the geometry of these grains are dictated by the specific purpose of the propellant. It is possible to design a propellant to have a constant mass burn rate. The simplest way to achieve this is to have a cylinder of propellant inhibited on the sides, when ignited it will burn like a cigarette. The drawback with this configuration is that the burn rate will be low, as the burning surface area is low, this will lead to a low powered rocket. A second disadvantage is the centre of gravity of the rocket will move as it is burnt. The power of the initial stage can be boosted by cutting radial slots and an axial conduit in the nozzle end.

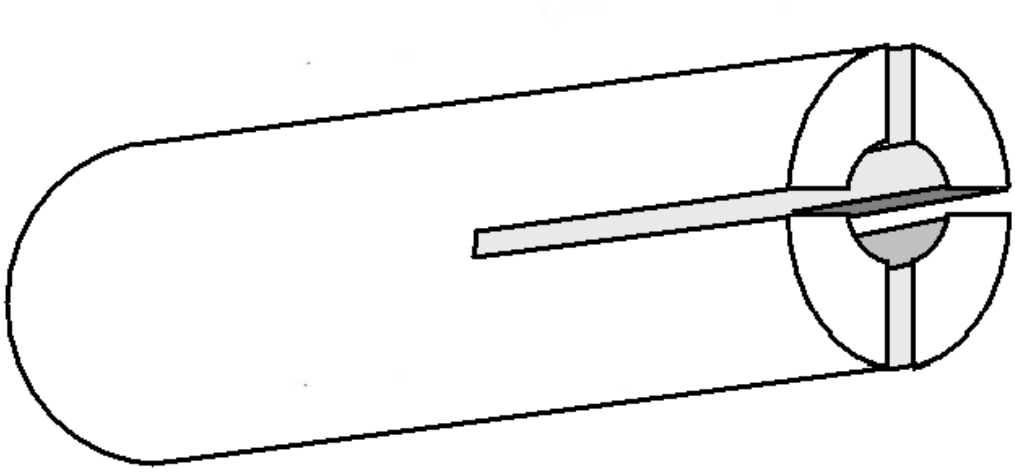

Figure 1-4 Rocket propellant grain with booster (8)

One way to increase the power during the whole burn on a cylinder propellant grain is to increase the burning surface area. With a cylinder with no conduit the only way to do this is to increase the diameter. This may not be desirable as this is likely to increase the aerodynamic drag of the missile or rocket.

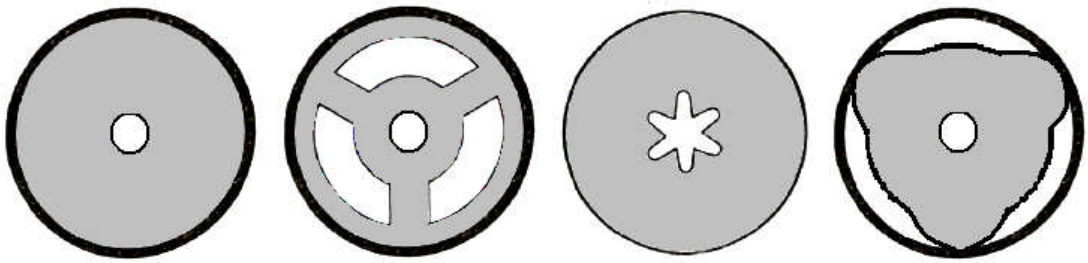

Figure 1-5 Conduit design for rocket grains

There are a number of propellant grain designs which increase surface area burn rate, these include longitudinal groves called conduits. One of the simplest (Figure 1-5 left) has a single cylindrical conduit extending the length of the grain, the grain burns from the inside out. This increases burn rate however the burn rate will increase during burning as the surface area increases. The three other designs shown (Figure 1-5) are intended to achieve nearer constant burn rates. These conduits allow control of the burn rate however they also weaken the propellant grain, stresses are concentrated at the corners, this makes the possibility of cracking more likely, this effect can be minimised by rounding the

edges of the conduits. The importance of mechanical integrity of propellants to their correct operation, is why the degradation of mechanical properties becomes the life limiting factor in some cases.

1.4 Methods of measuring decomposition processes

There are a number of ways in which the age and remaining safe life of a propellant can be determined. Commonly the stabiliser concentration is quantified using chromatography, though other methods have been reported.

As the propellant chemically decomposes over the course of years, the stabilisers are gradually consumed by the products of the denitration reactions. This means that the concentration of stabiliser is related to the level of decomposition. Analysing stabiliser concentration, involves extracting the stabiliser from the propellant. Then separately identifying and quantifying the stabiliser and stabiliser daughter products present. This can then be compared with the known starting concentration. This process can be monitored using chromatographic methods usually high performance liquid chromatography (HPLC) (5). The monitoring of stabiliser concentration provides an accurate measure of the chemical decomposition. As the safe storage life is dependent upon the stabiliser concentration, it provides a good monitoring option. However this method does rely upon efficient extraction of the stabiliser from the propellant, there have a number of methods that have been proposed for this. NATO Allied Ordinance Publication 48ed2, proposes two methods, there are others reported in journal articles. An assessment of all of these methods has been completed in chapter 8. The monitoring of stabiliser concentration provides no information about other decomposition processes, such as plasticiser migration, a process that is known to occur.

A method to quantify the nitration level in nitrocellulose using ion chromatography has been reported (9). The method involves an alkaline hydrolysis of the nitrate groups, followed by analysis of nitrate ions using ion chromatography.

The majority of the gas that is released from a double based propellant are nitrogen or a nitrogen oxide N_2, NO, NO_2, in addition there are some carbon oxides CO, CO_2. A link between the relative gas concentrations released from the nitrocellulose and the decomposition occurring has been investigated (10). There a number of ways to detect gas evolution, the first is to directly detect the gas (11) this could be done using spectroscopic methods, the second is to measure the gas's reactions with a sensitive medium such as an anthraquinone dye (10), and the third is to look at mass loss (12). These methods have been used to calculate activation energies for the denitration and chain scission. In all cases, measuring the gas evolved from a sample requires the sample to be monitored continually in a lab since manufacture, samples cannot be taken from in service munitions.

The thermal and mechanical properties are likely to vary as a function of time as the nitrocellulose molecular weight, nitrocellulose level of nitration and plasticiser distributions can change. DSC and bomb calorimetery can be used to assess the chemical energy stored within the sample, this can be used as a measure of the sample's age if compared with the analysis of an un-aged material.

The service life of propellants may be limited by the changes in mechanical properties of the propellant, or by changes in thermal transition temperatures. Though the quantification of stabiliser using HPLC provides an excellent method for the remaining safe storage life of a propellant. It would be useful to also monitor the property that is directly limits the service life of the specific propellant, which may be a change in glass transition temperature, the hardness of the propellant or a reduction in tensile of compression strength. Thermal analysis using DSC can also provide the thermal transition temperatures, these are likely to change as the material ages. Analytical methods such as tensile testing have been used to monitor the mechanical properties of propellants. It is considered by the author that DMA will be a useful

technique as it is capable of providing both thermal and mechanical data, and with fewer samples than destructive tensile testing.

2 ANALYTICAL TECHNIQUES

2.1 Dynamic mechanical analysis (DMA)

2.1.1 Outline of technique

Dynamic Mechanical Analysis (DMA) applies a small sinusoidal oscillating force to a sample that is continually deformed as depicted in Figure 2-1. Traditional mechanical testing applies a force to a sample which is gradually increased and ultimately deforms the sample sometimes irreversibly. In DMA the deformations incurred are very small and do not fatigue the sample. This means that the sample will respond to each sinusoidal oscillation in the same way (Figure 2-1). The material properties such as modulus, elasticity and viscosity, are calculated from the two sine wave curves.

There is very wide range of possible experimental conditions that a DMA can perform. The precise experimental conditions that have been used in this thesis are detailed in the experimental sections of the subsequent chapters.

One of the major advantages of using DMA over other mechanical tests is that the samples are not damaged during the analysis (temperature range dependent), the mechanical properties can be measured as a function of another variable, such as temperature or frequency. This allows a great quantity of information to be collected from a sample, reducing the need for a large number of samples, an advantage if the samples are rare, expensive or in this case explosive.

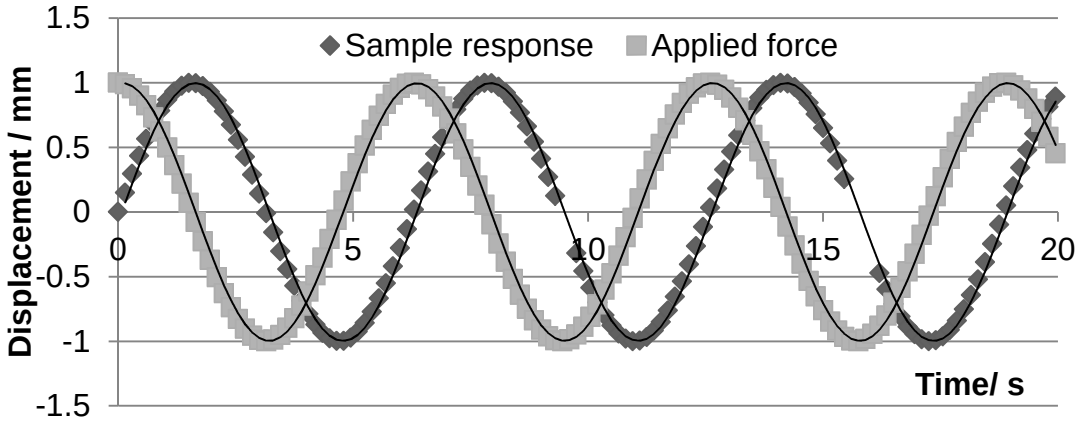

Figure 2-1 Typical DMA sinusoidal force and response

2.1.2 Testing geometry

There are a number of variables that can be investigated in a DMA. These include: temperature, humidity and the frequency of the applied force. Samples of various shapes and sizes can be analysed. There are different testing geometries to suit a variety of samples, as shown in Figure 2-2. Every testing geometry has an associated mathematical expression, which contains terms for the size of the sample and is used in the calculation of the material properties such as the complex modulus (2-1). The full list of geometry factors is given in (Appendix 10C.1). It is very important that the sample is accurately prepared, as the terms for length width and height in the geometry factors are often squared or cubed, which multiplies the error in the measurement, leading to inaccuracies in the data collected. It has been recommended that the test specimen be prepared to an accuracy of 0.5% of the smallest sample dimension, for a 2mm sample this means a precision of ±0.01mm (13).

$$E^* = \left|\frac{F}{y}\right| \frac{1}{j} \qquad \textbf{(2-1)}$$

E^* = Complex modulus, F = Force, y = Displacement, j = Geometry factor

When analysing a cuboid sample in either 3-point bend, single or dual cantilever bending geometries a 5% error in the length of the sample will lead to a 15.7% error in the modulus value. The full calculations are given in Appendix C.1.

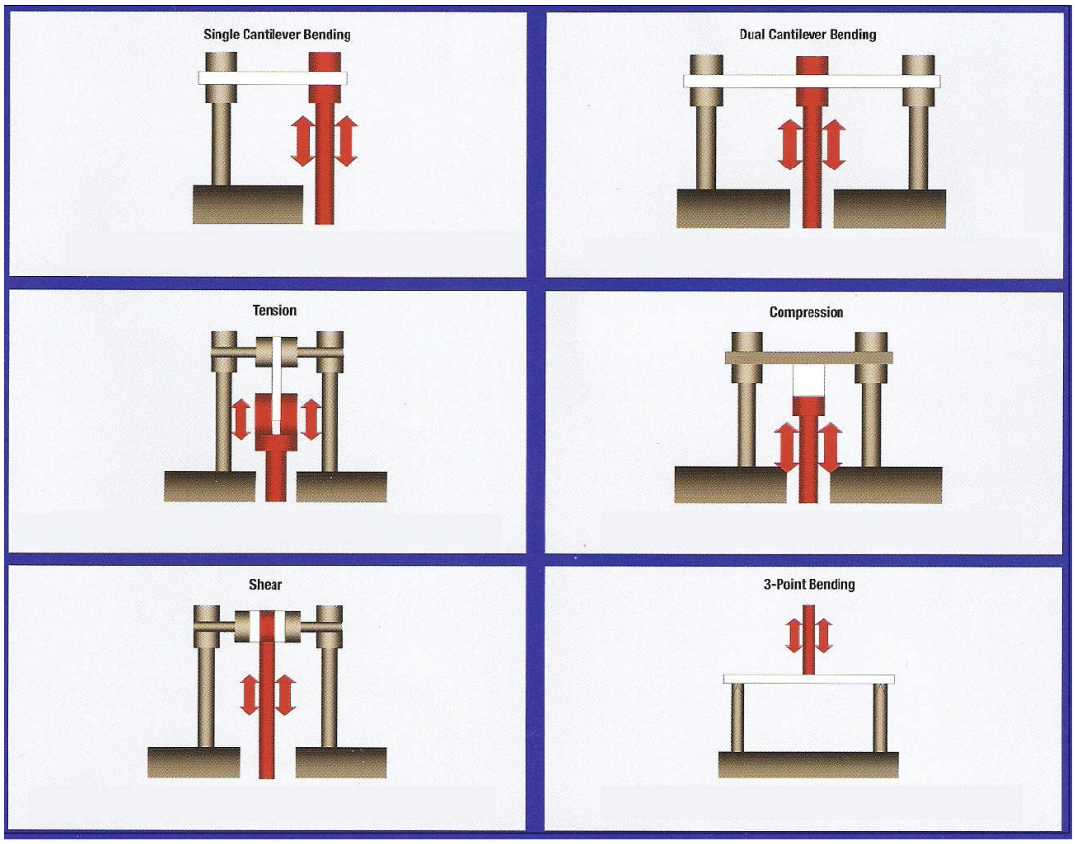

Figure 2-2 The analysis geometries in DMA (14)

Choosing the sample geometry is a very important consideration for DMA analysis. Some geometries are intrinsically stiffer than others. A plank of wood requires far less force to bend than to achieve the same displacement in tension. This variety in the inherent stiffness associated with sample geometry allows DMA to analyse a wide range of modulus values, however it also means that careful selection of sample geometry is important to collect good results. Geometries can be ranked in order of stiffness.

Shear> Compression> Tension>Dual Cantilever Bend>Single Cantilever Bend> 3- Point Bend (14) Figure 2-2.

Shear, being the most inherently stiff geometry suits the low modulus samples, such as soft rubbers or gel like materials. It has also been noted as useful for irregularly shaped and difficult to mount sample. Tension has been used well with film samples, as the low thickness of the sample compensates for the stiffness of the geometry. Dual and Single cantilever bending operate in the middle of the stiffness range, it is therefore a good starting point for the analysis. The advantage of single cantilever over dual cantilever bending is that it allows for a little lateral movement. This prevents thermal expansion causing a concentration of stress within the sample which would alter the results. Three point bend operates with very stiff materials typically an order of magnitude stiffer than clamped bend. It is very good for obtaining an absolute modulus value as there are no clamping stresses, it is important to ensure that the sample are completely flat as a twisting force could otherwise result (15). If analysing at very low strain amplitudes then it is possible that the sample will simply be settling in the clamp not bending. There can also be a frictional force between the sample and the clamp and this would lead to an increase in the tanδ (which is a ratio of the viscous and elastic material responses) as a frictional force would be measured as a viscous response. There is a valid modulus range for each sample geometry.

2.1.3 Viscous and elastic behaviour

Material responses can be considered as the result of two extreme contributing behaviours, elastic and viscous. Elastic behaviour is described by Hooke's law and viscous is described by Newton’s law.

2.1.4 Elastic behaviour

Hooke's Law states that ‘the deformation of a spring is linearly related to the force that caused it', the two are related by the spring constant, equation (2-3). Stress is defined as the force applied divided by the area upon which it is applied, units of pressure are Nm^{-2} or Pa. Strain is a measure of the deformation, it is usually given as a percentage of deformation, an equation can be written in terms of stress and strain to describe elastic behaviour equation

(2-2) (15). If the material is stiff then the spring constant will be relatively high. A perfectly elastic material gives a linear response to force as shown in the initial region of Figure 2-3.

$$F = -kx \quad \textbf{(2-2)}$$

k = spring constant, x = displacement

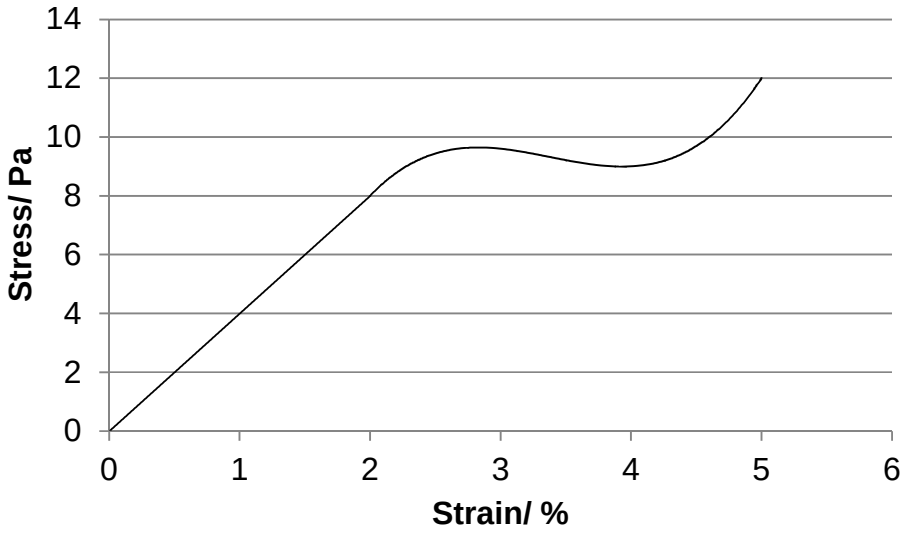

Figure 2-3 Elastic behaviour described by Hooke's law

The gradient of the initial linear region of the graph is the Young's modulus, it can be calculated from equation (2-2)

$$E\ (Young's) = {}^{\delta\sigma}/_{\delta\gamma} \quad \textbf{(2-3)}$$

E (Young's) = Young's modulus
σ = Stress
γ = Strain

A Hookean material will obey equation (2-3) when stressed. If a sufficient force is required then any Hookean material will cease to obey Hooke's law. This is the point at which the graph begins to curve, the curvature of the graph is a result of the material beginning to neck before breaking.

2.1.5 Viscous behaviour

Viscous behaviour is at the other end of the scale. The elastic model can be considered to be related to the return of energy, the viscous model is related to the loss of energy. The viscosity of a material is a measure of how readily it will flow, increasing viscosity means that a material increasingly resists flow.

$$\sigma = \eta \, {}^{\delta\gamma}/_{\delta t} \qquad \textbf{(2-4)}$$

η = Viscosity, t = time

The viscosity relates the stress applied to the rate of strain that it causes, an applied force will cause a fluid to continually deform at a fixed rate, which is linked to the viscosity. This relationship is described by equation (2-4). Materials that exhibit this type of behaviour are classified as Newtonian fluids. There are materials that don't exhibit this behaviour, their viscosity is not linearly related to the stress applied, and these materials are known as non-Newtonian fluids.

There are two modes that a DMA could operate stress and strain control. The stress is related to the force applied, in stress control the same force will be applied on every sinusoidal oscillation for the whole analysis, as the material properties change, the strain, or deformation incurred will change. So for example, if a material is becoming progressively softer, the material will be easier to deform and the strain or deformation will be increasing. If the analysis is a strain controlled analysis, the material is deformed to the same extent every oscillation. So for example if the sample is deformed to 2% strain, and it is getting softer as the analysis is carried out then the stress applied to the oscillation will be reduced as the sample becomes easier to deform, as it is not necessary to apply such a strong force. In both cases we are looking at the differences between the stress and the strain waves to calculate the material properties. The Perkin Elmer DMA 8000 used in this research operates in a strain control.

As the materials behaviour is considered to be the result of two limiting extremes. One is elastic, the other is viscous. When analysing the data from DMA we split the materials behaviour in to elastic and viscous components in order to calculate the material properties. The elastic component acts in phase with the applied sine wave, the viscous component of the material behaviour acts 90º out of phase with the sine wave. As analysis can be carried out in stress or strain control there is a mathematical explanation for both viscous and elastic components in both stress and strain control.

An elastic material response curve will be in phase with the applied force curve. This is because elastic behaviour is described by equation (2-2). The material exerts a force on the instrument equal and opposite to the force applied to it, and proportional to the displacement incurred. The materials response will be at maximum when the applied force/displacement it at maximum. The applied force and the opposing force from the sample are therefore in phase.

Viscous material response to a sinusoidal force is 90° out of phase with the applied force, it is described by equation (2-4). The materials exerts a force proportional to the rate of strain, this is zero at maximum displacement and maximum at zero displacement.

2.1.6 Calculating material properties from the DMA data

We can write a mathematical expression for the stress in a strain controlled analysis and for the strain in a stress controlled analysis, at the elastic limit and at the viscous limit. At the elastic limit for a stress or strain analysis, the stress at any point on the curve can be calculated using equation (2-5). Additional detail is given in (0)

$$\sigma(t) = \sigma_{max}\sin(\omega t) \quad \textbf{(2-5)}$$

ω = Frequency

The strain at any point can be calculated with equation (2-6)

$$\varepsilon(t) = \varepsilon_{max}\sin(\omega t) \quad \textbf{(2-6)}$$

ε = Dynamic strain

These equations have a striking resemblance, this is because at the elastic limit the samples response to the applied force is in phase with the applied force. It therefore doesn't make a difference to the equations whether the stress is kept constant and the strain is measured or the other way around. The derivation of these equations in given in Appendix C.

The mathematical expressions for the viscous limit are a little more complex, as the sample response is out of phase with the applied force by 90º. The sine curve representing the stress always precedes the wave representing the strain since the sample cannot incur a strain until a stress has been applied. It is important to remember that the sample response curve indicated the force applied by the sample to the instrument, resisting the force applied to it, not the displacement of the sample. In a stress controlled analysis the strain wave will occur at +90º, in a strain controlled analysis the stress curve will occur at -90º. The mathematical expression for the stress in a stress controlled analysis at the viscous limit is also equation (2-6), and for the strain in stress control at the viscous limit equation (2-7).There is a +π/2 term, this is equal to +90º.

$$\frac{\sigma_{max}}{\eta}\frac{1}{\omega}\, sin\omega t + \frac{\pi}{2} = \varepsilon \quad \textbf{(2-7)}$$

The expression for stress in a strain controlled analysis is equation (2-8), it contains a -π/2
term, this is equal to -90º.

$$\sigma = \eta\varepsilon_{max} sin\omega t - \frac{\pi}{2} \quad \textbf{(2-8)}$$

We have established that there are two limiting behaviours, elastic and viscous, and we have seen from the mathematics, that the elastic component acts in

phase with the applied force. We also see that the viscous acts 90° out of phase with the applied force, in both stress and strain controlled systems. In real life we observe a material behaviours that lie between these two extremes.
In the analysis we will apply a sinusoidal deformation, then measure the sample's response to this, which would take the form of equation

$$\varepsilon(t) = \varepsilon_{max}\sin(\omega t + \delta) \quad \textbf{(2-9)}$$

δ = phase angle

Figure 2-4 Viscous and elastic limits

The symbol δ is the loss angle or how out of phase the response is. As δ approaches zero the material is becoming elastic and as it approaches 90° the material is becoming viscous. We established that the materials will have a response to the applied sine wave and that this response will be the result of elastic and viscous contributions Figure 2-4, the relationship can be expressed using trigonometry.

$$\varepsilon(t) = [sin\omega t\, cos\delta + cos\omega t\, sin\delta] \quad \textbf{(2-10)}$$

Figure (2-10) is a trigonometric relationship, it can be broken into two components.

$$\varepsilon^{i}(t) = [\varepsilon_{max} sin\omega t].cos\delta \quad \textbf{(2-11)}$$

$$\varepsilon^{ii}(t) = [\varepsilon_{max} cos\omega t].sin\delta \quad \textbf{(2-12)}$$

Now we have broken the response into an expression for the elastic equation (2-11) and the viscous equation (2-12) responses. The triangle in Figure 2-5 The trigonometric relationship Figure 2-5 visually represents how the properties are related. We can calculate the elastic and viscous modulus values using equations (2-13) and (2-14) respectively.

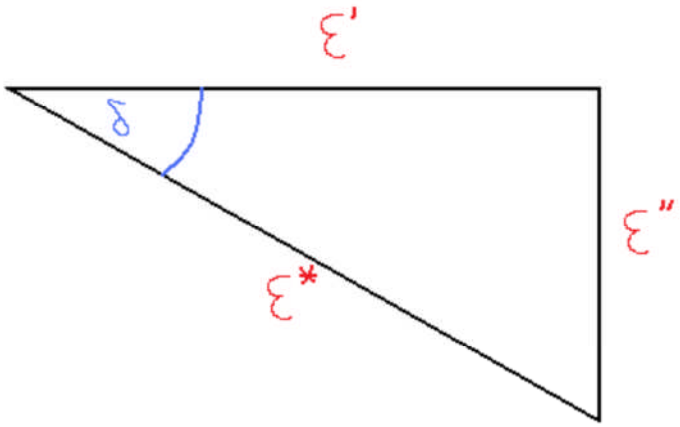

Figure 2-5 The trigonometric relationship

$$E^{i} = \frac{\sigma_{max}}{\varepsilon_{max}} cos\delta \quad \textbf{(2-13)}$$

$$E^{ii} = \frac{\sigma_{max}}{\varepsilon_{max}} sin\delta \quad \textbf{(2-14)}$$

E^{i} = Storage modulus, E^{ii} = Loss modulus

The E* is the complex modulus, it is trigonometrically related to the storage and loss modulus, equation (2-15) representing Figure 2-5.

$$E^{*} = \sqrt{(E^{i})^{2} + (E^{ii})^{2}} \quad \textbf{(2-15)}$$

Tanδ is often used to measure the materials properties as it is a ratio of viscous to elastic material behaviour, equation (2-16) .

$$Tan\delta = \frac{sin}{cos} = \frac{viscous}{elastic} \quad \textbf{(2-16)}$$

2.2 Interpretation of DMA data

Identifying peak maxima of tanδ or loss modulus curves from DMA results can be difficult. The highest data point may not represent the true maximum value, because of; overlapping peaks, a random error when collecting one data point or because data points are collected at each oscillation and the true maximum value may have fallen between two data points.

A method is required which allows interpretation while minimising these sources of random errors. In single peak analysis, a second order polynomial expression can be used to fit a curve. In these cases the temperature at which the data peaks can be determined by differentiating the polynomial of the curve, and rearranging it to determine x when y=0. This has been performed in Figure 2-6, the results of this analysis are shown in Table 2-1.

Table 2-1 Comparison of data collection method for single peak system

Peak determination method	Peak value /°C
Highest data point	46.1
Polynomial curve fit	46.2

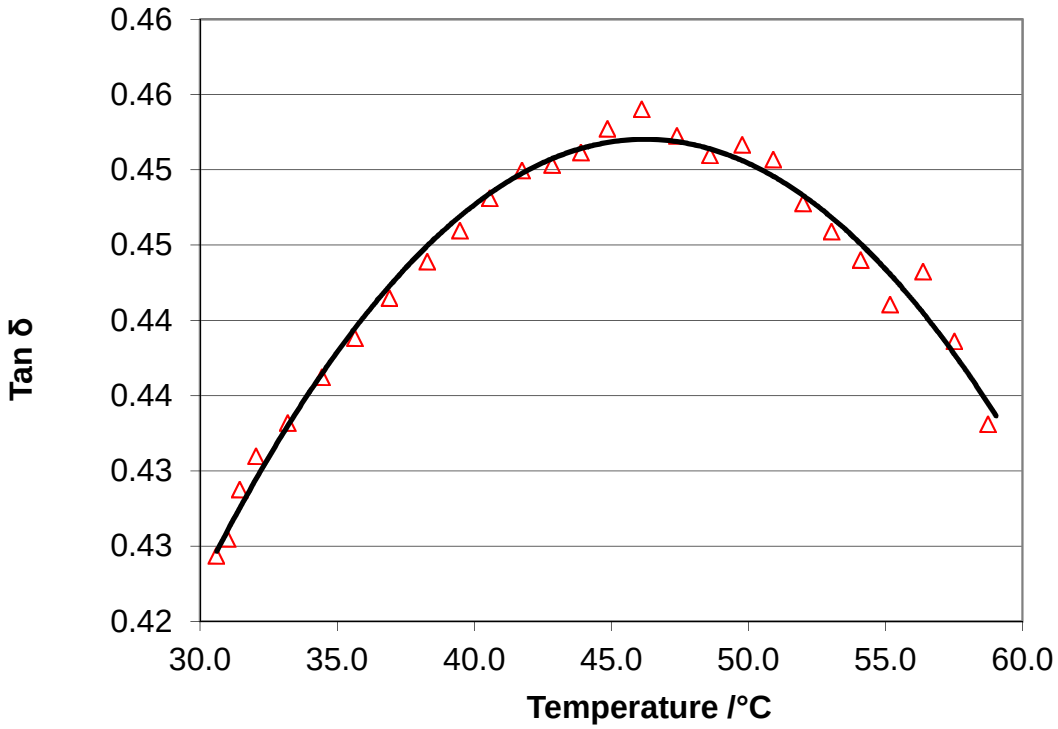

Figure 2-6 Determining peak value using polynomial. Extruded double base propellant (specifically 'Double base I') 10Hz heated at 5°C/minute

In the case of two peaks overlapping, often one is larger than the other, and a peak with a shoulder is the result. The smaller peak maxima point is obscured and it would be difficult to reliably visually identify the maxima of the event from which it has originated, such as in Figure 2-7.

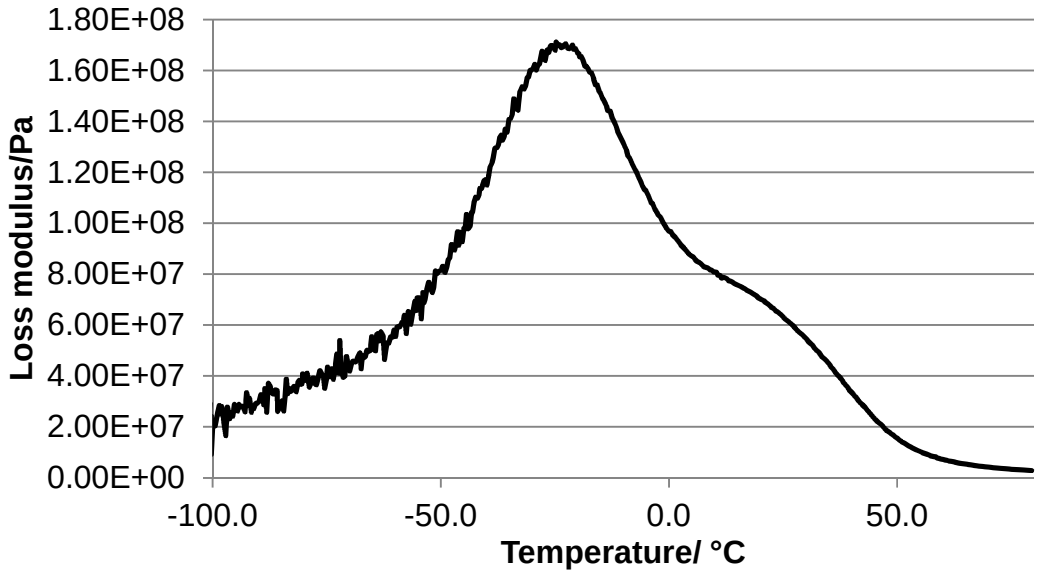

Figure 2-7 Overlapping peaks in loss modulus curve. Extruded double base propellant (Specifically 'Double base II') 1Hz heated at 2°C/minute

A method is needed that can be used to identify the separate peaks, then the individual areas and maxima can be evaluated. A mathematical approach is required, alleviating the need for operators to visually identify peaks. A method that will be easily reproducible from one lab to another.

The temperature at which a thermal event occurs may be frequency dependent and it therefore maybe possible to use the frequency dependence of thermal events to separate them, thermal transitions may not all be shifted by the same amount due to any given frequency shift. It is possible that a range of measurements at different frequencies could be carried out to determine a frequency at which the peak of interest is separated from others. This method may be unworkable when comparing data collected using different methods, by other workers.

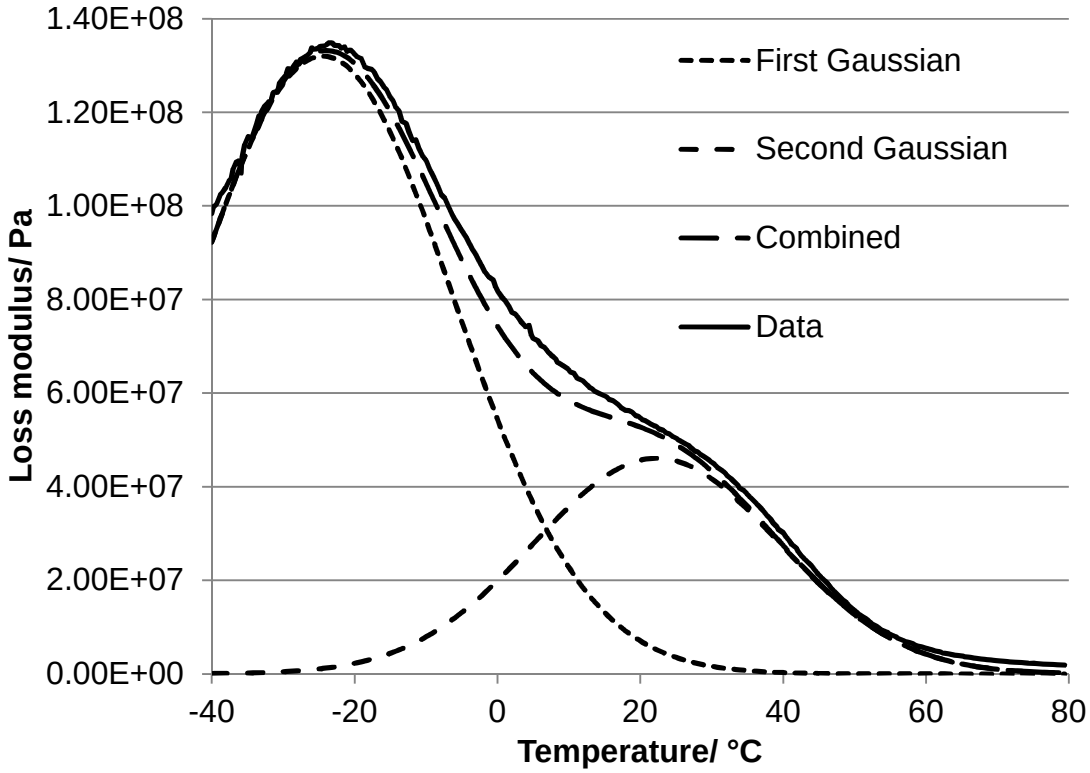

Figure 2-8 Loss modulus data from DMA analysis, curve of best fit derived from a linear combination of two Gaussian distributions both Gaussians are also shown. Extruded double base propellant (Specifically 'Double base II') 1Hz heated at 2°C/minute

A method is required that mathematically rather than experimentally separates the peaks. It is important that the mathematical expression used to model the data is related to the chemistry occurring, for example a high order polynomial expression could be used to fit a curve to any set of data Figure 2-9 however this will not necessarily provide new information about the sample in question. Only the maximum value would be determined, in a multiple peak system this may not represent the transition midpoint as the second peak may be distorting the first.

A method that had been reported (16) useing tangents fitted to the curve near the peak, extrapolation of the tangents to determine the intersection point, which is taken as the peak value. This method still won't provide a satisfactory method as there will be operator error associated with the point chosen to take

the tangent from (17). The method would not be workable for determining a value for the midpoint of a thermal event where the thermal event only leads to a shoulder in a peak.

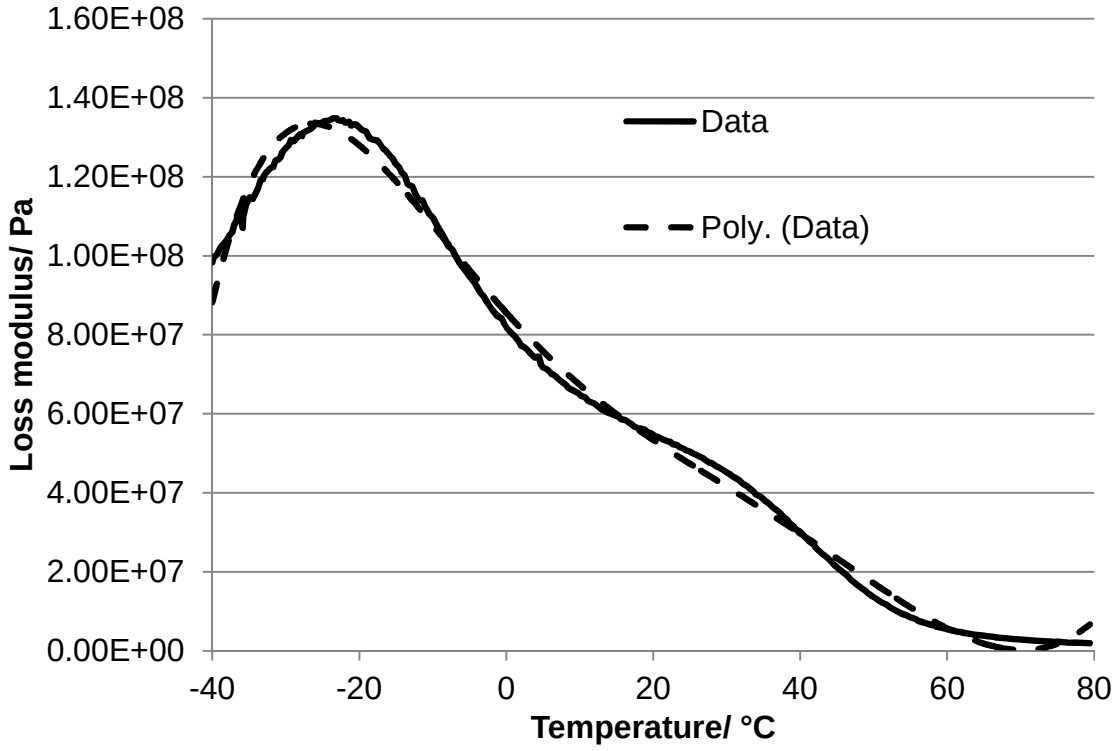

Figure 2-9 Loss modulus data from DMA analysis, curve of best fit derived from 6th order polynomial. Extruded double base propellant (Specifically 'Double base II') 1Hz heated at 2°C/minute

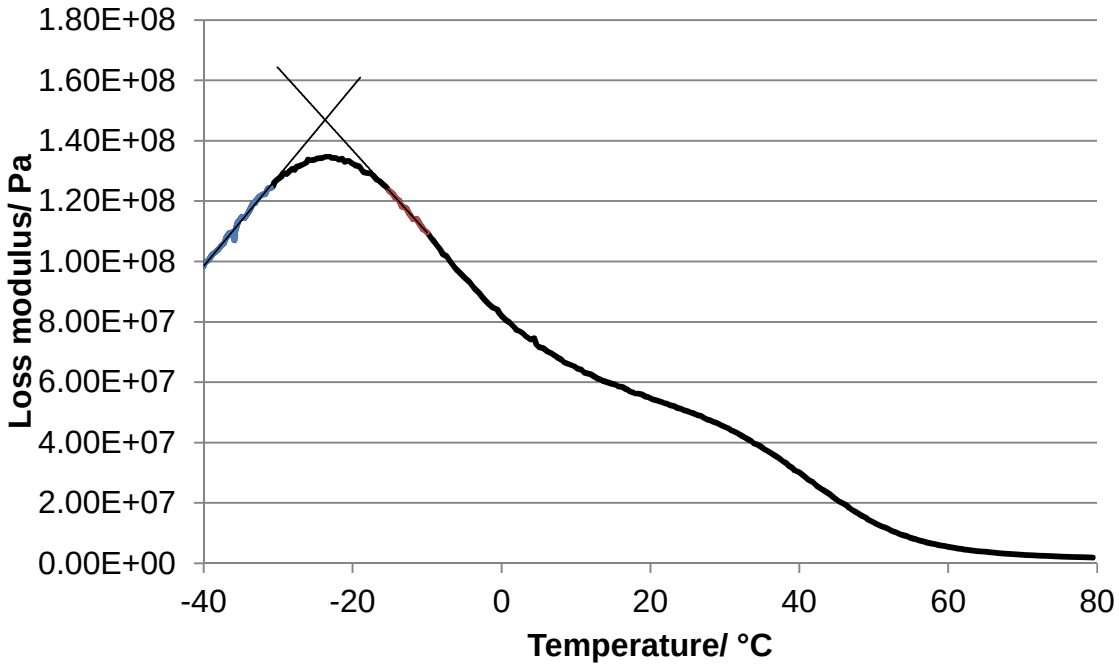

Figure 2-10 Loss modulus data from DMA analysis, peak determined by fitting tangents. Extruded double base propellant (Specifically 'Double base II') 1Hz heated at 2°C/minute

It is suggested from a review of literature published in the area, that the thermal events occurring in the temperature region under investigation are related to the lengths of the nitrocellulose polymer chains in the propellant (14). The processes have been hypothesised to be the glass transition and an interaction between the plasticiser and polymer chains (18). GPC analysis shows that for un-aged samples of propellants, the distribution of polymer chain length is roughly 'Normal' or 'Gaussian', this is discussed in chapter 7.

As the thermal event temperatures are linked to nitrocellulose molecular weight which follows a Gaussian distribution. It is reasonable to use a Gaussian distribution model to fit the data where a transition is occurring, and use an expression based on a combination of Gaussians to fit data where a number of transitions are occurring. The number of Gaussians in the model should equal the number of thermal events occurring, then each model will fit each transition.

The equation for the curve of best fit can then be used to calculate the parameters of the transitions. It is likely that increasing the number of Gaussians more highly will improve the data fit, however if this is done then the condition where each Gaussian component represents one transition is lost, and data can't be calculated from the curve of best fit.

Increasingly complex mixed Gaussian models could be used to fit the data, such as exponentially modified Gaussian and log normal distributions. It might not always be appropriate, the reason for using the Gaussian distribution in the first place is because it represents a tangible chemical aspect of the material. In the determination of peak maxima this method may be questionable as the author believes that unless there is evidence to indicate that the chemistry follows this distribution then it is unjustified. There are cases when is it likely that these models could be used appropriately, such as when nitrocellulose is aged thermally, chain scission is known to change the distribution of molecular weights, an analysis using GPC will indicate whether a more complex model can now be used (19).

2.3 Effect of heating rate in thermal analysis

As DMA can carry out temperature scan experiments, heating rate is an important variable to consider. The heating rate needs to be low enough to allow the sample to equilibrate in temperature. As the sample size is increased the time needed for the temperature to equilibrate also increases. There is then a clear advantage having a small sample, however the smaller a sample is the more significant any error in measurement of sample size will be. If the heating rate is too low then the analysis may take an unfeasibly long time to complete. The sample may be aged by the extended period of time at elevated temperature. In the case of a double base propellant, the nitroglycerine may migrate and or chemical decomposition reactions could occur to permanently alter the substance. Table 2-2 shows the sample thickness and heating rate of a number of analyses that have been reported in the literature.

Table 2-2 Sample sizes and heating rates reported in literature

Source	Sample size/mm	Heating rate/°Cmin^{-1}	Analysis geometry
(18)	22x2.5x5	0.4	
(20)	1.5x6x30	5	Single cantilever bend
(20)	2x6x30	5	Single cantilever Bend
(16)	2x10x14	2	Single cantilever bend
(16)	1.6x3x17	5	
(21) (22)	50x10x2.5	2	Torsion
(17)	40x10x5	0.5	

It has been reported that when using a higher heating rate the temperature at which the glass transition occurs is increased (23). This phenomenon has been observed in; differential thermal analysis (DTA), DSC and TMA. Therefore it is logical to anticipate an effect in the DMA. Strella investigated the effect of heating rate on two polymers using DTA (24). It was observed that in both cases the glass transition temperature was higher with faster heating (24). The effect of heating rate in TMA was investigated by Schwartz (23), where a sample of double base propellant was heated from 150°C to 27°C at: 1.04, 2.08, 4.16 and 8.32 °C/min. The results from this analysis were interpreted as a linear relationship between glass transition temperature and the heating rate. This is illustrated as the black line in Figure 2-11. (23). Schwartz reported that the slope of the regression line has a statistically significant deviation from zero, which means that T_g really is a function of heating rate. The true transition temperature at a theoretical 0°C/minute could then be calculated. These results suggest that the kinetics of the reaction are slow, this means that there is a time delay between the sample reaching the glass transition temperature and the sample actually transitioning. As the heating rate is increased the temperature at which the T_g is measured also increases, glass transitions are discussed in chapter 3.

This simple explanation does seem to fit the narrow data set collected by Schwartz adequately (23). However in my opinion the data fits a curve more

accurately, shown as the dashed line in Figure 2-11. There is a more complex explanation for the heating rate effect that does explain the presence of the curved line. A more detailed analysis of these thermal events using DSC and "Hyper DSC™" (a fast scanning DSC) have provided more evidence that a complex process is occurring (14). The current concept to explain the link between heating rate and glass transition temperature is based upon the concept of annealing.

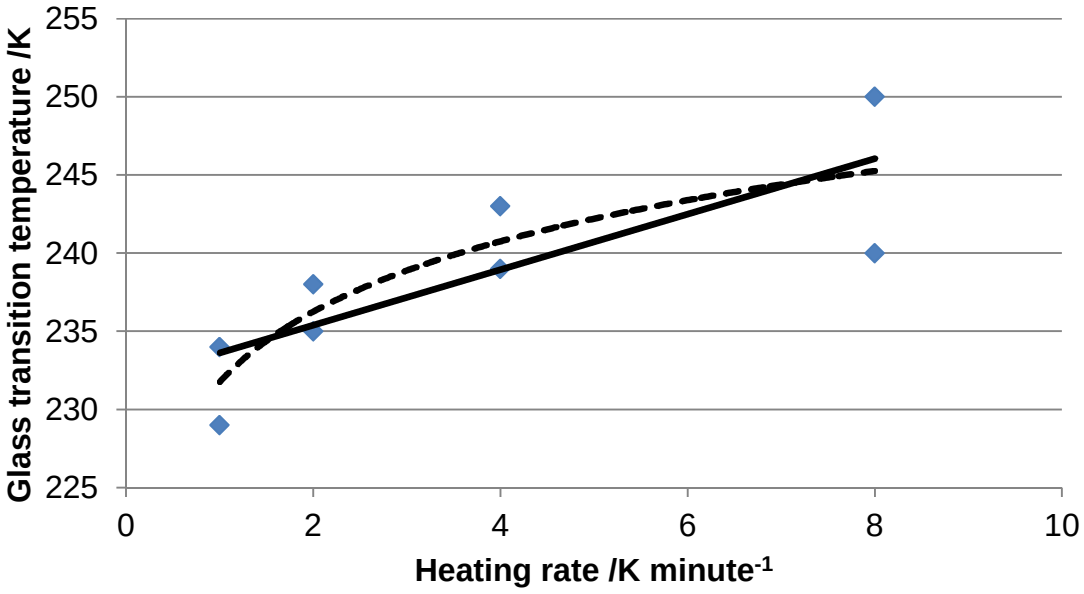

Figure 2-11 The effect of heating rate on glass transition temperature (23)

2.4 Annealed samples

If a sample is cooled very slowly through the glass transition region or annealed at a temperature just below the glass transition region then the sample will relax into a low energy state, Figure 2-12. If the cooling rate is slightly higher then the enthalpy state into which the sample relaxed will be slightly higher Figure 2-12. A material is annealed by cooling it very slowly or by holding it at a temperature below the T_g. During this process it relaxes in to a lower enthalpic state, the line labelled slow cooling in Figure 2-12. The kinetics of the thermal transition are slowed due to the lower enthalpic state. When heating an annealed sample of Polystyrene at a heating rate of 10ºC/min, the glass transition is passed before

the material has time to transition Figure 2-14. The material enters a non-equilibrium state, energy is absorbed to retain equilibrium, an endothermic step is measured as a consequence in the DSC Figure 2-13. The T_g onset is increased progressively as the heating rate is increased up until very high heating rates, in PS approximately 200ºC. The inconsistencies that are observed at higher heating rates for the larger sample sizes can be attributed the uneven heating of the sample.

2.5 Un-annealed samples

The un-annealed samples are less significantly affected by the heating rate, Figure 2-15. The explanation for all of these results is simple that at very low heating rates the samples are being annealed during the early stages of the heating, before the glass transition is approached. Once in the lower enthalpy state their behaviour is the same as those samples that have been annealed, this includes a lower glass transition temperature. Furthermore if the sample was heated to fast and the T_g overshot then there would be an endothermic on the DSC after the T_g, this would occur as the sample would have been heated in to a region where it is in a lower energy state than the equilibrium, therefore an endothermic process would need to occur for the equilibrium to be regained. This would be observed as an endotherm in the result.

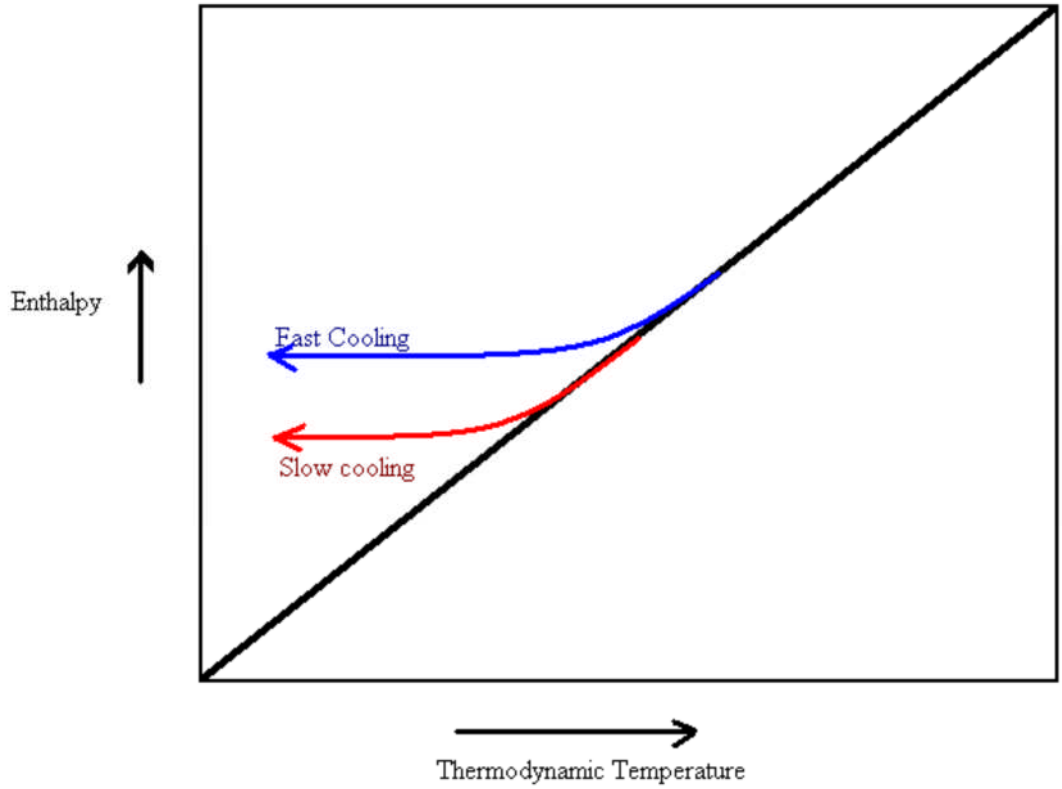

Figure 2-12 Enthalpic states after cooling (14)

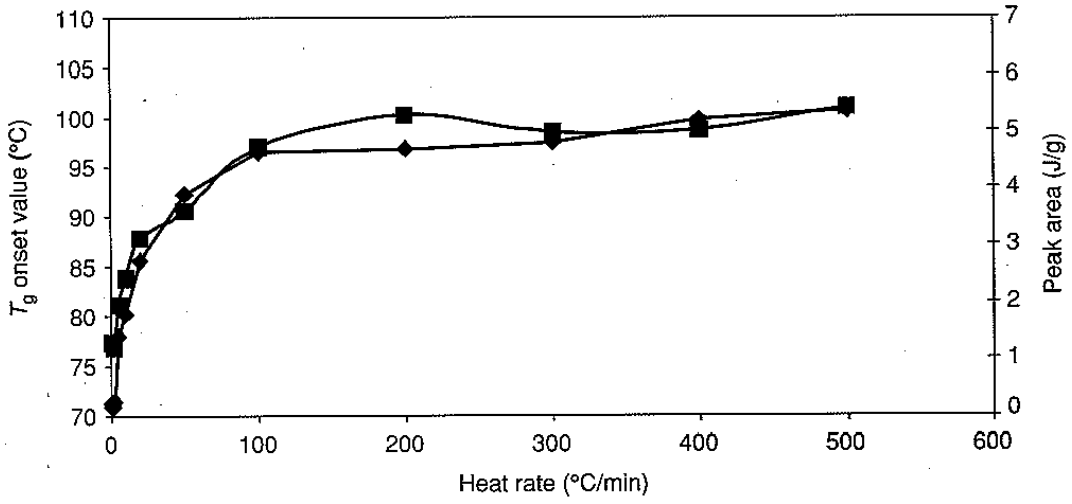

Figure 2-13 The glass transition of indomethacin at 10°Cmin^{-1} after cooling from melt at 1°Cmin^{-1}, two data sets indicate repeats (14)

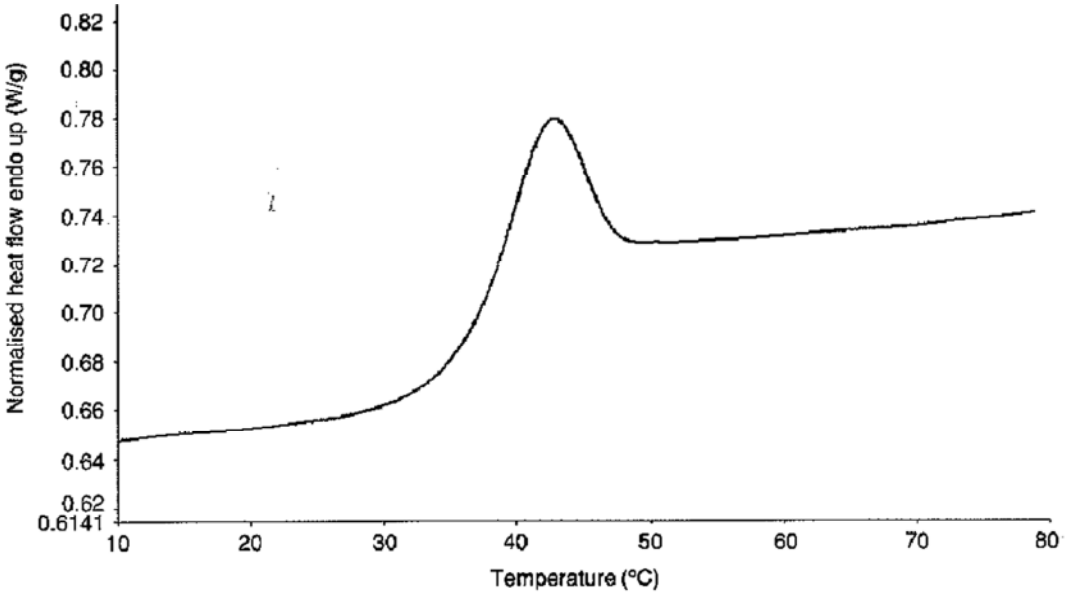

Figure 2-14 Effect of high heating rate on glass transition of polystyrene after slow cooling (14)

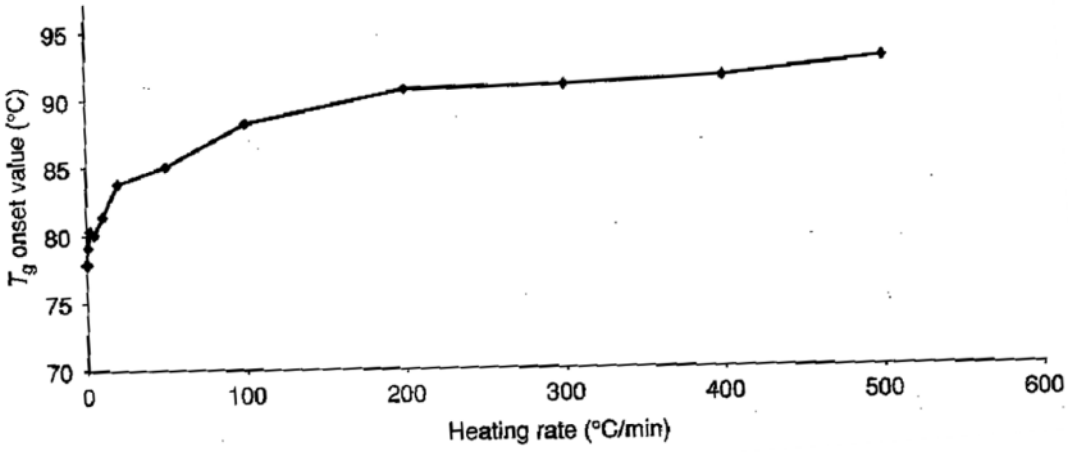

Figure 2-15 Effect of heating rate on polystyrene after fast cooling (14)

3 LITERATURE REVIEW

3.1 Thermal transitions

A thermal transition can be described as a temperature region through which the mobility of sections of chains in a polymer changes. It influences a range of the material properties.

3.1.1 Glass transition

Glass transitions can be considered to be changes in the free volume of the polymer. The free volume is related to the mobility of atom (25). As a polymer is warmed from a very low temperature the free volume increases. Molecules transition from being tightly compressed with little or no free volume, to localised movements. As the temperature and free volume increases so does the molecules ability to move. Eventually the polymer will become a liquid and the individual molecules have significantly increased freedom of movement.

As the temperature of the material is increased the energy is also increased. This increase in energy allows more movement, vibration and rotation of chemical bonds (26).

Rotation of some chemical bonds may be difficult as there are bulky groups sterically hindering complete rotation, as the energy is increased the activation energy for the complete rotation may be reached and so it can occur. Glass transition temperature will be influenced by the chemical composition. As bulky groups sterically hinder rotation, increasing the activation energy of the rotation, the glass transition temperature is increased by the presence of these bulky groups (26).

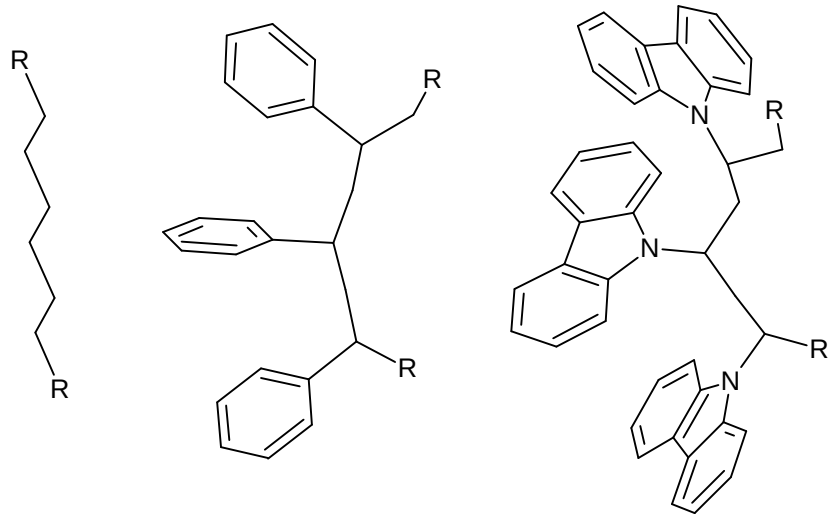

Figure 3-1 Polyethylene, Polystyrene, Poly(9-vinylcarbazole)

Polyethylene has only hydrogen atoms bonded to the polymer backbone which means there is low steric hindrance to rotation. Polystyrene has greater steric hindrance, increasing the energy barrier to rotation. Poly(9-vinylcarbazole) has the bulkier groups attached to the polymer backbone leading to the higher steric hindrance to bond rotation, and highest energy barrier to bond rotation. As a higher energy barrier to bond rotation corresponds to a higher glass transition, the size and numbers of bulky chain substituents has a significant influence on the glass transition (26). In chapter 7 of this thesis, this principal is discussed with reference to the loss of nitrate groups from nitrocellulose, which occurred due to ageing.

The addition of a plasticiser can also have an influence on the glass transition. The inter molecular bonding forces need to be overcome to allow the movement of chains to take place. A plasticiser interacts with the chains, forming intermolecular bonds thereby preventing as many intermolecular bonds bridging between chains, and softening the material. The nitrocellulose in double base propellant is plasticised by the nitroglycerine, low molecular weight nitrocellulose and often small concentrations of other chemicals such as di-butylphthalate (26).

3.1.2 Other thermal transitions

In terms of double base propellant it is likely that the nitroglycerine content, nitrocellulose chain length and degree of nitration will have measurable effects on the transitions measured. The transitions, as shown in Figure 3-2 are assigned by counting back from the melting point. It is convention to label the peak using the Greek alphabet counting back from the melting point, in the diagram the T_g is the T_α.

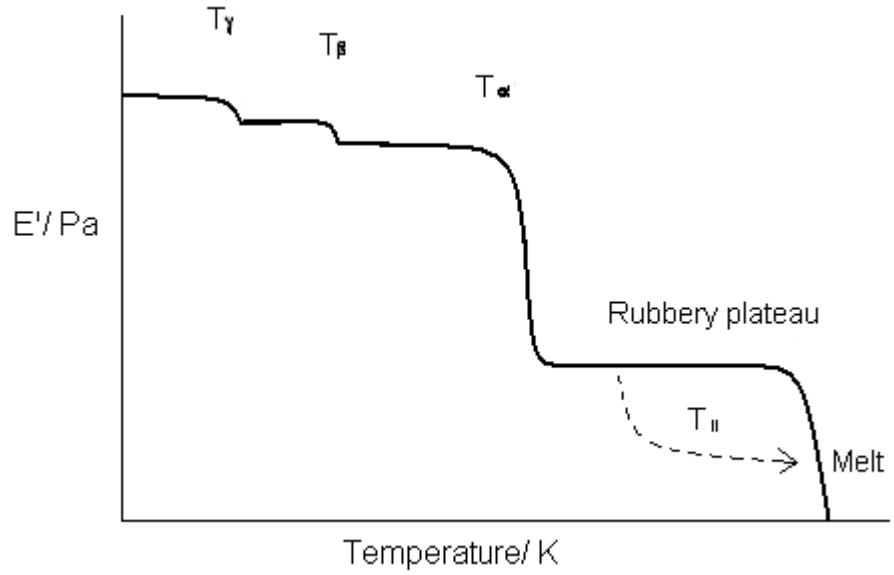

Figure 3-2 Idealised thermal transitions (15)

Attributing the microscopic process to the transitions that we observe in a DMA, is not simple. The transitions T_β and T_α are often called the sub-T_g transitions as they occur at the lower temperatures. These are often associated with the stretching and bending of side groups. These transitions have been observed in DSC and thermal mechanical analysis (TMA) however as they are normally subtle transitions they are difficult to measure accurately with these techniques (15). The T_g is the glass transition (discussed in section 3.1.1), it is also often designated the T_α as it is often the first sub melting point transition. The rubbery plateau lies between the glass transition and the melting point, the rubbery plateau is affected by the molecular weight between cross links. The

change in the modulus of this region can give us information on the relative changes in the number of cross links. Within this plateau region there are a number of transitions that can occur. In completely amorphous materials the sometimes another transition may occur between the melt and the glass transition it is often given the symbol T_{II} (15) and is indicated as the dotted line in Figure 3-2, this is associated with increased chain mobility.

In the following review of literature, the transitions reported to occur in double base propellants, are discussed along with attribution of chemical processes thought to occur. The term glass transition is avoided and transitions are simply labelled α and β. This is to eliminate confusion as various authors have claimed different transitions as the glass transition.

3.2 Temperature scan in dynamic mechanical analysis

Thermal transitions can be measured in the DMA using a temperature scan. There are a number of parameters that can be used to measure the changes in the material. The elastic modulus E', the loss modulus E'' and the tanδ can all be used to detect transitions. However the temperatures recorded for a transition using each of these quantities are not always the same, in some cases the temperatures measured for the transition varied up to 30K (17), therefore care must be taken to ensure the experimental conditions are quotes with the transition temperatures. It is important to define the experiment parameters that the measurements were carried out under, such as the frequency, heating rate, stress and strains applied and the geometry of test can all have an effect on the data gathered. These transitions, do not always occur at an exact temperature, rather they occur over a temperature range (15), this can be related the distribution of molecular weights within a polymer.

3.3 Evaporation of nitroglycerine from propellant samples

The evaporation of nitroglycerine from double base propellants at elevated temperatures has been measured by Matecic and Suceka (22). At temperatures above 70°C nitroglycerine evaporation was measured using thermal gravimetric

analysis, and became very significant at temperatures above 90°C, this is indicated in Figure 3-3 where the solid line deviated from the dotted line (analysis were carried out on 2g samples at a heating rate of 2°C/minute). Nitroglycerine has a boiling point of ~60°C, within the polymer matrix it forms interactions with the nitrocellulose, which increases the energy required for it to change state. This is why the loss of nitroglycerine from the propellant occurs at temperatures higher than the boiling point of nitroglycerine. This indicates that at these temperatures the chemical changes that can occur are different to those occurring at ambient temperature, and it is therefore interesting to consider how the concentration of nitroglycerine is likely to influence the propellant properties.

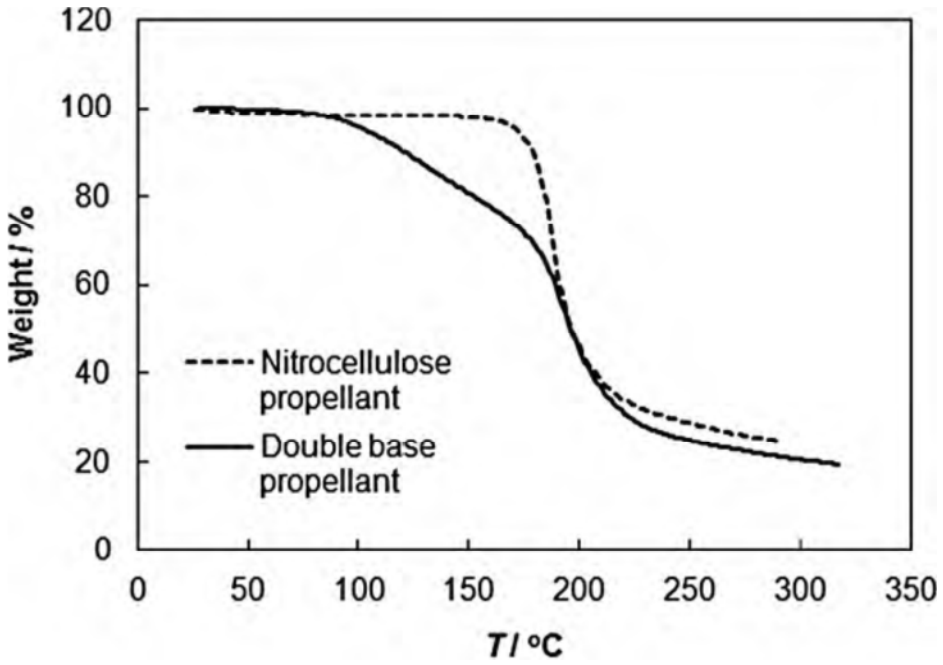

Figure 3-3 Non-isothermal thermal gravimetric analysis curves of nitrocellulose and double base propellant samples (2g) heated at 2°C/minute (22)

3.4 Effect of plasticiser concentration on tensile mechanical properties

As nitroglycerine acts as a plasticiser, the effect of varying the nitrocellulose nitroglycerine ratio has a significant effect on the mechanical properties of a propellant. As the concentration of nitrocellulose is reduced and the concentration of plasticiser increased, the tensile strength of the material is significantly reduced as shown in Figure 3-4. In this case the plasticiser was a combination of nitroglycerine and triacetin. The effect of increasing the plasticiser concentration is greater as the temperature is increased. Steinberger wrote that a propellant with higher nitrocellulose content will usually have higher tensile strength, higher modulus and lower elongation (27). This is observed as the plasticiser reduces the energy required for chains to slip past one another, reducing the force required to deform a sample.

3.5 Effect of plasticiser concentration on dynamic mechanical properties

Steinberger (27) reported, that the plasticiser concentration has a significant effect on the temperature at which thermal transitions occur. In research carried out by Townend and Warren the effect of plasticiser concentration on the dynamic mechanical analysis of double base propellants was investigated (21). The investigation showed that nitroglycerine concentration significant affects material properties. The change in nitroglycerine concentration had an effect on the modulus at temperatures greater than -30°C. A reduction in nitroglycerine concentration corresponded to an increase in modulus values Figure 3-4. The temperature of the thermal transitions were also clearly influenced, however it is difficult to identify the precise temperatures at which the thermal transitions occur from the modulus plot. Thermal transitions often appear as peaks in the tanδ and loss modulus plots of the temperature scan, this makes the onset, middle and end temperatures identifiable.

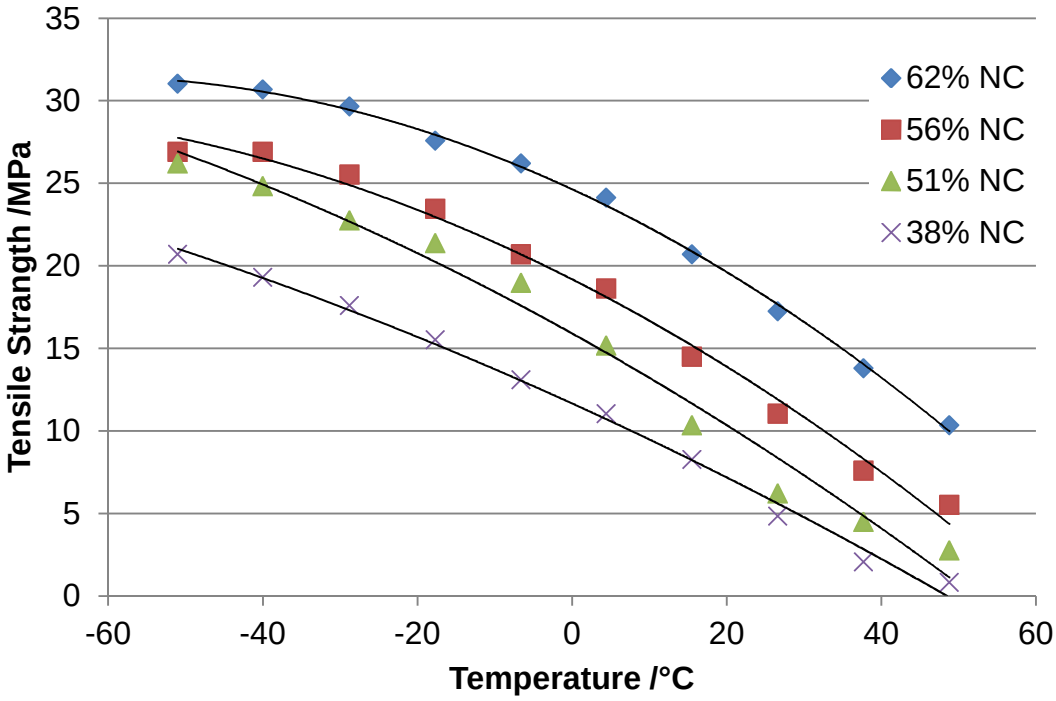

Figure 3-4 The tensile strength of double base propellant with varying plasticiser concentration as a function of temperature (27)

3.5.1 The α transition

In the research carried out by Townend and Warren on samples of double base propellant, the first transition designated α, occurred in the temperature region from 110 to 55°C for a moderately gelatinised sample, this can be seen in both the modulus and tan δ plots Figure 3-5, Figure 3-6, though it is easier to identify changes using the tan δ Figure 3-5. The temperature of the α transition, was dependent on the nitroglycerine content. The temperature at which the α transition was observed in the tan δ decreased by 60°C, corresponding to an increase from 10-60% nitroglycerine content (21). This is consistent with the data collected later by Warren, where a decrease from 133°C to 56°C was observed due to an increase in nitroglycerine concentration from 0% to 45% (28). Both of these investigations show that the α transition is shifted lower by an increase in plasticiser concentration. Townend and Warren claimed that there was no significant change in the magnitude of the tan δ peak for the α transition Figure 3-5. In my opinion the data was not accurate enough to

discuss whether there is a trend, as the variation in the α peak of the tanδ plot is very slight. It was also noted that this alpha transition was accompanied by a more significant drop in the elastic modulus than the β transition. The same trend has been observed in an analogous inert system based on cellulose acetate and an inert plasticiser (27).

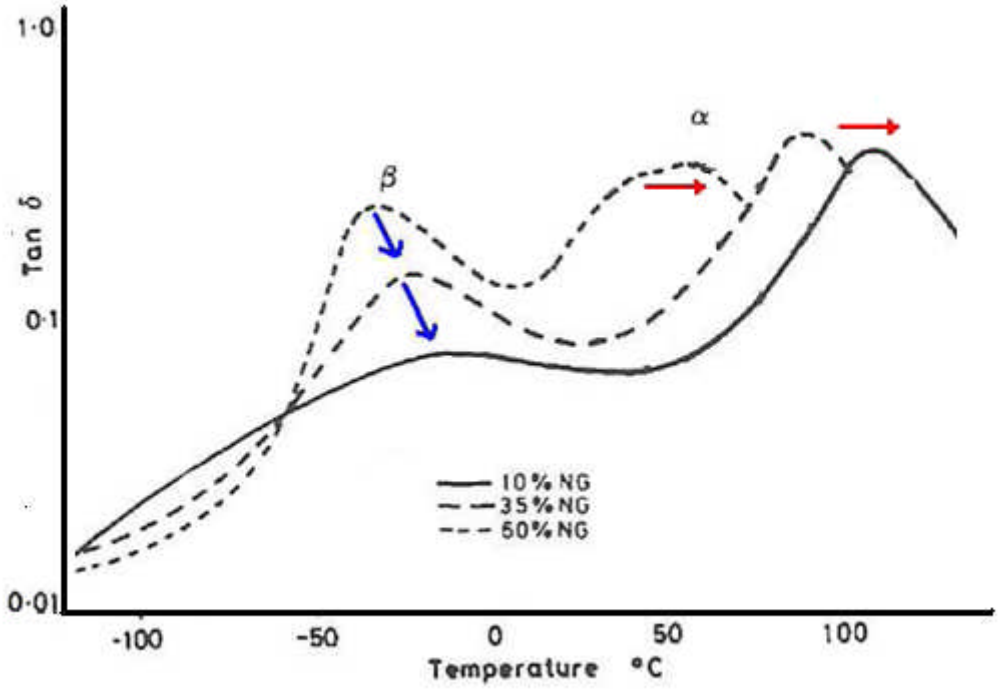

Figure 3-5 The tan δ curve for temperature scans of three samples of double base propellant containing varying amounts of plasticiser (21)

3.5.2 The β transition

Townend and Warren showed that the temperature of the β transition decreased from 15 to -33°C as measured by the tanδ curve. This is a decrease of 24°C for the same 50% increase in nitroglycerine concentration discussed before. The thermal transition occurred at lower temperature in samples containing more nitroglycerine, just as observed in the α though the β is less influenced. Interestingly the magnitude of the β transition peak (tanδ) varied significantly, showing a significant decrease in magnitude as the nitroglycerine concentration decreased, by 10% nitroglycerine concentration the β transition was very slight, possibly diminishing to zero at zero concentration (Figure 3-5,

Figure 3-6). This result agrees with the results obtained with inert analogues (29). The β transition was accompanied by a much smaller change in the modulus than the α. It has been observed that there is a significant peak in the differential scanning calorimeter analysis (21) and a thermal mechanical analysis peak (23) at the β transition, which may indicate that this is a glass transition process (14).

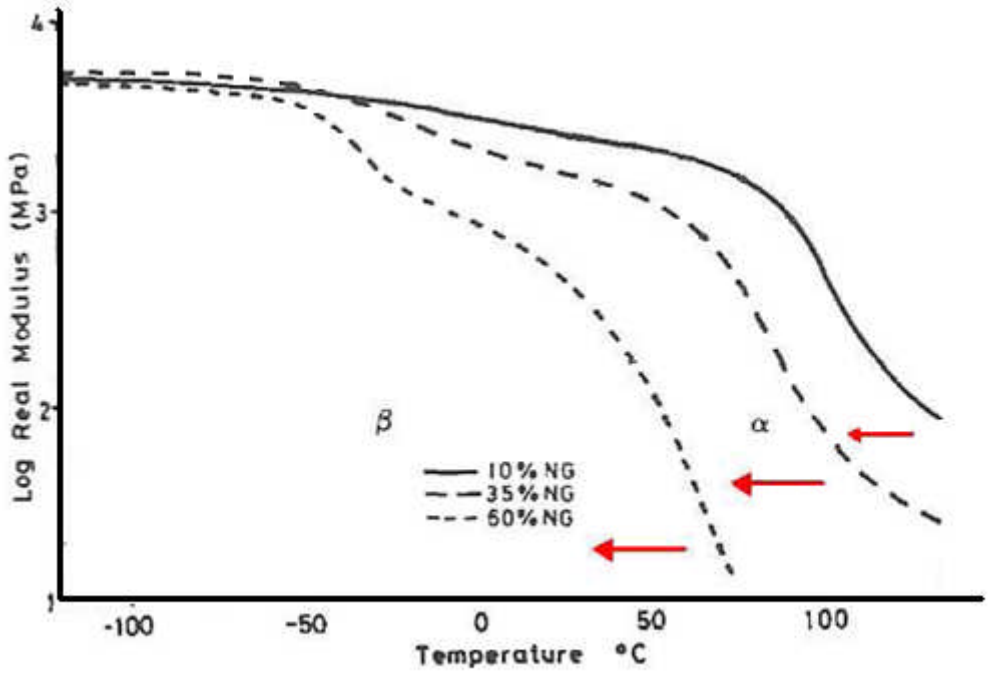

Figure 3-6 The storage modulus curve (real modulus) for temperature scans of three samples of double base propellant containing varying amount of plasticiser (21)

3.5.3 The γ transition

A transition named here as the γ has been reported at -80°C in a sample containing 10% nitroglycerine (21), and in samples containing 10% and 0% nitroglycerine at similar temperatures (16). This peak was not observed at higher nitroglycerine concentrations. It is difficult to consider the chemical processes that lead to this transition based upon such little information.

3.6 Effect of gelatinisation on dynamic mechanical properties

3.6.1 Gelatinisation

The regularity of the crystalline structure of cellulose and the level of intra-molecular hydrogen bonding between the cellulose and polymer strands, have an effect upon the mechanical and thermal properties. Gelatinisation is the extent to which the regular crystalline structure of the cellulose has been broken. Thus gelatinisation is likely to affect the mechanical properties of a sample. The effect of gelatinisation on mechanical properties has been investigated (21). Poorly, moderately and well gelatinised products were synthesised. Samples of varying degrees of gelatinisation were prepared by varying ratios of acetone and ethanol as a processing solvent (21). It is important to note there is no quantitative measure of gelatinisation.

3.7 Chemical processes, thermal and mechanical transitions

It would be useful to try to attribute chemical processes to the thermal and mechanical transitions observed in literature. These can then be carried forward and developed when interpreting experimental results.

3.7.1 Thermal transitions measured between ~-90 and -80°C in double base propellant samples

The peak and modulus values are affected by the concentration of plasticiser and by the level of gelatinisation. A transition has been reported to occur at -80 to -90°C in nitrocellulose / nitroglycerine mixtures (18) (16). Baker and Privet suggest that this process was due to the presence of residual solvent from manufacturing however it has been highlighted (20) that this peak increased as the solvent was removed. Therefore this suggestion is unlikely to be correct. Bradley and Carr observed the T_g transition at -90°C in cellulose and it was attributed to the motion of the alcohol side groups (30), while Townend and

Warren attributed a transition in nitrocellulose to the motion of the nitro groups. These two conclusions are analogous as the alcohol in cellulose is equivalent to the nitro group in the nitrocellulose (30). These seem consistent with the idea that the lower temperature transitions are due to small group movements.

3.7.2 Thermal transitions measured in the range ~-33 to ~15°C (β) and ~56 to 133°C (α) double base propellant samples

A transition at -40°C was measured in cellulose acetate butyrate (29). The authors attribute this transition to ring motion. These measurements were made using non-volatile plasticisers. The transition is close in temperature to the β transition, therefore will be included in our discussion of β transitions. As shown in Figure 3-5 the β peak height in the tan δ is significantly affected by the concentration of nitroglycerine. The β transition has been attributed to an association of the plasticiser with the side groups of the polymer (30). This attribution explains the apparent reduction of the β transition as nitroglycerine concentration decreases. It is likely that this process will have a thermal effect, and there have been DSC peaks observed at this transition.
The alpha transition measured was 20°C lower in samples with “good” gelatinisation compared with those with “bad” gelatinisation. As the product was gelatinised to a greater extent, reduced intra molecular bonding between the chains caused by gelatinisation will reduce the energy or temperature required for the movement of chain sections, this is consistent with the Tα being associated with slippage of chain sections past one another. The β transition is unaffected by the degree of gelatinisation, which suggests it is not related to large scale movement of chain sections.

3.8 Frequency effects

Increased frequency leads to an increase in the modulus and in the temperature at which the transitions occur. A range of frequencies between 0.1 and 50Hz were analysed (27). The α transition shifting by 6ºC, the β transition has also

shifted. Warren (16) reported that the temperature of the α transition increased by 15°C due to an increase of frequency from 0.33 to 30Hz as measured by the tan delta (16). The activation energies for the transitions were calculated by Pachman (17). The activation energy for the transition was calculated from data series of temperature scans at different frequency. A plot of log frequency vs 1/transition temperature gave a linear correlation, the gradient of which was – activation energy/gas constant. The activation energy calculated varied depended upon which point was taken to represent the transition, as the curve was not shifted by the same amount at every temperature.
At a higher frequency the material behaves like it is at a lower temperature. This is described as the equivalence of time and temperature. The principal is discussed in greater depth in chapter 7 where TTS calculations are performed on frequency scan data.

3.9 Measuring ageing using DMA

3.9.1 Samples age at ambient conditions

The influence of age on the mechanical properties of a double base propellant was investigated by looking at a series of samples that have been taken from in-service munitions (31). Samples up to 15 years old were analysed using DMA. As the samples were taken from in service munitions it could not be guaranteed that the samples had been subjected to the same storage conditions. An increase in T_α (identified by the author to be the glass transition) of 0.4°C per year. In Figure 3-7 the α transition is plotted against year of production , the line of best fit indicates a decrease over the time. There is a broad spread of data points, there is a difference of approximately 7°C between the two samples produced in 1985. This variation is approximately equal to the difference in transition temperature that would be predicted using the line of best fit suggested by the authors. The other parameters measured suffer equal variation across the range. The changes were attributed to the loss of nitroglycerine and chemical decomposition of the nitrocellulose, reducing the inter chain spacing and increasing the energy required for movement. These

attributions are consistent with the changes in mechanical properties due to nitroglycerine concentration reported by (21). In my opinion it is difficult to rely on these attributions as there was a very broad spread in the data collected Figure 3-7.

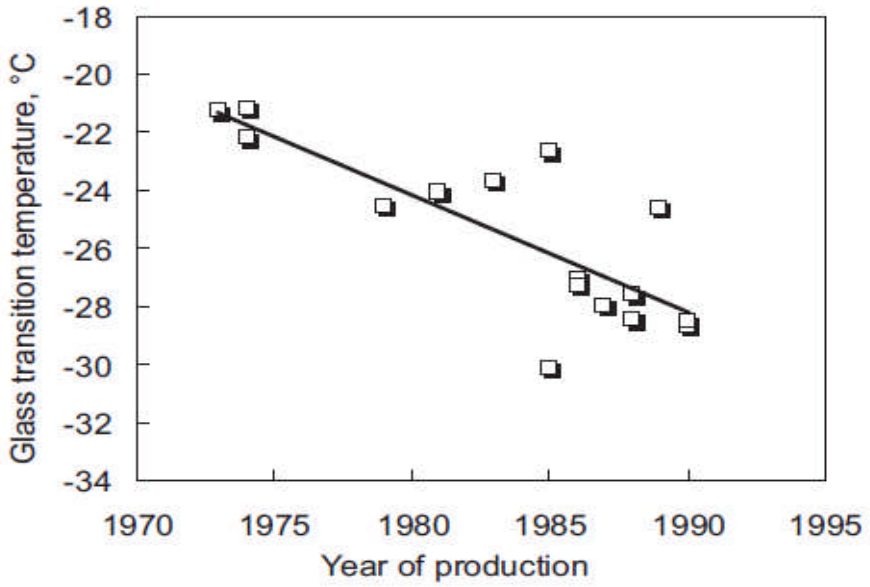

Figure 3-7 The α transition temperature of propellant samples aged at ambient conditions (transition identified as the glass transition by the author). Measured from DMA temperature scan loss modulus data 1Hz 2°C/minute

3.9.2 Samples aged artificially at elevated temperature

The changes that occur in a double base propellant during accelerated thermal ageing has been investigated by Matecic and Suceka (32). A sample measuring 50x10x2.5mm was aged at 90°C for 82 days. It was analysed periodically using DMA in a temperature scan between -120 and 100°C with a heating rate of 2°C/minute.

The results showed that the storage modulus decreased between -50 and -110°C after ageing, and increased between 30 and -20°C (Figure 3-8). The loss modulus peak between -20 and -80°C reduced in height and broadened (Figure

3-9). In the tan δ plot (Figure 3-10), the peak at approximately -20°C decreases in height progressively throughout ageing, and by 82 days of ageing it has almost entirely disappeared. The tanδ peak at 75°C was shifted to higher temperature, above the measured temperature range, the analysis doesn't go to a high enough temperature to fully analyse the effect on this peak.

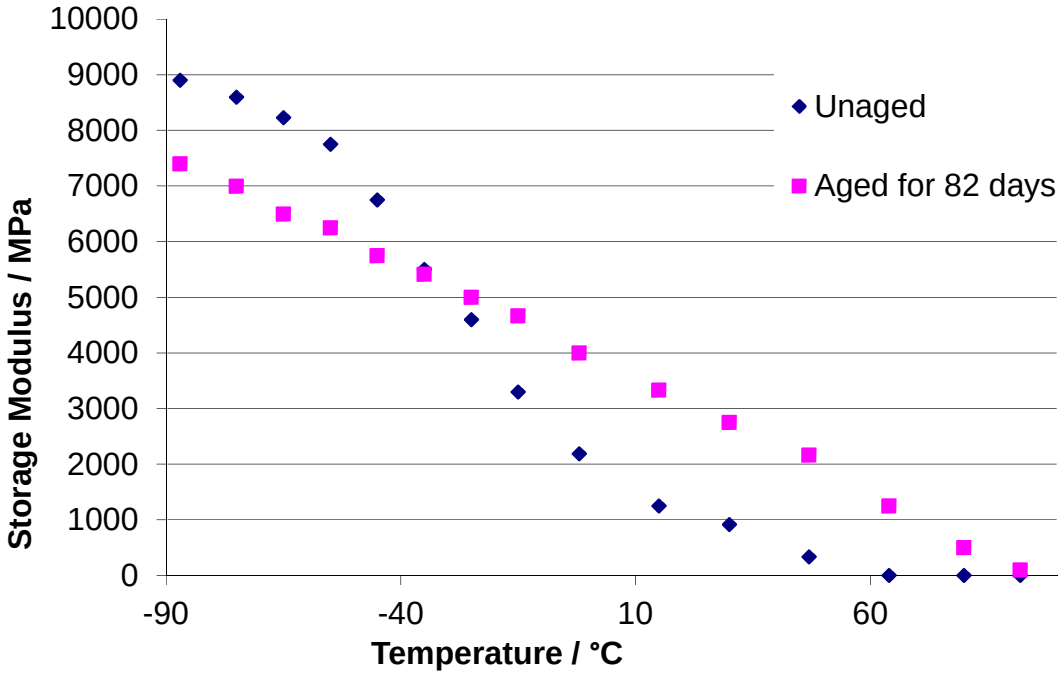

Figure 3-8 Storage modulus versus temperature for samples aged at 90°C (32)

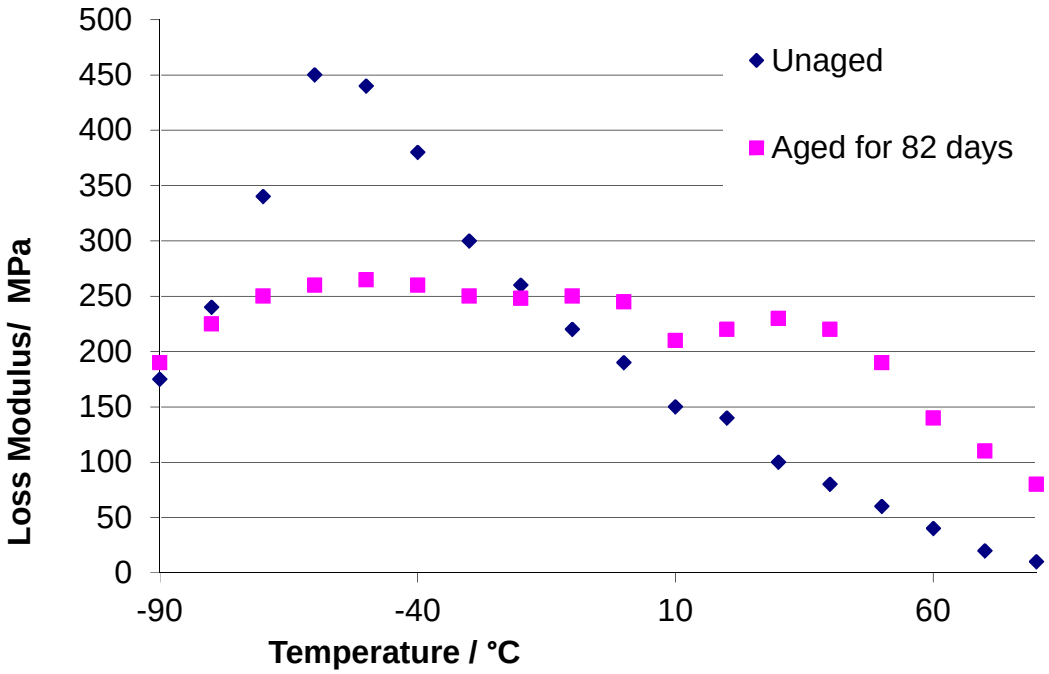

Figure 3-9 Loss modulus versus temperature for a sample aged at 90°C (32)

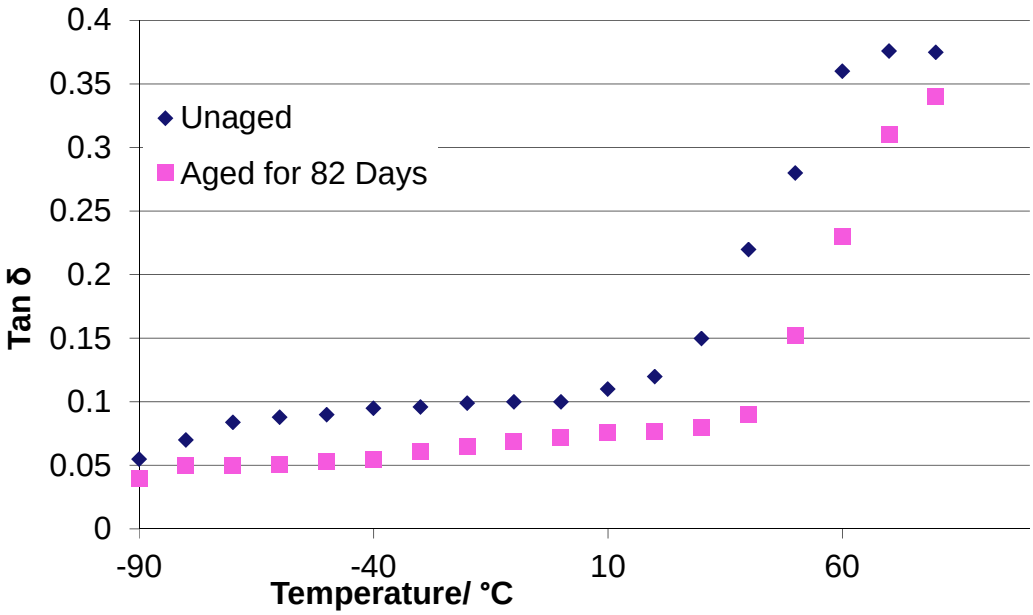

Figure 3-10 Tan δ versus temperature for sample aged at 90°C (32)

Matecic and Suceka (32) suggest that the increase in storage modulus between -20 and 70°C and the increase in the temperature of the tanδ peak which occurs initially at 75°C in an un-aged sample, are caused by a loss of chain mobility was due to plasticiser loss. This is a reasonable attribution as nitroglycerine migration is known to occur, and the research of Townend and Warren showed that the storage modulus of these propellants increases if the concentration of plasticiser is reduced (21). Matecic and Suceka suggest that chain scission reactions would also contribute to the increase in storage modulus between -20 and 70°C, as they believe it would enable closer interaction between chains leading to an increase in the modulus. I disagree with this, I think that chain scission reactions would act to reduce the storage modulus, as the shorter chains could move more easily and is possibly the explanation for the reduction observed between below -50°C. It would be useful to analyse the mechanical properties of propellant samples prepared with differing polymer chain lengths, before this attribution could be relied upon.

Matecic and Suceka (32) attribute the broadening of the loss modulus peak to an increase in heterogeneity caused by chain scission. I consider this to be reasonable. Gel permeation chromatography analysis could help to quantify this, as the distribution of polymer chain lengths could be analysed.

The tan δ plot Figure 3-10 provided further information about the ageing processes that had taken place (32). It had been identified that the β transition is dependent upon plasticiser concentration, as the plasticiser concentration is reduced the peak height is reduced (21). The changes to the β transition observed by Matecic and Suceka (32) Figure 3-10 are consistent with those measured by Warren (21) as a result of reduced plasticiser concentration. It is reasonable to attribute this peak loss to the migration of the plasticiser, this attribution was not made by Matecic and Suceka who stated that the effect of plasticiser loss was in a general increase in stiffness.

In general Matecic and Suceka (32) have attributed the changes observed to chain scission and plasticiser migration, however they have given little evidence to indicate which process is dominant. Simply claiming that the plasticiser migration occurs over the first 40 days and after that chemical degradation dominated. It would be useful to separate the ageing process's effects on the DMA. This would allow for a more detailed understanding of how the ageing is occurring. The extent of the chain scission was also not quantified, this could have easily been achieved using gel permeation chromatography.

In my opinion the experimental procedure used by Matecic and Suceka was flawed for a number of reasons:

Matecic and Suceka reanalyses the same DMA sample which is an undesirable practice as heating the material such that it will soften, as it will relax and deform in the clamps, leaving marks on the sample, it may not be exactly the same size and shape in each analysis. If the sample is becoming slightly thinner at the point at which is clamped then it will give a false indication that it is softening, whereas in reality less material is being analysed.

Migration of nitroglycerine is known to occur (22), in this research little effort was made to mitigate this. The DMA samples were small and had a high surface area, this is unfortunately unavoidable. It means that plasticiser migration is likely to occur at a far greater rate than in a real propellant grain. The samples were aged in glass vials, this allowed an airspace, and surface oxidation was more likely to occur. A better way to age the samples may have been to use sealed evacuated aluminium bags. Thermal gravimetric analysis was used to analyse how much nitroglycerine had evaporated from the samples, a technique that the authors describe as giving a rough measure of the nitroglycerine migration. HPLC could have been used to provide a more accurate measure. The temperatures (up to 100ºC) used during the ageing were higher than AOP 48 ed2 suggests should be used.

I believe that the excessively high ageing temperatures and duration coupled with poor consideration to nitroglycerine migration and the reuse of the same DMA sample, means that the experiment is unrepresentative of any likely real world ageing.

An accelerated thermal ageing trial was completed by Husband (33). In this work ½ gallon cartons of propellant were aged at temperatures between 25 and 73.8°C for 200 days. After ageing samples were taken from within the bulk not the surface and analysed

In Husband's investigation the tanδ and the thermal transitions were not reported, this is unfortunate as they can provide useful information about the sample.

The storage modulus values were affected by the ageing processes. The increase in storage modulus (at ambient temperature) is shown in Figure 3-11.

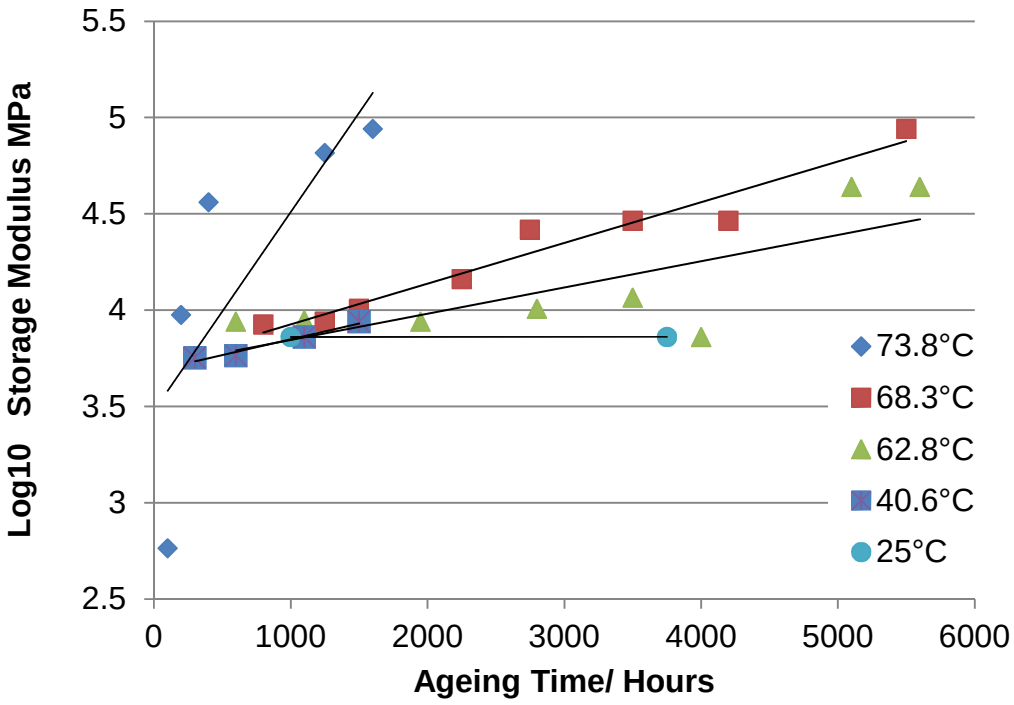

Figure 3-11 The effect of thermal ageing on the storage modulus of the propellant sample (33)

Husband (33) has identified the temperatures at which the three processes are occurring.

1. At temperatures less than 40.6°C the physical changes were attributed to slow physical processes (33), without explanation of what slow physical processes are,
2. At temperatures 40.6 and 62.8°C was attributed to the volatilisation of plasticiser.
3. Finally between 62.8 and 73.9°C the kinetics were describes as being consistent with the chemical decomposition of the propellant.

These attributions were based upon the data shown in Figure 3-12, in this graph is seems that Husband has simply connected the data points. In my opinion the line of best fit is very poor and this data could easily be correlated by a single linear relation. Considering how poorly the data in Figure 3-11 (the source of data for Figure 3-12) fits the lines of best fit, it seems unjustified to pick out such subtle changes in data as separate processes. It has been subsequently shown that at temperatures of 70°C nitroglycerine evaporates from double base propellants, this is slightly above the boiling point of nitroglycerine because the nitroglycerine forms interactions with the nitrocellulose, increasing the energy required for evaporation (Discussed 3.3) (22). It is still unclear looking at the results of Husband's research how significantly the physical process of plasticiser migration is responsible for the ageing observed, and how significantly the chemical decomposition reactions have influenced the result. In Husband's experimental method there is no indication regarding measures taken to minimise nitroglycerine migration, or whether the migration of nitroglycerine was quantified, this represents a serious issue with the method. Nitroglycerine has an impact upon the mechanical properties of the sample, it is therefore important to understand how this variable is changing during ageing.

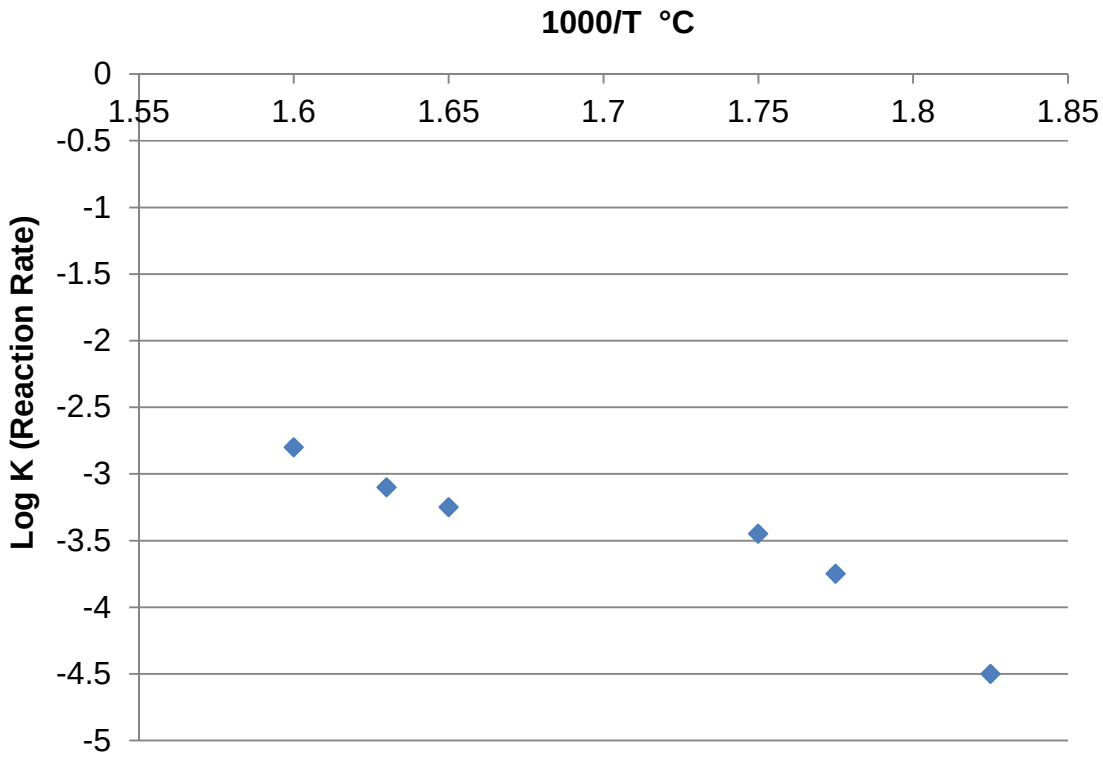

Figure 3-12 Reaction rate calculated for each propellant sample aged in Husband's work (33)

In Husband's research the samples were aged for the same length of time and different levels of ageing were achieved by using a selection of temperatures as opposed to using the same ageing temperature and increasing the ageing time to produce a sample that is aged to a greater extent. This means that the balance of how much plasticiser migration and how much chemical decomposition reactions are responsible for the total ageing is unlikely to be the same. This raises the question of how valid the comparison of the ageing is, further highlighting the need to understand how the plasticiser is migrating, and to consider whether this leads to a representative aged sample. In Husband's work the same samples were used throughout the analysis, it is probable that the ageing processes that occur at the surface of the material were not the same as those that are occurring within the core of the sample. These surface reactions would not be representative of the ageing processes that occur in munitions. If HPLC and GPC had been carried out on the samples in addition to

the DMA, then it would be possible to quantify ageing processes such as denitration and chain scission, it would then be possible to consider more reliably how certain chemical changes influence the mechanical properties. The work carried out by Husband does not provide sufficiently accurate results to draw many conclusions.

3.10 Effect of extrusion and re-extrusion on polymeric materials

During the extrusion process the polymer chains are submitted to high thermal and mechanical stresses, these promote chemical reactions within the polymer. It is widely accepted that extrusion as a process, due to these reasons changes the mechanical and physical properties of a polymer. The chemical reactions can cause chain scission or branching depending upon the individual conditions.

The exact chemical composition of a polymer will influence the extent to which chemical changes that occur. The decomposition reactions observed in other polymer can only serve as a guide to the processes that may occur in nitrocellulose. In the following sections the decompositions measured in a number of polymers is reported. The information gathered with these polymers demonstrates the importance of carrying out research in this area with propellant compositions.

3.11 Investigating the effect of extrusion on nitrocellulose based materials

The effect of extrusion and re-extrusion on the nitrocellulose within the propellants has not been reported in the literature. However it has been reported in other polymers that the forces and pressures of extrusion can cause chain scission and cross linking. These factors would both have an influence upon the mechanical and chemical properties of a propellant grain, it is therefore interesting to understand these effects in more detail. This can be

studied using DMA to measure any change in the mechanical properties and gel permeation chromatography to investigate the associated changes in molecular weight due to; chain scission and cross-linking.

Repeated extrusion has had a significant effect on polymers reported in the literature, inducing changes that resemble that of conventional ageing, it would be interesting to research this further.

3.11.1 Effect on polypropylene

The change in weight average molecular mass and number average molecular mass of polypropylene as a result of extrusion was investigated by Badia (34). A screw extruder was used. It was found that chain scission occurred, decreasing the molecular weight significantly at first and after 20 extrusions less significantly.

In this work (34) the screw extruder operated at a constant rpm, it is possible that the less significant decreases in the weight average molecular weight after approximately 20 cycles could be because the polymer is becoming softer and easier to extrude, therefore the forces experienced would have been reduced, there may be a linear relationship between the forces used and the chain scission. It was also noted that the polydispersity of the composition actually decreased, this was attributed to the Bueche effect (where the longer chains are more likely to break in the centre), yielding to polymer chains of half the originals size. The molecular weight data was collected using gel permeation chromatography. A further measurement of this work was that there appeared to be little oxidation, this was analysed from FTIR spectra.

3.11.2 The effect on polyethylene

At high oxygen concentrations the forces of extrusion promoted the chain scission reactions and at low oxygen concentrations the cross linking reactions occur. It was reported that in the first 5 extrusions the chain scission reactions dominate and in subsequent extrusions cross linking reactions were dominant.

The authors discuss that the oxygen molecules trapped in the polymer matrix react over the course of the first 5 extrusions causing scission and cross linking reactions dominate (35).

3.11.3 Effect on poly(ethylene teraphthalate)

The effect of repeated extrusion of poly (ethylene teraphthalate) has been investigated. A dramatic loss in the deformation capabilities and an increased fluidity of the polymer was observed, these changes were attributed to chain scission reactions. The storage modulus of the material was increased both above and below the glass transition region and after 4 extrusions the polymer was too brittle to analyse with DMA (36). These effects are similar in nature to those observed during the thermal ageing of nitrocellulose.

3.11.4 The propellant extrusion process used to manufacture propellant samples ‘Double base (I and II)’ investigated in this thesis

The chemical reactions reported in the previous sections in polymeric materials provide a guide to the sorts of process that can be expected during the extrusion of nitrocellulose. They highlight the importance of understanding the process.

The propellant samples ‘Double base I/II’ have an extrusion limit of 3, this means that if an exudate fails inspection for any reason it can only be re-extruded two times. This limitation comes from the manufacturing company’s policy.

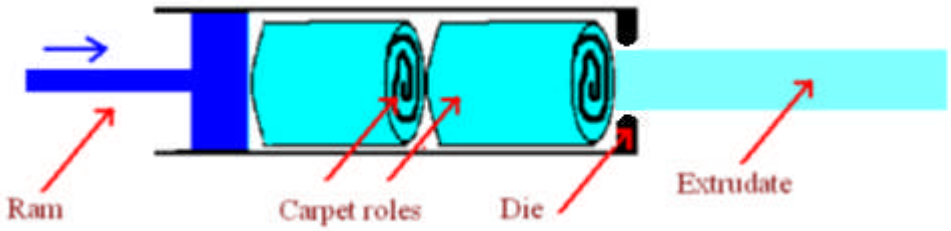

Figure 3-13 The carpet roles are loaded into the extruder

The forces of extrusion may vary across the grain, there are higher shear forces at the edges of the grain than in the middle, as illustrated in Figure 3-14. This variation in the intensity of the forces exerted on the polymer across the grain may lead to variation in polymer damage, across the grain. It would be possible to investigate the effect across the grain, such an investigation would yield information on the homogeneity of the product.

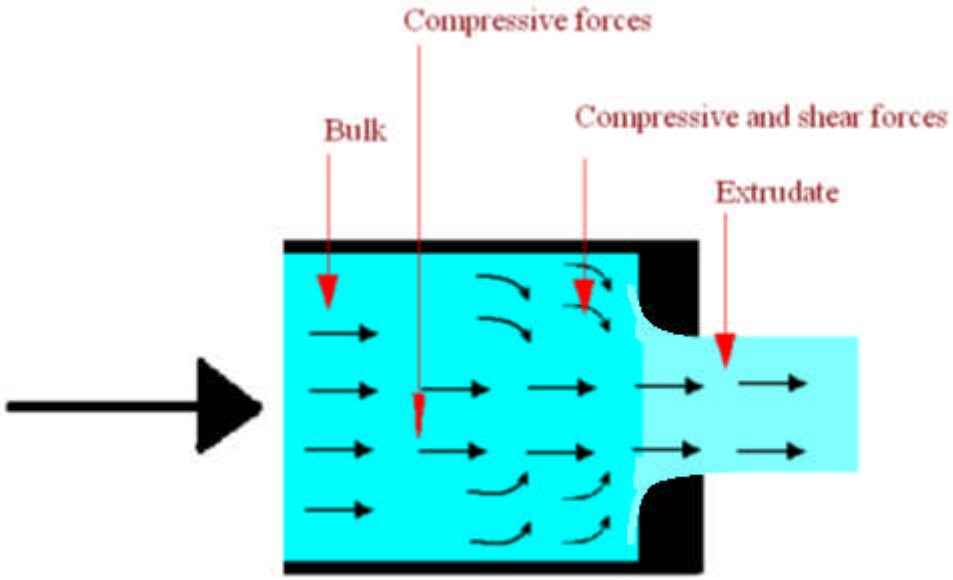

Figure 3-14 The possible shear forces during extrusion

The importance of understanding the effects of extrusion on nitrocellulose based propellant compositions has been highlighted. The area is studied in chapters 4 and 5.

4 RESULTS: CHEMICAL AND PHYSICAL EFFECTS OF MANUFACTURE ON EXTRUDED DOUBLE BASE PROPELLANT

The chemical and physical effects of the solventless manufacturing process for extruded double base propellants were analysed. A reduction in weight average molecular mass (Mw) was observed stepwise throughout the production process during both the rolling and extrusion stages. This was attributed to denitration of the nitrocellulose. Differential scanning calorimetery data indicated that the first extrusion stage is critical in ensuring the nitroglycerine is completely mixed into the nitrocellulose.

4.1 Introduction

This research aims to investigate how each stage of the `Solventless' manufacturing processes for double base propellants, affect chemical composition of the propellant material.

The nitrocellulose chemically degrades in two ways. De-nitration of the nitrate ester groups occurs, this has a reported activation energy of about 120kJmol^{-1} (5), this process affects the energy content and the mechanical and thermal properties (36). The second decomposition process that takes place is chain scission, breakage of the 1,4 glycosidic bond, the process has an activation energy of approximately 80kJmol^{-1} (5). Chain scission reduces the nitrocellulose's ability to act as a binder, the influence of chain scission on mechanical properties is studied in chapter 7. The thermal transition temperatures which affect the thermal operating range of the propellant, are also effected by chain scission (37). These decomposition processes compromise the propellants ability to function effectively, therefore the extent of the decomposition must be monitored (37).

Cellulose is a naturally occurring polymer, it occurs in large quantities in plants. In the plant material its structure has both crystalline and amorphous regions

(1), these are depicted in Figure 4-1 (1). It is desirable to have a propellant material that isn't hard and brittle (38) for reason discussed in section 1.3.3, it is important to 'gelatinise' the nitrocellulose, to remove the crystal structure which would make the propellant brittle. This gelatinisation can be achieved in a number of different ways. The solventless process relies upon hot rolling and extrusion to gelatinise the propellant (38) (39) (2). It is possible that the temperatures and pressures experienced during production are sufficient to induce the decomposition reactions similar to those reported to occur in aged samples.

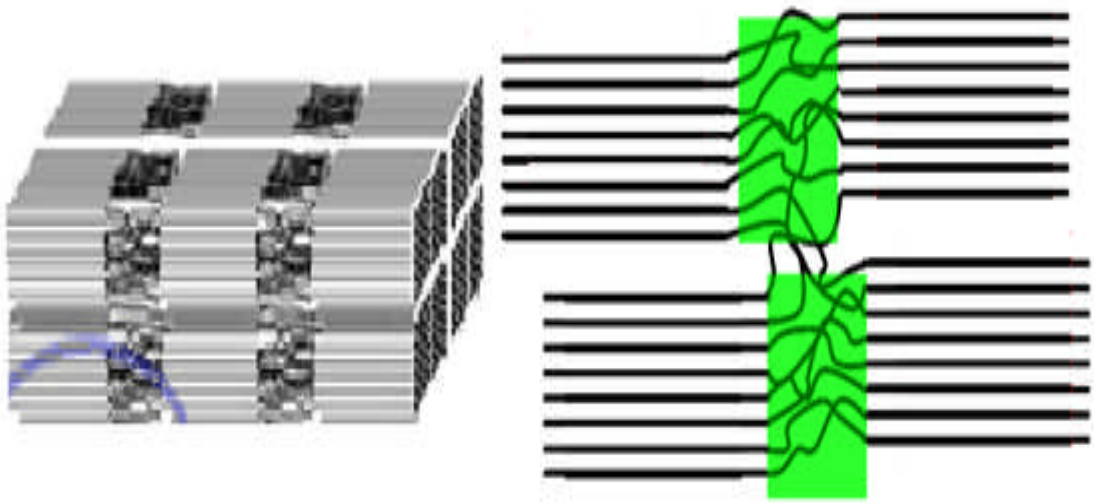

Figure 4-1 The amorphous and crystalline structure of cellulose found in plant material, left image ~25nm in length with enlargement on right ~10nm (1)

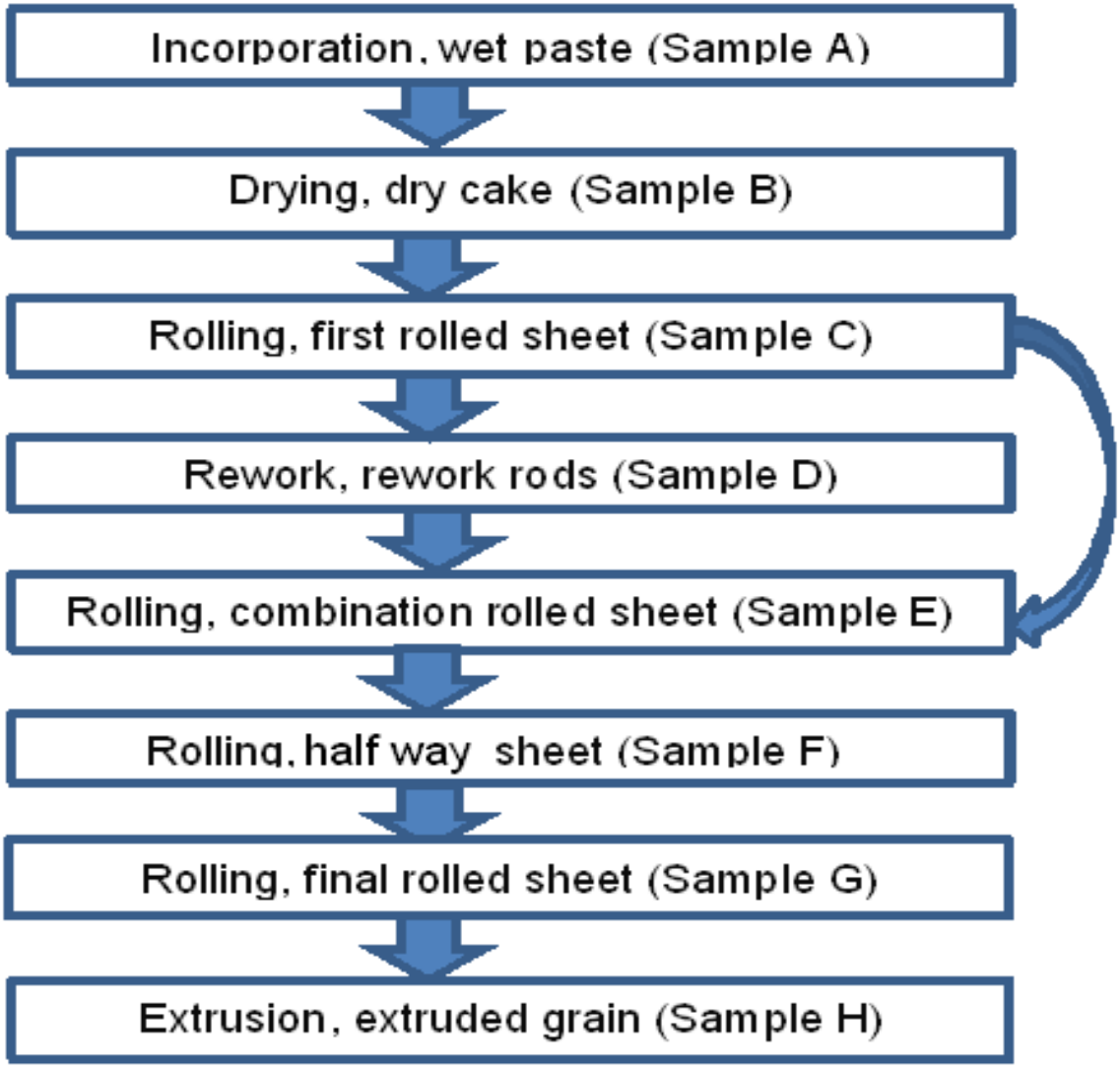

Figure 4-2 The production process for 'Double base II' (Table 0-1) propellant. Samples names are indicated in brackets.

The incorporation phase, a water wet paste of NC, NG and other additives such as stabilisers are mixed, producing 'wet paste'(Sample A Figure 4-2). The water is then removed during the drying stage, producing 'drycake' (Sample B Figure 4-2). Dry cake is passed through hot rollers typically 60-70°C, producing 'first rolled sheet' (Sample C Figure 4-2). Half of the first rolled sheet is reworked by passing through an extruder, this 'reworked' (Sample D Figure 4-2) material is recombined with the other half through rollers, producing the 'combination' (Sample E Figure 4-2) rolling material. A number of further rollings

are carried out , the ‘final’ rolled material (Sample G Figure 4-2) is passed through an extruder to produce the EDB propellant (Sample H Figure 4-2).

4.2 Analytical techniques

4.2.1 Reverse phase High Performance Liquid Chromatography (HPLC)

Instrument. Waters 2695 HPLC and Waters detector 996 PDA. The column, set to 30^{o}C, was an Inertsil 5mODS-2, 250 x 4.6 mm (Varian Inc., Palo Alto, California, USA). The flow rate was 1 ml/min and the mobile phase 65% MeOH, 35% H_2O.

Sample preparation. The AOP 48 ed2 (Shaking) method for stabiliser extraction was followed [8] , using a IKA KS 501 digital shaker at 300rpm, as it has been shown to be the most effective method (40). Analysis was carried out in duplicate; the result for each is the average of two injections of 20ml. The stabiliser and nitroglycerine concentrations were measured by a UV photo diode array detector at a wavelength of 254nm.

4.2.2 Gel Permeation Chromatography (GPC)

Instrument. Viscotek VE1121 GPC solvent pump, a Kontron Instruments DEG-104 degasser, Waters 717 Plus auto-sampler and Waters 2410 refractive index detector. set at 35°C. The mobile phase was THF and the flow rate of 1 ml/min was maintained through two columns in series (PLgel 10 mm mixed phase B columns, 300 x 8 mm, manufactured by Polymer Laboratories (part of Varian Inc.)) held at 35°C using a column heater. The injection volume was 100 ml. The calibration method detailed in (41) was used.

Sample preparation. Samples (50mg ±5mg) of propellant were dissolved in THF for 24 hours, the concentration of this solution was 0.15% weight (NC)/volume (THF). Injections of 5 replicated were carried out.

4.2.3 Differential Scanning Calorimetery (DSC)

Instrument. Mettler Toledo DSC 1 Stare System, Liquid N_2 cooled. Samples were analysed between -50°C and +80°C, heating rates of 5,10 and 20°C/minute were used.

Sample preparation. Samples were cut using a scalpel from the bulk, ensuring a flat surface so good thermal contact is made with the sample pan. Samples of approximately 5mg (±0.1mg) and sealed in aluminium sample pans. Analysis carried out in triplicate.

4.2.4 Dynamic Mechanical Analysis (DMA)

Instrument. Perkin Elmer DMA 8000. A temperature scanning mode was selected, samples were analysed between -100 and +80°C at a heating rate of 2°C/min in a single cantilever bending geometry.

Sample preparation. Samples taken from the pre extrusion stages were cut using a scalpel to approximately 3mm x 4mm x 20mm ±0.5mm, cuboids as they were too soft to machine using a CNC mill.

The extruded sample was prepared using a CNC mill fitted with slot drills. The milling process carried out using a 3mm slot drill at: 1000rpm with a maximum cutting speed of 30mm/min and was air cooled by ambient air. The sample was prepared to the same measurements ±0.01mm.

4.2.5 Helium Pycnometery

Instrument. Micromeritics AccuPyc 1130 Gas Pycnometer, using Helium. Three samples were taken for each material, each sample was analysed five times by the instrument to generate an average.

Sample preparation. Samples were cut using a scalpel to approximately 0.5g pieces, they were weighed out to 0.001g.

4.2.6 X-ray Diffraction (XRD)

Instrument. PANalytical X'Pert PRO Multi-Purpose Diffractometer with Cu radiation. A PIXcel detector was used to collect data over an angular range of 10 - 80°/2Θ with a step size of 0.0263 °/2Θ and a count time of 23.97 seconds at each step (2Θ is the diffraction angle).

Sample preparation. Samples were cut into thin slices (~5mm thick) using a scalpel, these were mounted on a silica sample holder.

4.3 Results

4.3.1 Molecular Mass Distribution (GPC).

The GPC showed a statistically significant reduction in the weight average molecular weight (Mw) of nitrocellulose throughout the manufacturing processing Figure 4-3, error bars indicate 2x standard deviation. The Mw decreased progressively throughout the samples measured. The most significant decreases were observed after extrusion, between samples C and D and between samples G and H. This is likely due to the high pressures involved at this stage. No such changes in Mn or polydispersity were observed Table 4-1, Figure 4-4, Figure 4-5.

It was concluded that denitration was the dominant mechanism taking place. The scission factor ‘S’, which is defined at the apparent number of chain scissions per molecule was calculated using equation (4-1). The value of the scission factor was >1. It has been reported that a scission factor of >5 is an indication of chain scission. It was concluded that chain scission was not the dominant process. The changes in Mn and Mw indicate that the extrusion process has produced degradation of the highest molecular weight chains with a consequent narrowing of the polydispersity. The longer chains connect between regions of order in the matrix and their degradation will lead to loss of ultimate mechanical properties

$$S = \frac{Mn_{Initial}}{Mn_{Final}} \quad \textbf{(4-1)}$$

Denitration reduces the weight average molecular mass of the polymer, as the hydroxyl groups which replace the nitrate groups are smaller. As a decrease in weight average molecular mass was measured and there was no significant change in the number average molecular mass, it was concluded that denitration was the dominant process (42) (43).

Sample B (dry cake) material had a very high surface area, as it was highly porous in form, as a result Mw may have been reduced by surface oxidation since manufacture more significantly than any other. Subsequent samples would not have been stored in this porous state for such a significant period of time, and therefore not incurred this decomposition. This may account for the lower than expected molecular weight observed in sample B.

The findings of the GPC analysis correlate with published research studying the effects of extrusion. It had been reported that extrusion causes reduction in Mn and Mw of polypropylene (35). The precise influence of the pressures and forces that occur during extrusion will depend upon the chemical composition of the polymer and exact extrusion conditions. It is therefore not surprising that the changes observed in polypropylene, where both Mn and Mw decreased, were not the same as those measured for nitrocellulose, where a decrease in Mw only was observed. It is also quite possible that if the nitrocellulose were subjected to repeated extrusion, changes in Mn may occur. These results demonstrate that the manufacturing processes of rolling and extrusion are having an influence on the polymers molecular structure, in addition to disrupting the macrostructure of fibrils which is present in the cellulose initially (3).

Table 4-1 Gel permeation data of 'Double base II' samples taken from throughout the manufacturing process

Sample	Average Mw	Std Dev	Average Mn	Std Dev	Polydispersity
B	309085	8568.2	84005	2141.5	3.68

C	317720	17881.4	86757	10312.6	3.66
D	293030	5880.8	78557	1369.1	3.73
E	290220	7441	77313	3576.6	3.75
F	281230	3492.2	85161	5175.8	3.30
G	279840	2330.4	77910	3264.4	3.59
H	238874	2206.6	83930	2261.2	2.85

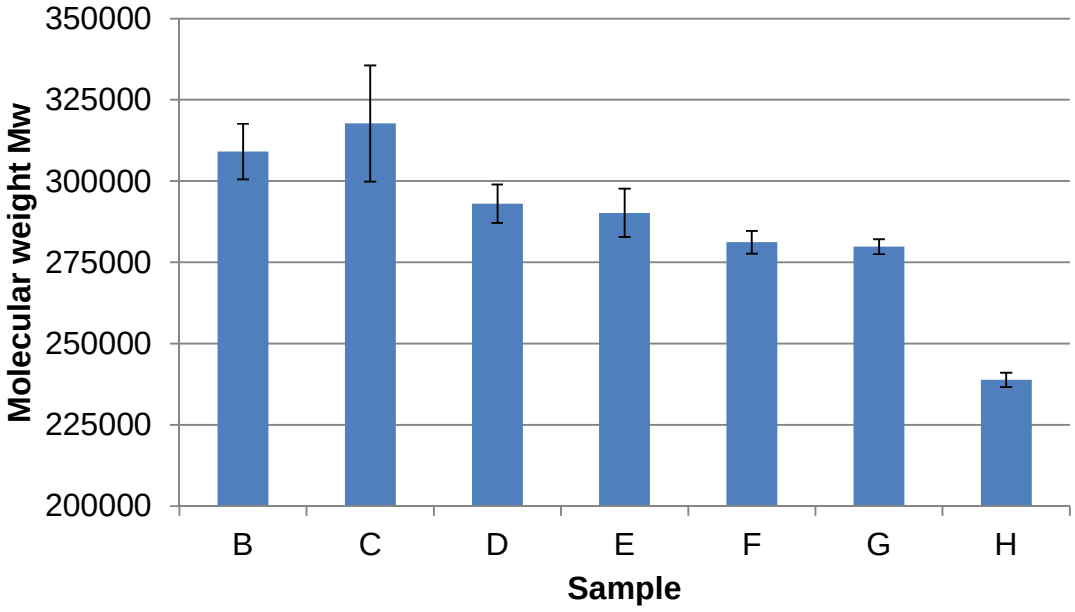

Figure 4-3 Molecular weight variation throughout the manufacturing process, error bars indicate 2 standard deviation

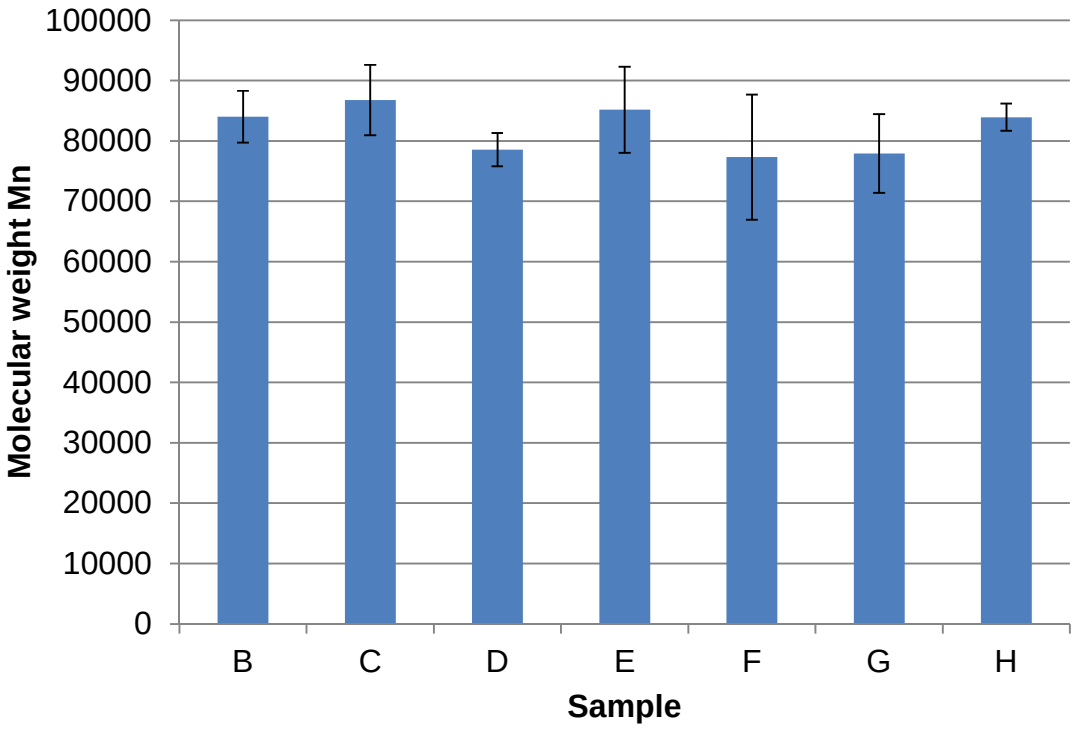

Figure 4-4 Molecular weight Mn variation throughout the manufacturing process, error bars indicate 2 standard deviation

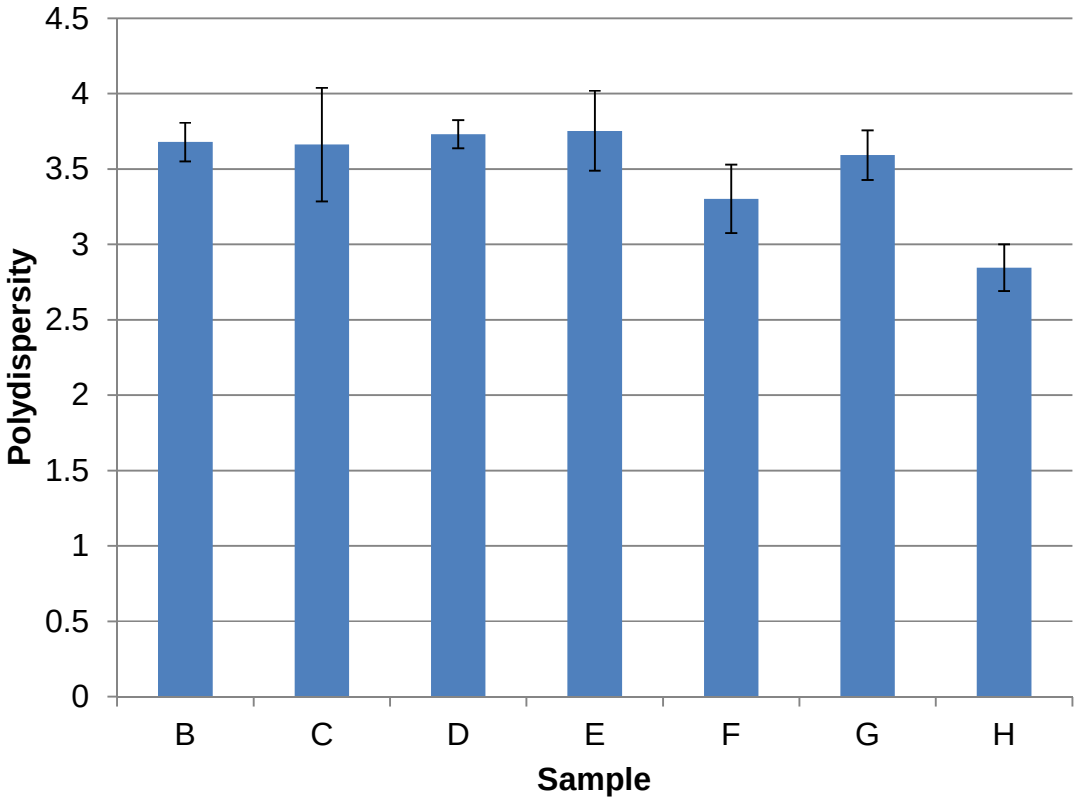

Figure 4-5 Polydispersity variation throughout the manufacturing process, error bars indicate 2 standard deviation

4.3.2 Thermal Transitions (DSC)

The DSC analysis of all samples measured two thermal events. The first occurring within the region -30 to -10°C, the second occurring within the region 60 to 80°C. Thermal transitions within these regions have been previously reported in double base propellant (18) (16) (41) (21) (23). The thermal event occurring between -30 and -10°C is typical of a melt process, as it appears as a peak in the heat flow trace (14) , the integral of the peak remained constant within standard deviation (Table 4-2). Previous work has linked thermal events in this region to the concentration of nitroglycerine, discussing how the nitroglycerine may associate with the nitrate ester side group of the nitrocellulose (21). Though the melting point of nitroglycerine is 14°C (2) when

pure, in nitrocellulose the nitroglycerine may be melting as this temperature is passed, as it can form interactions with the nitrocellulose, enabling it to interact more freely with the nitrocellulose. The temperature at which the thermal event occurred was invariant with respect to the standard deviation. The standard deviations were far higher in samples B and C, than for samples D,E,F and G Figure 4-7, Table 4-2. I believe that the variations are due to incomplete mixing of the nitrocellulose and nitroglycerine in samples B and C. That the pressure involved during the extrusion of rework rods (sample D), leads to the largest single gelatinisation of the nitrocellulose. This indicates that the rework stage is critical to ensure that nitroglycerine is evenly distributed within the propellant. This most intimate mixing would likely have an influence of the burn rate as localised high concentrations of nitroglycerine may burn faster and low concentrations burn slower. These fluctuations were only measured using the DSC as the samples (5mg ±0.5mg) were at least an order of magnitude smaller than other techniques.

The indication that the reworking stage forming sample D aids in the mixing of the nitroglycerine, suggests that there may be other constituents that are distributed during the rolling and reworking stages. It is possible that the stabiliser is only distributed completely during these stages, this would mean that the long term stability of the propellant may be influenced.

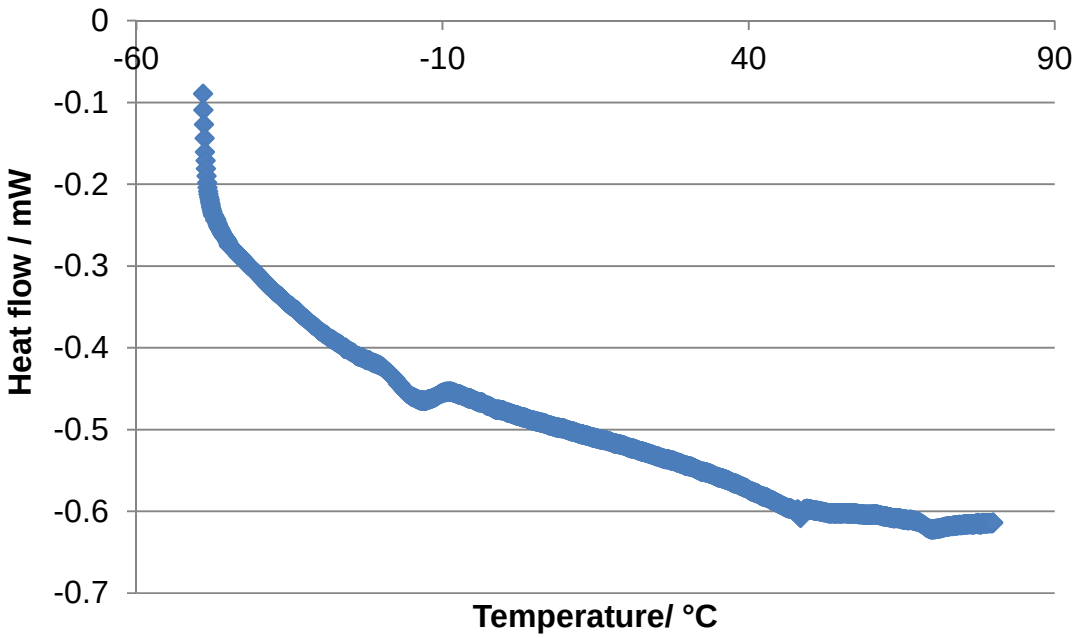

Figure 4-6 DSC analysis of propellant measured at 20°C/minute

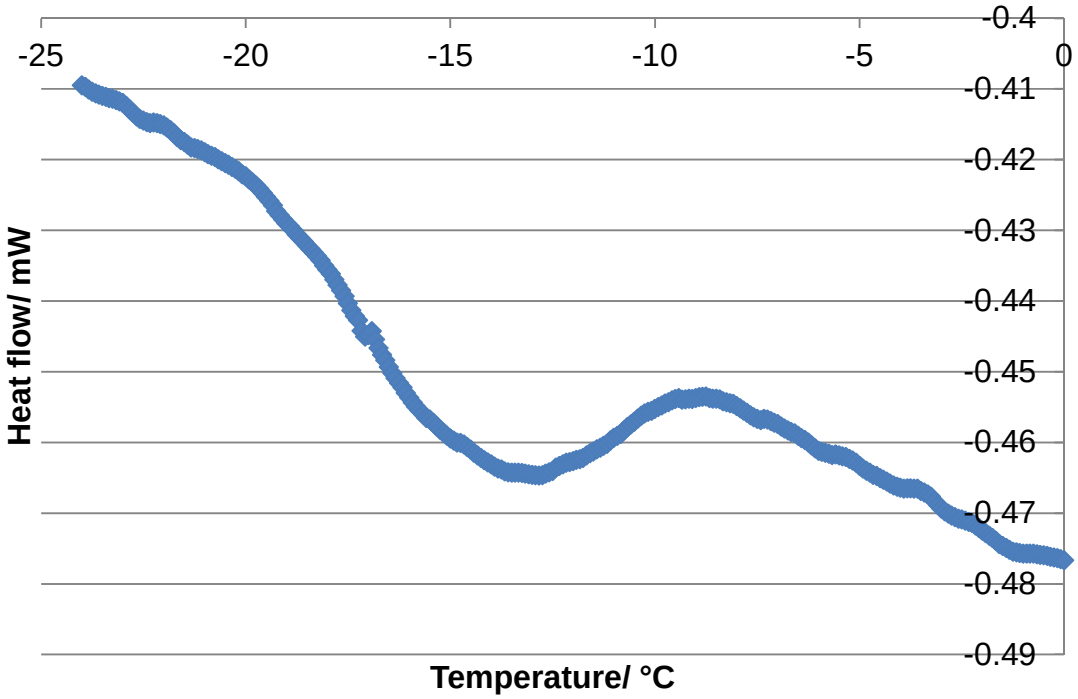

Figure 4-7 Endotherm measured in differential scanning calorimeter analysis, measured at 20°C/minute

Table 4-2 Endotherm measured in differential scanning calorimeter analysis

Sample name	Average endotherm /°C	Std dev	Endotherm area J/g	Std dev
B	-20.94	6	0.37	0.05
C	-16.65	4.64	0.41	0.08
D	-13.85	0.51	0.44	0.08
E	-14.23	0.65	0.38	0.07
F	-14.34	0.73	0.42	0.03
G	-14.23	0.49	0.38	0.08
H	-14.11	0.52	0.39	0.08

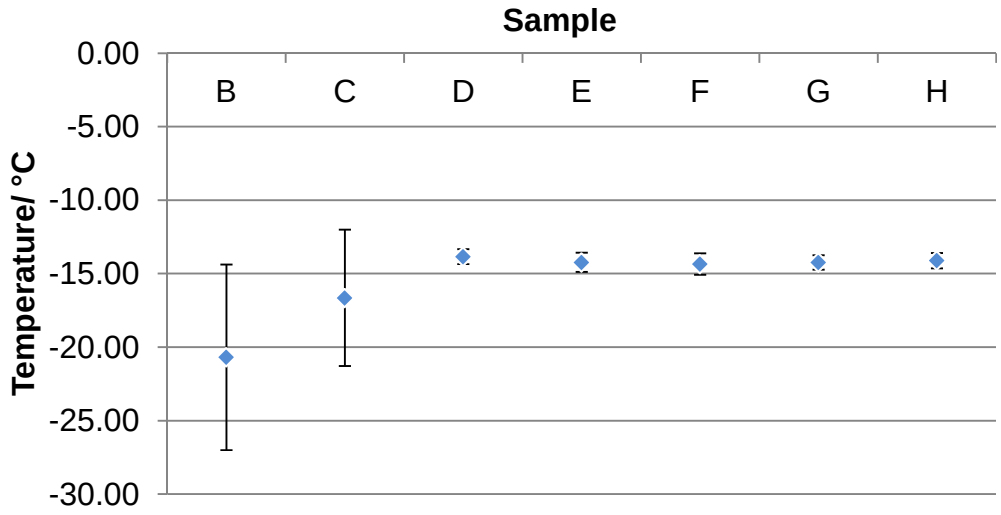

Figure 4-8 The average endotherm temperature measured by differential scanning calorimetery, indicated with 2 standard deviation

4.3.3 Dynamic Mechanical Properties (DMA)

Two thermal changes were observed in the DMA. The storage modulus decreased in two steps. The loss modulus peaked at -40°C with a shoulder in the region of ~15°C (Figure 4-9). To determine the midpoints of the events the Gaussian deconvolution method described in section 2.2 was used.

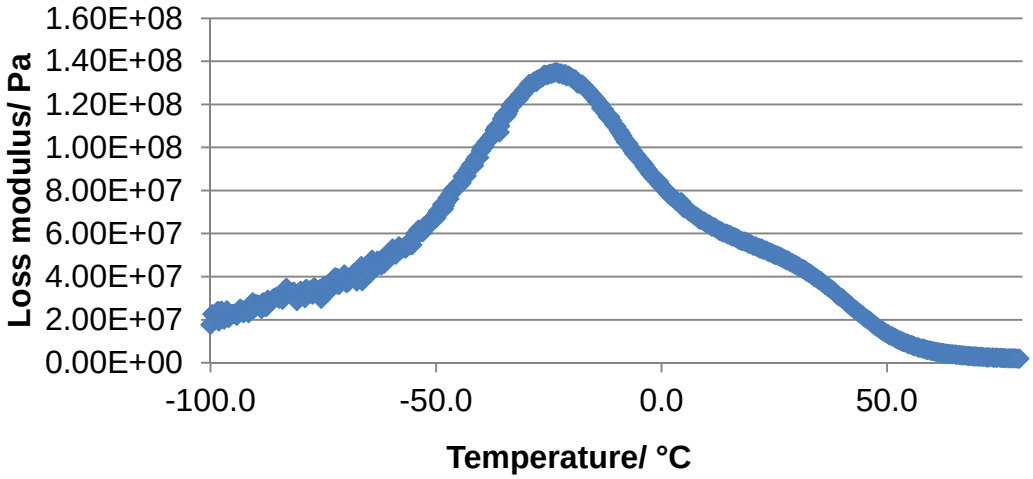

Figure 4-9 Loss modulus curve of sample D measured at 1 Hz and 2°C/minute

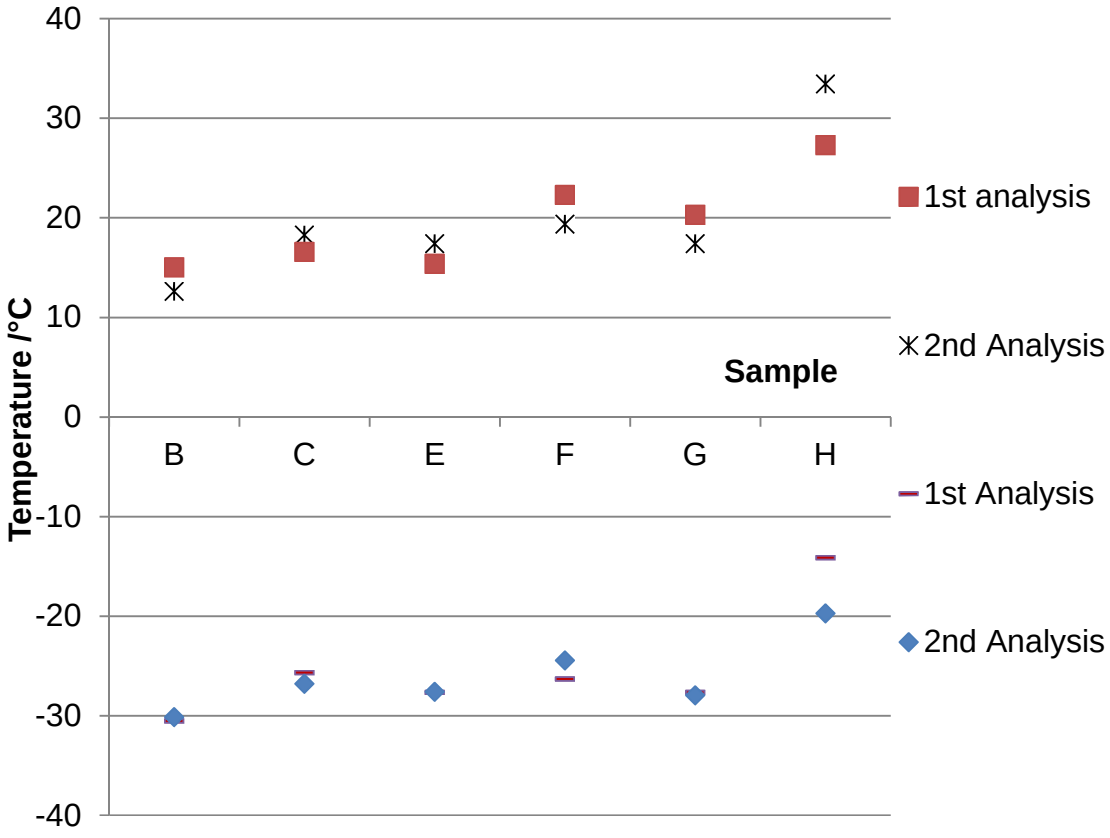

Figure 4-10 The two thermal event midpoints calculated from Gaussian deconvolution of loss modulus curves. Samples B to H

Table 4-3 DMA and DSC thermal average data, DMA data collected from Gaussian distributions fitted to curves of loss modulus

Sample	B	C	E	F	G	H
Loss modulus lower 95%	-44.92	-38.27	-39.94	-38.39	-41.79	-26.18
Loss modulus mid	-30.33	-26.24	-27.64	-25.39	-27.64	-19.73
Loss modulus upper 95%	-16.40	-12.48	-13.52	-12.34	-14.61	-13.45
DSC endotherm	-20.69	-16.65	-13.85	-14.23	-14.34	-14.23

The data collected from DMA loss modulus curves indicate that the thermal transition midpoint temperatures remained constant, except for sample H which was ~10°C higher Figure 4-9, Figure 4-10 and Table 4-3. The DMA loss modulus data was evaluated using curve fitting functions.

A mixed Gaussian model containing two Gaussian terms was employed (19)(as discussed in chapter 2.2). The temperature at which each event occurs was determined, these results are displayed in Figure 4-10. The upper, lower 95% and midpoint was then calculated from the curve's equation for the lower temperature transition to aid in comparison with DSC data. The DSC data correlated well with the upper 95% DMA data in all cases (including sample H), indicating that transitions are occurring in the same temperature range. The temperature at which the glass transition occurs is influenced by the method used to measure it, so it is not surprising that there is no exact match.

A progressive increase in the temperature of the transition occurring between 10 and 30°C is observed. This is consistent with the theory of denitration occurring throughout manufacture, a theory proposed based on the GPC measurements. The nitrate groups soften the cellulose as they reduce the intermolecular bonding between polymer chains, as they reduce the number of hydroxyl groups available for hydrogen bonding. This reduces the energy required for movement. This transition is associated with the movement of polymer chains past each other (20) (21), if denitration is occurring then it is likely that the temperature of the transition would increase.

4.3.4 Stabiliser and plasticiser analysis (HPLC)

The concentration of nitroglycerine was analysed in all samples. As sample 'A' was taken from a wet stage of production, it contained an unknown %wt of water. This meant that it was not possible accurately weight a sample out. To ensure accurate determination of nitroglycerine concentration, the stabiliser was used as an internal standard. The validity of this analysis is dependent upon assuming that the stabiliser concentration remained constant. To ensure that this was the case the HPLC separations were analysed for stabiliser daughter products, none were found. The results indicate that the nitroglycerine concentration remained constant (±0.5%wt).

4.3.5 X-ray Diffraction analysis of samples (XRD)

X-ray diffraction analysis was carried out on samples C and H (Figure 4-11 Figure 4-12), to investigate whether any variation in crystalline structure could be measured. The diffraction pattern clearly showed the crystalline CuO (CuO reference shown in Appendix D). Small variation between the two analysis can be seen, though further analysis is required before variations between samples can be clearly identified and quantified. The results from further analysis could be used to investigate which stages of manufacture disrupt the organised fibril structure of cellulose (3).

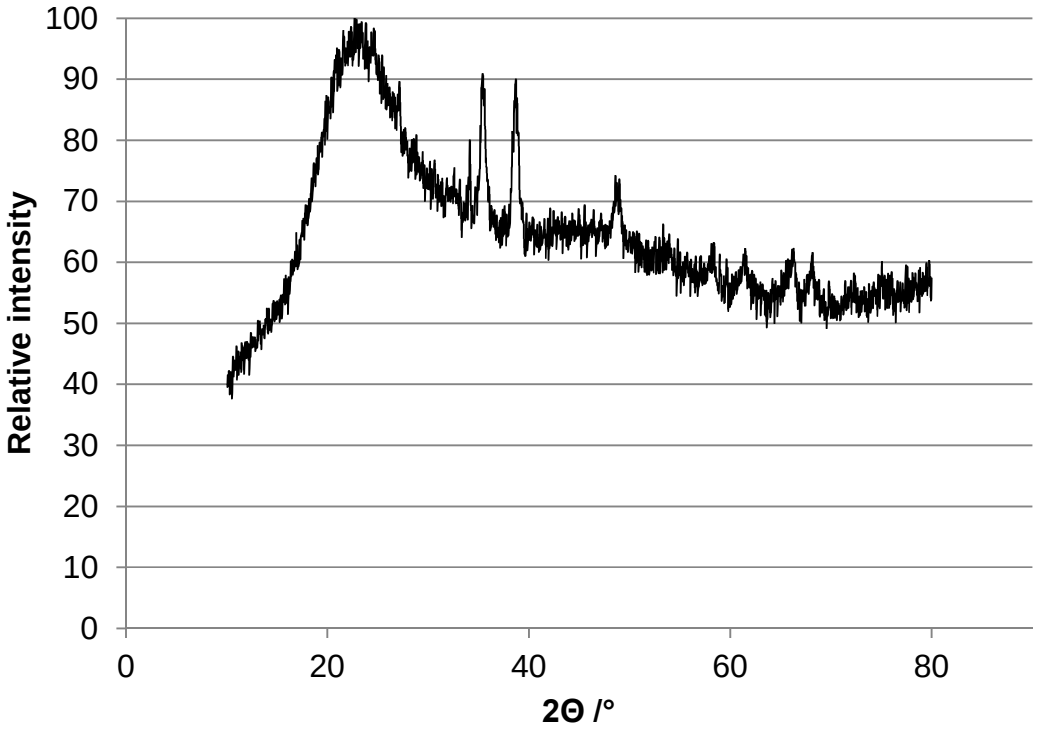

Figure 4-11 X-ray diffraction pattern of 'Double base II' sample C

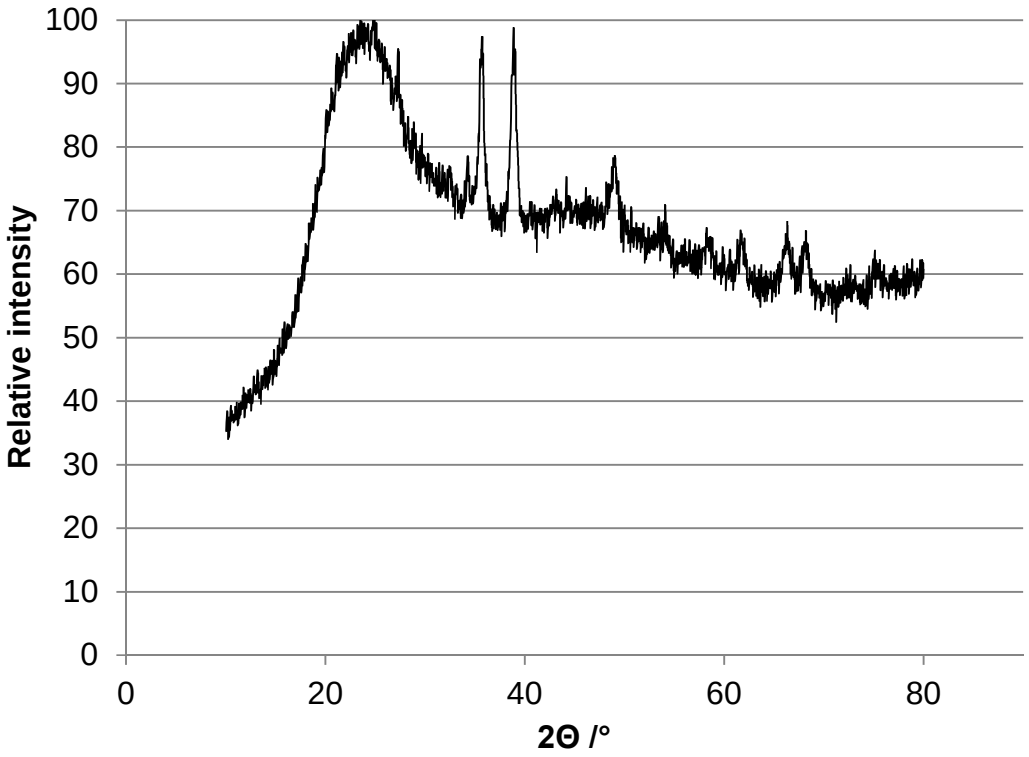

Figure 4-12 X-ray diffraction pattern of 'Double base II' sample H

4.4 Conclusion

This research investigated how each production process affects the physical and chemical properties of the propellant.

The density of the propellant remained at a constant 1.6 gcm^{-3}(±0.01). This was measured using a gas Pycnometery method, which calculates density based on pressure measurements, giving an accurate measure of density.

X-ray measurements could not quantify any change in crystalline structure, but indicated some variation through production. A further investigation should include samples of the nitrocellulose taken from before the incorporation stage and more detailed analysis of samples taken from the production processes. This may enable a quantification of how the crystal structure present in the fibrils of cellulose is changed, this would allow a more complete understanding of the chemical changes occurring to the cellulose polymer. It was noted that the CuO constituent of the propellant which showed clearly in the diffraction patterns measured, could be used as an internal standard to aid in the quantification of the peaks.

The Mw of the nitrocellulose reduced throughout the production processing. This was not surprising as the high temperatures and pressures involved in the extrusion and rolling stages of propellant production provide energy to break bonds. The reduction in the Mw was considered to be likely due to the process of denitration, which is a known ageing process in nitrocellulose. This is a very important finding as a reduction in nitrogen content of nitrocellulose reduces the energy content and increases the intermolecular bonding between polymer chains (26) (14). The increase in intermolecular bonding has the effect of increasing the attractive forces holding polymer chains in place, which increases the energy required for chain movements, changing the thermal properties of the propellant. The change in the thermal and energetic properties

of the propellant are a very serious consideration as they may influence the service life of the propellant.

Thermal analysis showed that the rework and rolling stages are crucial to the homogenisation of the propellant, indicating that this is not completed during the incorporation phase. It is likely that the complete homogenisation can only be achieved once the majority of the crystal structure has been broken down, as the additives such as stabilisers and ballistic modifiers are unlikely to penetrate crystalline structure. This attribution may be confirmable from further work analysing >5mg samples with HPLC. This is an important finding as the energetic content of the propellant is partially due to the nitroglycerine concentration. Ensuring that nitroglycerine is well distributed within the propellant is crucial for achieving the desired burn rate. It would be desirable to continue research to consider how influential the rolling and reworking stages are for distributing other propellant constituents, such as ballistic modifiers and stabilisers. As the distribution of stabilisers within the propellant composition will have a profound influence on the long term stability of the propellant.

5 RESULTS: THE EFFECT OF THE EXTRUSION PROCESS ON PROPELLANT

This work investigates the effect of the extrusion on the mechanical, thermal and polymeric of the nitrocellulose. Samples were analysed using Dynamic Mechanical Analysis (DMA), Micro hardness testing and Gel Permeation Chromatography (GPC). The thermal transition events that occur in an extruded double base propellant have also been investigated with differential scanning calorimetery (DSC) and DMA.

5.1 Introduction

During the extrusion process, the polymer chains are subjected to high thermal and mechanical stresses (5). The effect of repeated extrusion on the NC and the effects across the diameter of the extrusion have not been reported. However it has been reported in other polymers, that the forces and pressures of extrusion can cause chain scission and cross linking (34). In the previous chapter (chapter 4) reduction in Mw of the nitrocellulose was reported throughout the rolling and extrusion stages of the manufacture, this was attributed to the loss of nitrate groups from the nitrocellulose. It was considered that the process of extrusion on the nitrocellulose in propellant compositions should be studied further. The results of a further study could be used to develop and improve the manufacturing processes for propellants.

Polymers are often extruded at elevated temperatures, the cooling to ambient would occur at different rates throughout the propellant grain. It is possible that different areas of the propellant relax into different enthalpy states. One aim of this research is to investigate whether extruded propellants are homogeneous, or whether the process of extrusion affects the surface of the grain in a different way to the centre. Greater shear forces could occur at the edge of the grain, leading to chain scission and denitration. A second area of interest was to investigate how DMA correlates to DSC as a thermal tool, a thermal transition between -50°C and 0°C has been reported to occur in DBP (5) (36).

5.2 Experimental

Materials

The extruded ‘Double base I’ (Table 0-1) propellant, measuring ~72mm diameter with a star conduit Figure 5-1, was supplied by Chemring Energetics UK Ltd. with a nominally composition of 50% NC, 25% NG, 20% Triacetin and stabilized with Ethyl Centralite (EC). Standards were obtained from Sigma-Aldrich Ltd (Gillingham, Dorset, UK). NG was purchased from Qmx Laboratories (Halstead, Essex, UK). Acetonitrile was HPLC grade and obtained from Fisher Scientific (Loughborough, Leicestershire, UK). Tetrahydrofuran (THF) was HPLC grade stabilised with 100 ppm BHT and was obtained from Rathburn Chemical Ltd (Walkerburn, Scotland, UK). Milliput Super Fine White Epoxy Putty was obtained from Amazon.co.uk.

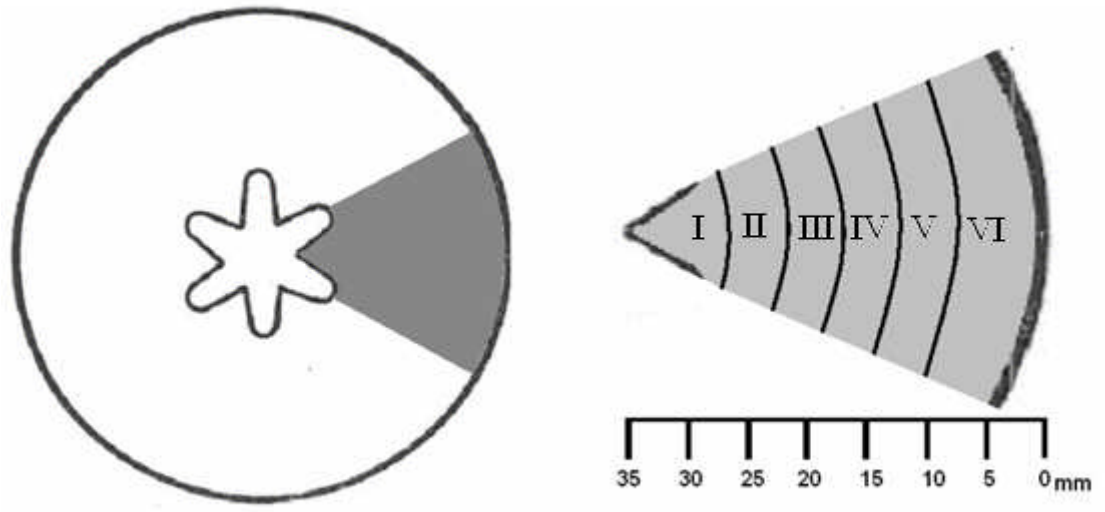

Figure 5-1 Propellant grain (Double Base I) with star conduit (left). The grey area (enlarged right) illustrated how samples I - VI relate to the propellant grain as a whole

5.3 Analytical techniques

5.3.1 High Performance Liquid Chromatography (HPLC) Analysis

Instrument.

As detailed in 4.2.1

Sample preparation.

A sample was taken from the bulk solution and filtered with a 0.2µm nylon syringe into a HPLC sample vial. The STANAG (stirring) method for stabiliser extraction was followed (5). Analysis was carried out in duplicate; the result for each is the average of two injections of 20µl. The EC and NG were measured by a UV photo diode array detector at a wavelength of 254nm. The Triacetin was analysed at a wavelength of 220nm.

5.3.2 Gel Permeation Chromatography (GPC)

As detailed in 4.2.2

5.3.3 Dynamic Mechanical Analysis (DMA)

Instrument. Measurements were performed on a Perkin Elmer DMA 8000 with a temperature scan from -100°C to +20 °C with a heating rate of 5°C per minute in a single cantilever bending geometry, the analysis were repeated to ensure that the sample wasn't damaged during analyse. Single Cantilever Bend geometry was selected because it can be used for a broad range of sample modulus values (14), the sample modulus falling well within the range for single cantilever bend.

Sample preparation. The samples for DMA analysis were prepared to 3x5x15mm ±0.25mm, using a CNC milling machine fitted with slot drills. The milling process carried out using a 3mm slot drill at: 1000rpm with a maximum cutting speed of 30mm/min and was air cooled.

5.3.4 Microhardness

Instrument. Measurements where performed on an Indentec HWDM-7. The analysis was carried out using a 10g mass to create the indentation. The indentation was measured manually through the microscope fitted to the indenter.

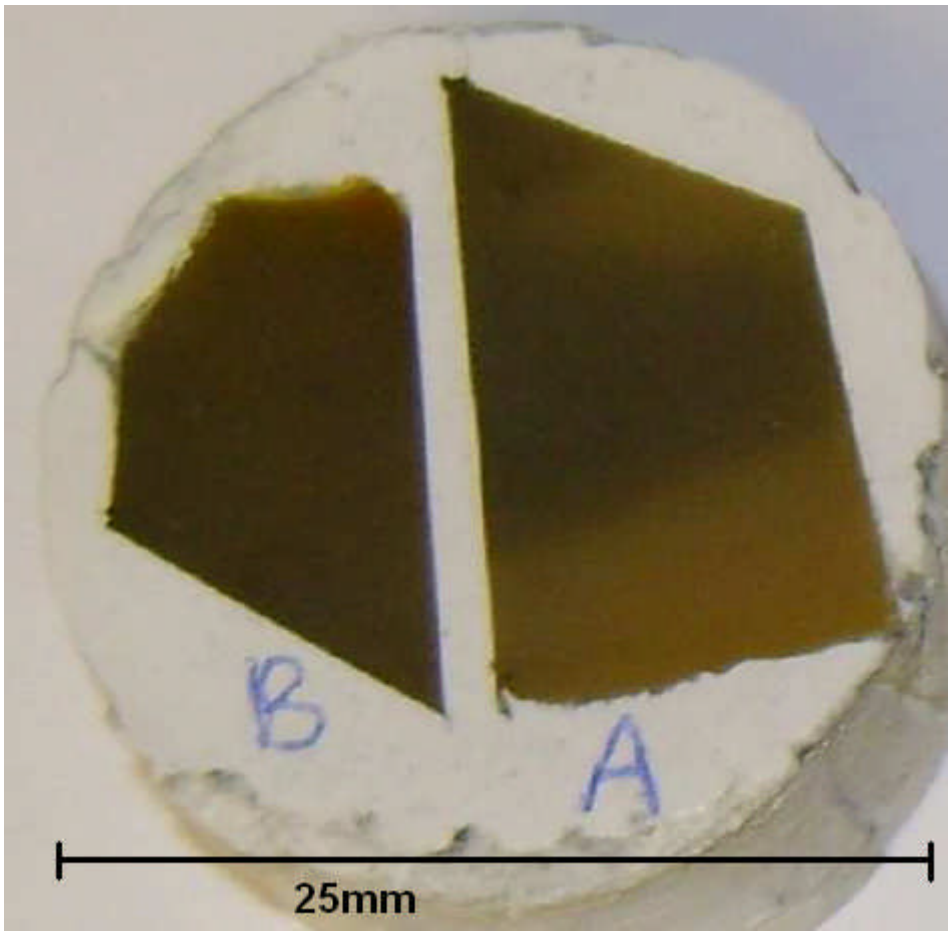

Figure 5-2 Two samples of EDB propellant mounted in epoxy putty for micro hardness testing

Sample preparation. A sample of the propellant ~5mm thick was mounted in epoxy putty (Figure 5-2). The surface was then polished, firstly with very fine sand paper, and secondly with a plastic disk grinding disk with a 4μm diamond solution to provide the abrasive surface.

5.3.5 Differential Scanning Calorimetery (DSC)

Instrument. Measurements where performed on a Mettler Toledo DSC 1 Star$_e$ System, Liquid N_2 cooled. Analysis between -100°C and +100°C, heating rates of 5,10 and 20°C/minute were used.

Sample preparation. Samples of 0.05g were weighed to an accuracy of 0.001mg and sealed in aluminium sample pans.

5.3.6 Optical microscope photographs

Instrument, Light Microscope, Polyvar Met with Polaroid DMC2 camera

5.4 Results

5.4.1 Stabiliser and plasticiser analysis (HPLC)

The concentration of Ethylcentralite remained constant within all samples. The results varied by 0.01% (Table 5-1). This result confirms that during the manufacture of the propellant, the mixture of constituents is entirely homogeneous. The concentration of the plasticizer (NG,Triacetin) also remained constant throughout the propellant grain Table 5-1, Figure 5-3. This result is important as NG and Triacetin effects both the mechanical properties and the energetic content of the rocket, variation in NG concentration could therefore dramatically alter the performance of the rocket.

Table 5-1 HPLC analysis of 'Double base I' propellant samples

Sample ('Double base 1 ')	Ethylcentralite %wt	Nitroglycerine %wt	Triacetin %wt
I	1.11	21.02	18.17
II	1.10	20.79	19.82
III	1.10	21.02	19.86
IV	1.09	20.89	17.78
V	1.10	20.95	19.17
VI	1.11	21.08	16.33

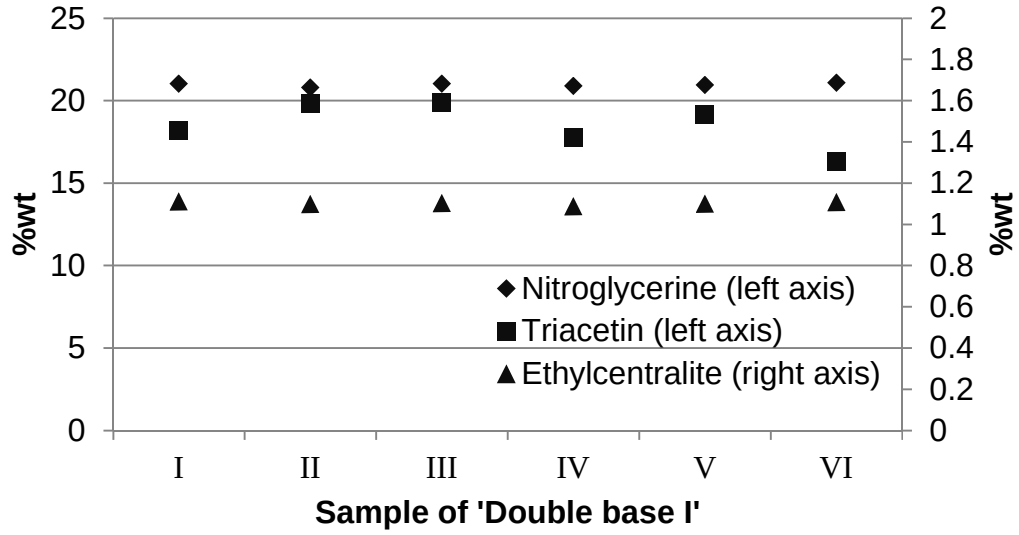

Figure 5-3 HPLC analysis of 'Double base I' propellant samples

5.4.2 Molecular mass distribution (GPC)

The Mw, Mn and Polydispersity measurements indicate no change between samples I, III, and VI. This result doesn't indicate whether there are changes occurring within the sample due to the extrusion process, simple that any changes affect the propellant equally across the grain.

Table 5-2 GPC analysis of 'Double base I' propellant samples

Sample	Mw	Std dev	Mn	Std dev	Polydispersity
I	86759	2284	424500	21189	4.89
III	86030	4722	445392	21637	5.18
VI	88265	4115	440694	28937	4.99

5.4.3 Micro hardness

Micro Hardness measurements were taken from the outside of the propellant grain to the conduit at the centre, at 2mm intervals. The results provide information about how the relative hardness changed.

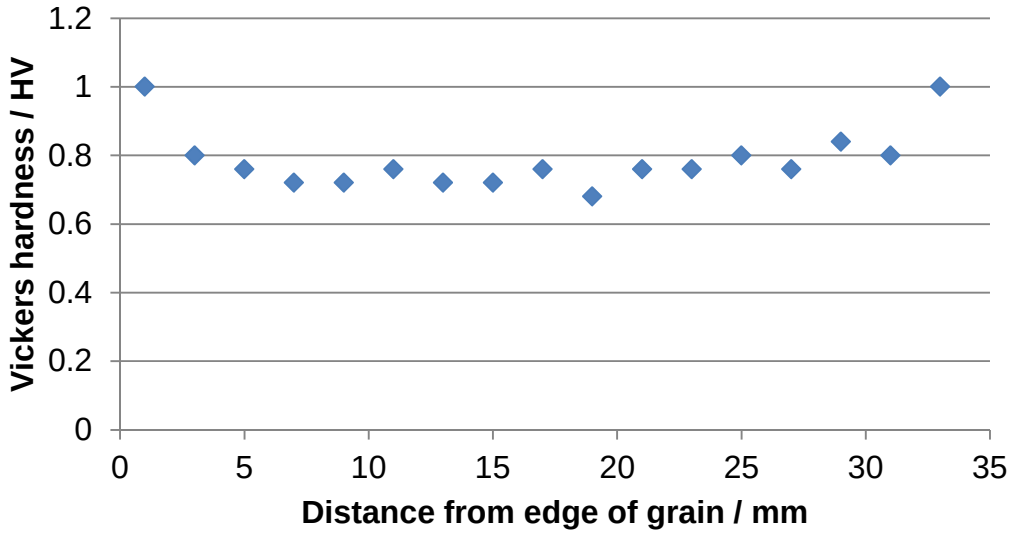

Figure 5-4 Micro hardness analysis of 'Double base I' propellant sample

The measured hardness of the propellant sample varied (Figure 5-4), at the outside and conduit surface the propellant sample was harder than in the centre. This increase in hardness at the surfaces only penetrated 3/4mm into the propellant sample. The variation is possibly due to: mounting of the sample, as the Milliput epoxy putty sets very hard, the measured hardness close to the edge on the grain could be caused by the epoxy putty supporting the propellant; or annealing process that grains are subjected to after extrusion. If it was possible to analyse un-mounted samples, measurements taken close to the surface would still be false as the material would behave unusually soft. The variation is shown in (Figure 5-4), which represents one of the three analyses that were carried out. The same trends were observed in all analysis. The variations in hardness between 5mm and 30mm are within the error associated with the instrument.

5.4.4 Dynamic mechanical properties (DMA)

The DMA analysed the mechanical properties as a function of temperature. The Tanδ curve represents the ratio of viscous to elastic material behaviour, there are peaks during thermal transitions.

The results from the tanδ curve show the same thermal transition in the region of -40 to 10°C, peaking at -8°C ±3, for each of the 6 samples Figure 5-5. The loss modulus curve indicates the transition is occurring at a lower temperature -17°C ±3 in each sample.

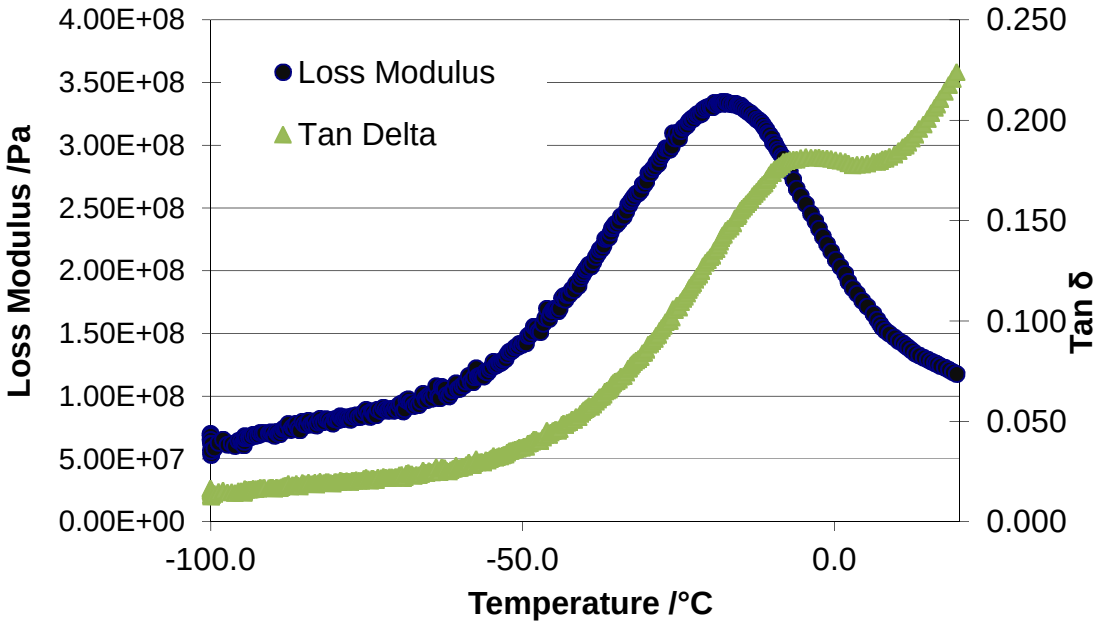

Figure 5-5 Dynamic mechanical analysis of propellant, ('Double base I')

5.4.5 Thermal transitions (DSC)

Table 5-3 DSC results for analysis of each sample ('Double base I') between -100 and +100°C using a heating rate of 20°C/minute

Sample	Transition onset temperature /°C	Transition midpoint /°C
I	-45.32	-33.91
II	-44.21	-34.56
III	-44.83	-35.13
IV	-45.2	-32.18
V	-44.6	-31.52
VI	-44.15	-34.94
Average	-44.72	-33.71

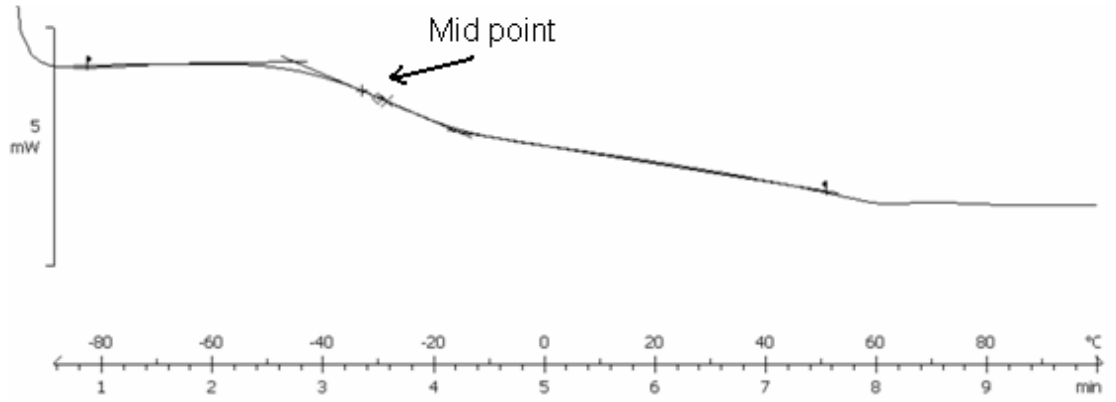

Figure 5-6 DSC analysis of sample II ('Double base I'). A thermal transition indicated by a step in the curve, the midpoint at -33.16°C

The DSC indicates a transition between ~- 45 and ~ -15°C in all samples, there was no difference measured between samples taken from different sections of the propellant grain. There is also an inflection in the DSC curve at approximately 60°C, it was not considered in this work, though it correlates approximately in temperature with transitions reported in literature (44).

5.5 Discussion

5.5.1 Analysis of the Effect of Extrusion across the Propellant Grain

The thermal transition at approximately -10°C observed in the DMA has been reported to be related to the concentration of NG (21) . It was expected therefore that the transition remained constant in all samples, considering that the HPLC confirmed that the concentration of NG was unchanged for all samples.

The micro hardness provided no information to indicate that the mechanical properties were changing across the grain, however a more sensitive instrument such as a nano-indentation machine may provide more precise and

useful data. Nano-indentation could be used to determine modulus values, which could be compared with DMA data.

The molecular mass distribution results indicated that there was no variation in Mw, Mn or polydispersity across the propellant grain. It is quite possible that changes do occur as a result of extrusion though in this case changes influenced the grain equally across its diameter. It is also possible that uneven degradation does occur however only in the outer 0.5mm, and was not detected in this analysis because the sample representing the surface was taken from the outer 5mm. A variation would then be masked by the quantity of bulk material included in the sample.
This result was consistent with the DMA results as the mechanical properties are known to be correlated to the Mw, Mn and polydispersity.

5.5.2 Thermal Analysis of EDB using DSC and DMA

The DMA results indicated a thermal transition occurring at sub ambient temperatures. The tanδ curve indicates the β transition is occurring within the region -40 to +10°C (Figure 5-5). The modulus curve indicates the thermal transition occurring between -50 and -10°C. It is known that the peak of the tanδ curve often represents a higher temperature than the transition measured in the modulus (45). Therefore data collected from the modulus curve is more likely to coincide with data collected in a DSC analysis. The frequency of the DMA will also have an impact upon the temperatures at which thermal transitions occur; higher frequencies increase the temperature at which thermal transitions occur, as discussed in chapter 3, measurements taken with DBP have shown an increase of 5°C between samples analysed at 1Hz and 10Hz (18). It is possible therefore that the temperatures measured in the DMA analysis will be higher than those collected by the DSC. To minimize this effect the data was collected at a low frequency of 1Hz. The DSC analysis shows that the gradient of the slope before and after the glass transition aren't exactly the same, this indicates that a second process is occurring, likely to be the onset of the α transition. We

had anticipated that this transition was associated with a minor change such as small areas of unprocessed crystalline NC (in the bulk) becoming amorphous, but the DMA indicates a large change in the modules which is inconsistent with such a potentially minor transitions as crystalline NC becoming amorphous. The small decrease in the tanδ before another increase supports this theory. The DMA data also shows that the β transition occurs at temperatures just below the α transition. The tanδ curve only dips slightly before increasing due to the α transition, just as had been reported in literature Figure 3-5. In this analysis temperatures high enough to analyse the α transition were not reached as it has been observed in previous analysis that that the sample softens significantly in the clamps triggering the ‘broken sample’ error in the DMA instrument.

It was very difficult to determine from the DMA which thermal event was the glass transition. The DSC analysis however indicates that the β transition was the glass transition as it has the step change in heat capacity that is typical of such a transition.

5.6 Conclusion

The present investigation did not indicate any inhomogeneity in the extruded propellant. This does not disprove the theory that more decomposition may occur at the edges of the grain in all cases. The propellant sample investigated was relatively soft as it contains ~45% plasticiser. If a propellant containing a lower plasticiser concentration was extruded, the forces required would be higher, as the propellant would be harder. In this case any difference between the decomposition that occurs at the surface and the centre would be more significant. The samples representing the surface were taken from the surface of the propellant to a depth of 5mm, it is possible that variations only occur within the first 1mm, and therefore the variations weren’t detected. Future work should investigate samples taken from across the grain of a propellant in narrower steps, this would allow a more accurate representation. Future work

should also use nano-indentation to study the mechanical properties as it will provide a more precise measure of material properties.

The thermal analysis using DMA and DSC provide complementary results. DMA analysis provides more information as it is more sensitive to thermal changes, however it is difficult to determine the glass transition from DMA as more than one thermal event may be occurring. The DSC analysis is very useful for determining glass transitions as there is a characteristic step in the DSC data. The DSC analysis can be carried out more quickly as the sample preparation is simpler, and uses a smaller quantity of sample.

6 RESULTS: APPLICATION OF DMA FOR ANALYSING NITROCELLULOSE BASED MATERIALS

6.1 Time temperature superposition

6.1.1 Introduction

Time temperature superposition (TTS) is based on the principal that the changes observed when altering the temperature are like those caused by a change in frequency. Data from frequency scans at a range of temperatures can be superimposed, generating a curve indicating the materials properties at frequencies outside the range of instrument measurement (15).

The diffusion of molecules in a polymer matrix, and the conformational changes of large sections of the polymer chain are slow. Unlike the movement of electrons which are nearly instantaneous (26). The time period over which observations are made, has an influence on the behaviour of the material observed. This is as the molecules require time to move.

In terms of DMA, the time scale is the frequency, which is measured in reciprocal time. At high frequency the time period for molecular motion to occur is small and the molecular motion observed will be low. At a lower frequency there is more time for molecular motion to occur, so more motion will be observed. As temperature is linked to the energy in the system, which is related to the rate of molecular motions, the temperature of measurements will influence the result. At a high temperature the rate of molecular motion is higher than at low temperature (15) (26).

In a glass state the molecular motions are slow, the changes observed will be lower than those observed in a rubbery state, where molecular motions are high, for analysis carried out at the same frequency. An analysis carried out at a lower frequency (longer time period) will observe a more significant change. When the sample is at a higher temperature, there is more energy in the system. As a result the molecular motions can take place more rapidly. This

means that during the same time period (frequency) more changes would be observed (26).

The glass transition can be viewed to occur at a temperature when the time required for molecular movement is equal to the time period of the measurement (26).

A time temperature superposition can be carried out on a series of isothermal frequency scans, at a range of temperatures, to produce a master curve. The amount of shift (shift factor) can be calculated using the Williams-Landel-Ferry (WLF) equation. The WLF is an empirical equation, the three constants are unique to the polymer studied.

$$-\log(a_T) = \frac{C_1(T - T_0)}{C_2 + (T - T_0)} \quad \textbf{(6-1)}$$

T = Temperature

T_0 = A constant and the reference temperature.

C_1,C_2 = Constants

6.1.2 Time temperature superposition. DMA Analysis

Instrument. Isothermal frequency scans between 0.01-35 Hz, at temperatures between -50 to 50°C in 10°C intervals were carried out. Tests were carried out in a single cantilever bending geometry.

A TTS master curve with a reference temperature of 0°C, was generated by the instrument software using the WLF equation.

Sample preparation. As described in 4.2.4 using ’Double base II’ (Table 0-1) samples

6.1.3 Time Temperature superposition results

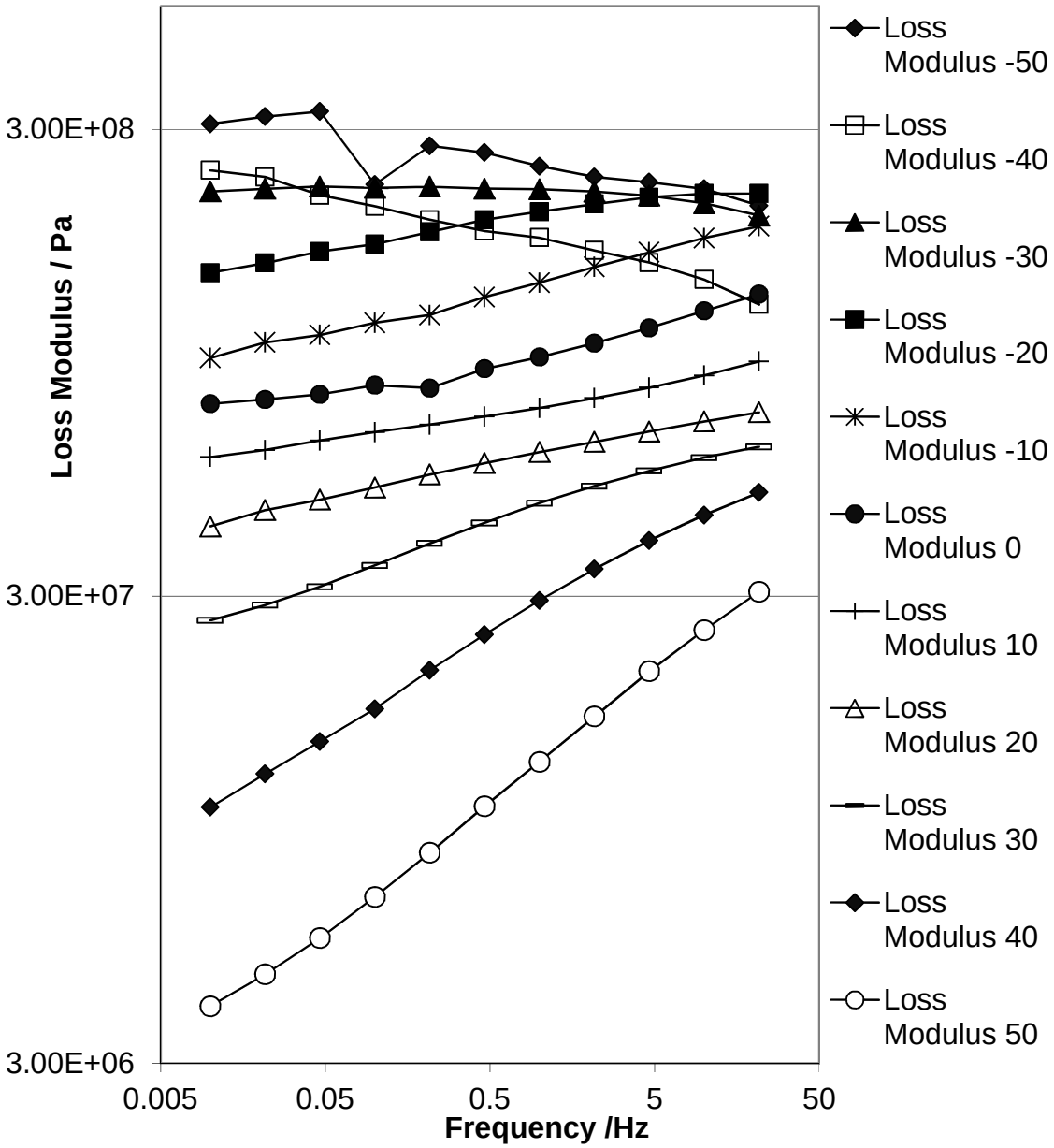

Figure 6-1 TTS before shift. Loss modulus data aged at 60°C 'Double Base II' analysis 1

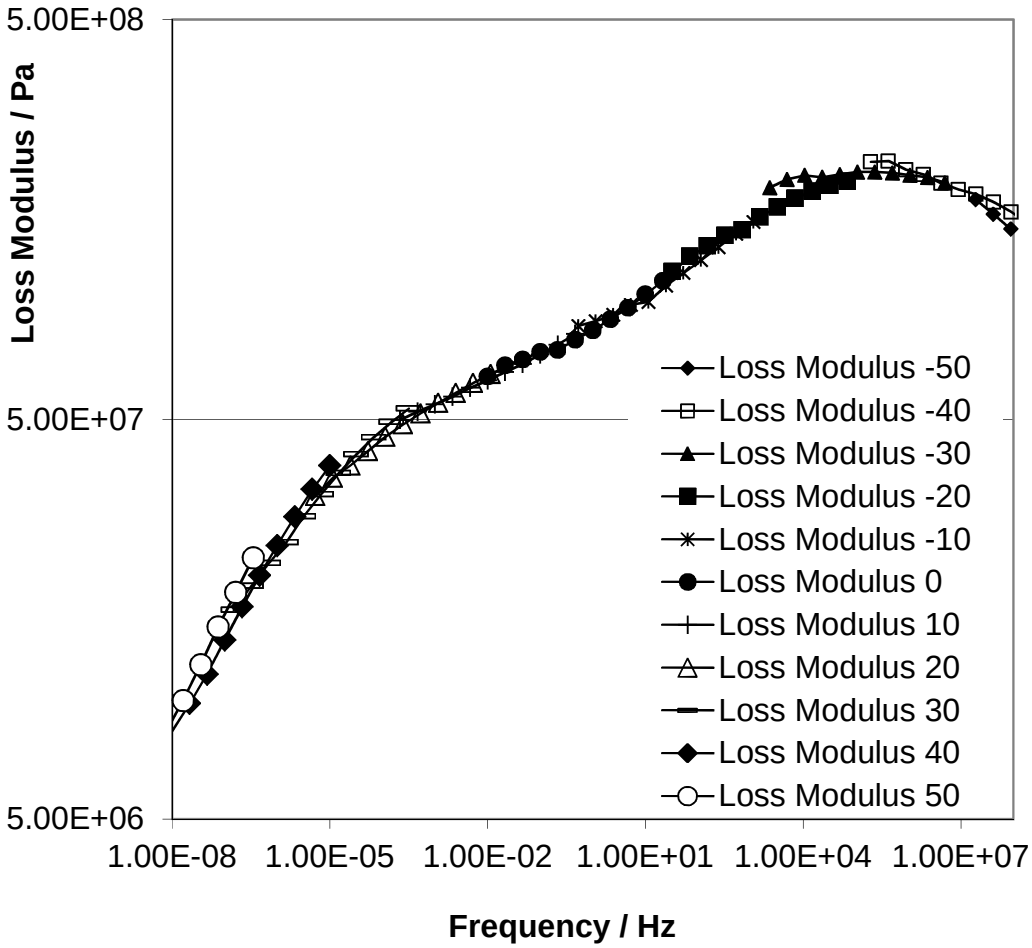

Figure 6-2 TTS loss modulus data aged at 60°C 'Double Base II' analysis 1

The propellant was found to superposition well Figure 6-1,Figure 6-2, despite being a complex material containing plasticisers and other additives including crystalline CuO, full results are detailed in (Appendix E).

The data was shifted by computer software using the WLF equation (10-15). The constants calculated for the un-aged and aged samples are shown in Table 10-1. There are differences between the constant calculated for the aged and un-aged samples, as only one measurement of each sample was made it is not possible to consider whether the differences indicate a difference between samples.

It is concluded that the material does superposition well, that this technique could be used to investigate the mechanical properties at frequencies higher than the operating range of the DMA instrument. This enables an estimation of how the propellant would react when subjected to high frequency loads in service.

6.2 Creep analysis

6.2.1 Introduction

A creep experiment involves a fixed load being applied to a sample nearly instantaneously. The subsequent strain incurred by the sample is monitored until the material reaches equilibrium.

This type of mechanical testing can be employed to investigate a number of material types, such as; metals, ceramics and polymers (46). When investigating polymeric materials which exhibit viscoelastic behaviour, such as those used in this study, it is crucial to determine the limits of the viscoelastic region.

The limit of the linear viscoelastic region for a given sample can be determined experimentally. A number of creep experiments can be carried out using a range of forces. The linear viscoelastic region is the region where the relationship between stress and strain in the equilibrium region is linear.

In Figure 6-3 the strain incurred by three samples of the same material as a function of time is plotted. Each sample was subjected to a different force. The data shows that the material is within its linear viscoelastic region up to a force of 2N (stress 2.433E+06 Pa), as the % strain incurred is linearly proportional to the force. The samples linear viscoelastic region may extend beyond, as these experiments didn’t indicate that the viscoelastic limit had been reached.

Viscoelastic material behaviour is complex, it contains elements which act like springs trying to return to its original shape (elastic) and elements which act like dashpots which resist change in displacement (viscous). When modelling the material response to creep experiments, a combination of spring and dashpot elements can be used. A number of models have been proposed:

The Maxwell model is composed from a spring and dashpot in series. This model describes a strain curve with sharply edged corners, equation (10-15). As the sample is stressed it incurs an instantaneous strain, as the elastic (spring) section extends, it then strains infinitely at a constant rate as the viscous (dashpot) component reacts.

The Voigt model is composed from a spring and dashpot in parallel. This model describes a continually curved creep response until maximum extension equation (10-16). The strain rate is initially high as the dashpot moves, it then gradually decreased as the spring extends to its limit progressively opposition further displacement.

These models both depict certain aspects of creep behaviour: The Maxwell model depicts the instantaneous response seen in many materials. The Voigt model depicts the curved response caused by dashpot dampening the springs instant response, this describes the time dependent response of the material.

A more complex model is required to satisfactorily describe the response seen in real creep experiments. The ‘Four element model equation(10-17) is a combination of the two previous models, it contains a number of key features which make it more useful; the instantaneous response to an applied force, the curved time dependent response and continual change increase in strain.

A plot of strain versus time allows identification of viscous, elastic and viscoelastic components of the four element model.

In Figure 6-4 the relationship between stress strain and time for a sample of double base propellant can be seen. Comparison with the four element model is valid as the material is within its linear viscoelastic region.

When a stress is applied there is an instantaneous response in the material. These is the independent elastic E1 of the material. The value can be calculated by dividing the stress by the strain. This can be qualitatively described as the spring extending and locking into its extended state immediately. This is analogous with the Young's modulus plot.

Once the E1 response has occurred the independent viscous and viscoelastic responses take place.

The independent viscous response will lead the material to start deforming at constant rate, continually and infinitely. η1 can be calculated by dividing stress by strain rate in the equilibrium region of the strain curve.

The viscoelastic region exists between the initial elastic and equilibrium viscous regions. In this region the Voigt component of the four element model and the independent viscous element are occurring.

The strain at any time in the four element model can be calculated using equation (10-17). The term η2/E2 is termed the retardation time of the polymer (τ), it is the time taken for a 63.21% deformation in the Voigt element. The retardation time is linked to the molecular weight. The principal limitation of the four element model is that it includes one 'retardation time' which is a limitation as polymeric materials are composed from a distribution of molecular weights. It is for this reason, and the distribution of molecular weight was changing throughout the ageing of samples, that the η2 and E2 were not investigated.

It is useful to understand how each aspect of the chemical composition of the material contributed to the materials response to creep testing.

I think that when a force is applied instantly the chain backbone stretches and the intermolecular hydrogen bonds between nitrate and hydroxyl groups stretch like springs. The chain twists, the steric hindrance C-O bond in the chain backbone is high and the backbone but doesn't easily rotate through the eclipsed state. This is the instantaneous E1 response which will be influenced by; molecular weight, intermolecular bonding, chain substituents which in turn

influence the activation energy of bond rotation. If the force is removed the material will return to its original shape.

If the applied force is maintained the breakage of intermolecular bonds between nitrates and hydroxyls, will allow movement of chain sections into free volume, in turn allowing less hindered bond rotation, as bulky substituents on the chain such as nitrates and hydroxyls can move more freely. This causes reversible deformation.

The two processes discussed are the two elements of the Maxwell model. An intermediate region exists between these two regions which described the damped elastic extension described by the Voigt model, which occurs where an elastic extension of the polymer is damped by the time dependent movements within the composition. Together these regions describe the 4 element model.

I suspect that the independent E1 elastic component and η1 viscous component of the materials behaviour is linked to the intermolecular bonding present between chains. If more intermolecular bonding is present then this would resist chain movement, preventing chains slipping past one another. As the material is flexed the bonds stretch and when the force is removed the bonds pull the material back to its original shape resulting in higher E1. When there is less intermolecular bonding, the chains are more able to slip past one another, increasing the η1 behaviour.

I suspect that as temperature is increased and there is more energy to overcome the cohesive forces of the intermolecular bonding, the E1 component will reduce and the η1 will increase.

The plasticiser will reduce the intermolecular bonding within the composition and lead to a reduced E1 and increased η1.

The chemical changes which occur with age will influence the creep response. I suspect that chain scission will lead to a reduced E1 and increased η1, as shorter chains will move more easily as they are constrained by fewer

intermolecular bonds. Denitration of the nitrocellulose is likely to increase hydrogen bonding and therefore E1.

The maximum extension of the Maxwell component of the material response is likely to be linked to crosslinking, however the time taken for the extension could be reduced by factors which reduce η1. As the propellant material is not known to crosslink throughout ageing, it is thought that this component will not change substantially.

6.2.2 Determining experimental conditions

The linear viscoelastic region of the propellant under the static loads experienced during creep testing was first determined.

A series of creep analysis between -50 and 50°C were carried out using at 2.0N. A plot of the strain incurred over a period of 100 minutes for the analysis carried out at 50°C, is shown in Figure 6-3. A plot of the strain incurred during the analysis at -50,0°C in shown in Figure 10-16, Figure 10-17.

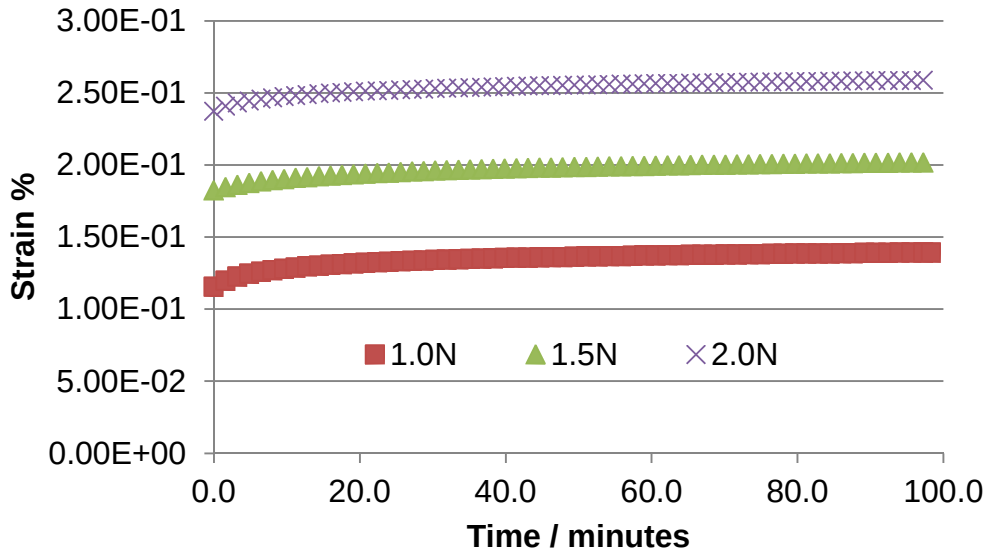

Figure 6-3 A series of creep experiments carried out at a range of forces at 50°C ('Double base II')

The strain incurred by the sample is linearly correlated to the force applied in all cases. This indicated that the propellant is within its linear viscoelastic region at all loads up to 2N. Samples analysed at 4N provided inconsistent results, often triggering the ‘broken sample detector in the instrument. The samples didn’t appear to be visible broken however could be slipping in the clamps. If the clamps are tightened further, visible distortion of the propellant occurs. It is for this reason that forces greater than 2N were not tested. Further creep tests were completed at 2N as this is the highest load that is known to provide reliable results, and it is within the linear viscoelastic region. Using the highest force allows the greatest accuracy in measurement as there are larger displacements incurred to measure.

6.2.3 Creep analysis of propellant. DMA Analysis

Instrument. Perkin Elmer DMA 8000.

Propellant samples ‘Double base II’ (Table 0-1), both aged and unaged were analysed between -50 and 50°C, at 10°C intervals for 100 minutes at each temperature, using a 2N load.

Sample Preparation. As detailed 4.2.4

6.2.4 Creep analysis of propellant. Results

The results of the analysis are displayed in Figure 6-4, Figure 10-18, Figure 10-19, 10E.2 Figure 10-20 and Figure 10-21.

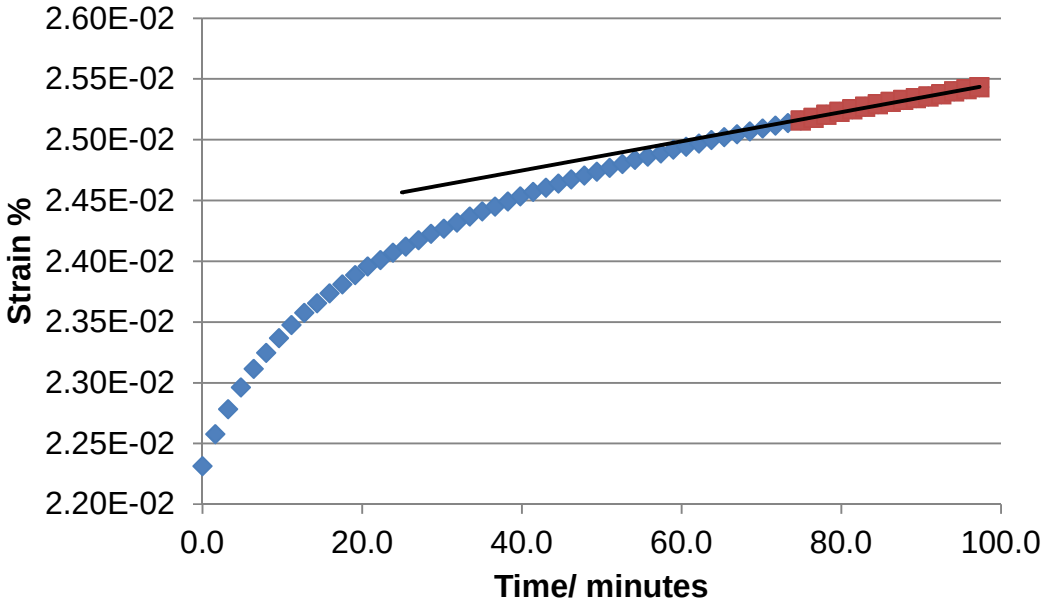

Figure 6-4 Creep analysis of unaged propellant at 0°C ('Double base II')

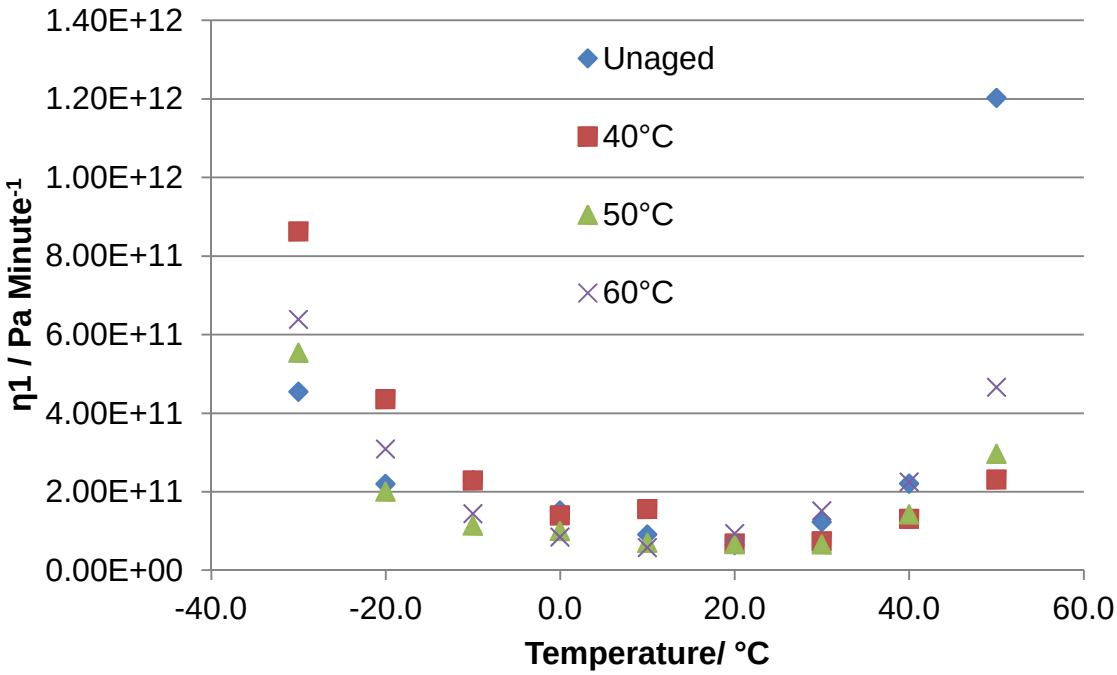

Figure 6-5 η1 values measured over a range of temperatures ('Double base II')

The η1 value for both aged and unaged propellant samples at a range of temperatures are shown in Table 10-2 and Figure 6-5. The lowest values correspond to least resistance to movement to flow.

6.3 Creep test discussion

The η1 viscous response was related to the temperature of the experiment. The lowest η1 values measured in the creep testing occurred at around 10 to 30°C, correspond with a peak of the loss modulus measured using a temperature scan experiment (Figure 4-9).

This result indicted that within 10 to 30°C this temperature range, the propellant creeps the most. More analysis of this sort could be used to determine the creep in a propellant grain occurring under its own weight. This is interesting to consider how the shape of a propellant grain could change. It is possible that performance could change due to this factor.

The η1 viscous response component of the creep analysis did not significantly change as a result of the ageing program. The ageing program simulated up to 8 years of ageing at 25°C. It is likely that if samples were aged further they would experience a change as denitration and change scission take a more significant, and measurable effect.

I would predict that the increased intermolecular bonding observed after denitration would increase the viscous components as it would further restrict the ability of chains to move past one another, restricting movement and reducing creep.

I predict that the effect of chain scission would have a broadly opposite effect to denitration, shorter chains would be less restricted, and would move past one another more easily.

As these two processes I believe have an opposite effect, it is not surprising that there are no significant changes observed. It is likely that their influences

are not exactly opposite and after a more significant ageing changed could be observed.

6.4 Conclusions

Time temperature superposition of a series of propellant frequency scan data was carried out. The frequency scan data superpositioned well, indicating that this technique can be used for propellant analysis. There wasn't time in this research to carry out a series of replicates, which would be necessary to ensure reliability. The application of time temperature superposition to propellant data would allow prediction of the material properties at frequencies higher than analysable in the DMA. It is advised that future work in this area start by considering the real world application of a propellant, and an investigation of the loads and forces to which is subjected.

Creep testing allows investigation of the tendency of the sample to continually deform. This enables determination of how the shape of a propellant grain will change due to the forces of gravity at any specific temperature. As the geometry of a propellant grain is fundamental to its function, investigating whether this may change during storage is of interest.

The propellant incurs the most significant η1 creep over the temperature range 10 to 30°C.

In the experimentation here, changes between aged an un-

aged samples in the η1 were not observed. If a more significant ageing regime was undertaken then the chain scission and denitration would likely influence the movement of polymer chains and in turn the creep properties.

7 RESULTS: AGEING TRIAL OF EXTRUDED DOUBLE BASE PROPELLANT

An accelerated thermal ageing trial simulating up to 8 years of ageing at 25°C was carried out to evaluate the storage characteristics. Reductions in: stabiliser concentration, number average molecular weight, weight average molecular weight and polydispersity compared with un-aged samples were observed. The glass transition temperature measured using differential scanning calorimetery decreased by ~3°C. The decrease was attributed to the initial denitration reducing the energy of bond rotation and shortening the polymer chains, both factors reducing the energy required for movement. Modulus values determined from dynamic mechanical analysis temperature scanning experiments, did not detect significant variation between un-aged and aged samples. Though it was considered that variations would be likely if a more extensive ageing program was completed.

7.1 Introduction

Double base propellants are known to degrade over time, eventually reaching a point where they are not fit for purpose. The aim of this chapter is to evaluate the way in which a number of analytical techniques can be employed to investigate the decomposition. When determining which techniques are most appropriate to use, it is important to understand how decomposition of the propellant might lead to the propellant failing. There are a number of possible failure modes.

Denitration of the nitrocellulose is known to occur (47). This reduces the energy content of a propellant composition, which may lead to loss of velocity and range of the projectile. In the case of sniper ammunition this may be particularly important as it is desirable to minimise variation in performance of rounds, so that the greatest accuracy can be achieved. A more significant variation may be acceptable in other ammunition. A variation would be considered ‘significant’ if it compromised the propellants ability to perform its intended application.

Stabilisers are included to react with the decomposition products of the thermolysis and hydrolysis reactions, preventing autocatalytic decomposition (Chapter 1.3.2). The concentration of stabilisers can be a safe storage life limiting factor (5).

Chain scission is known to occur in nitrocellulose, this is the breakage of the bonds between monomer units. It could have an influence on the mechanical strength and thermal properties of the material. The mechanical properties of a propellant are critical to its application. When a rocket is ignited the pressure builds up and acceleration causes extremely high stresses on the propellant. The pressure exerted upon gun and rocket propellants varies, typically for a gun propellant 1GPa and for rocket a pressure of 1-10MPa (48). As a result of the sudden mechanical stress the propellant grain could crack. The burning surface area would increase and the rate of burning would increase, leading to an increase in pressure. This cycle of increasing pressure could lead to a catastrophic failure of the rocket.

The Thermal properties of a propellant may change as a result of the denitration and chain scission reactions. At low temperatures the propellant could pass below its glass transition and become stiffer and therefore more likely to crack. At higher temperatures the propellant may become too soft and not retain its shape. The mechanical properties, and glass transition temperatures can change over the life of the propellant, reaching a point where the propellant is unsuitable for use. The changes that can occur have been reported in chapter 3.9, though this chapter concluded that more research was required to fully understand the nature of changes that occur.

7.2 Experimental

7.2.1 Propellant samples and accelerated ageing program

An accelerated thermal ageing program was carried out to simulate the effect of years of storage. The chemical and physical changes that occur over time were investigated.

Propellant was an extruded double base containing ~50% nitroglycerine and stabilised by 2-NDPA ‘Double base II’ Table 0-1.

In preparation for accelerated thermal ageing. Extruded cylindrical blocks of propellant material (35mm diameter, 30mm long) were treated in a humidity cabinet at 25°C and 65 % relative humidity for 48 hours. After which samples were immediately sealed into polymer lined foil bags. This is in accordance with AOP 48 ed2 (5).

The propellant samples were subjected to an ageing program at elevated temperature to simulate years at 25°C. Details of the ageing program are summarised in Table 7-1 and fully detailed in Table 10-5.

Table 7-1 Ageing program of propellant summary. Simulated ageing times were based on Arrhenius parameters stated in AOP 48 ed2 (5) ‘Double base II’.

Sample name	Ageing temperature/ °C	Duration/ days	Total simulated ageing/ days
Unaged	N/A	N/A	N/A
40a	40	90	580
40b	40	180	1160
40c	40	240	1548
40d	40	333	2148
50a	50	41	801
50b	50	70	1370
50c	50	88	1723
50d	50	101	1957
60a	60	16	937
60b	60	24	1406
60c	60	44	2579
60d	60	50	2931

7.3 Analytical techniques

7.3.1 DMA analysis

Instrument. Perkin Elmer DMA 8000. Temperature scan experiments were performed between -75 and 75°C at a heating rate of 2°C/minute, with a 10 minute isothermal soak at -75°C. Analysis took place in single cantilever bending test geometry at 1N force. Samples were clamped in place using a torque drive at 6mNm. Tests were carried out in duplicate.

Sample preparation. As detailed in 4.2.4.

7.3.2 HPLC analysis

As detailed in 4.2.1

7.3.3 GPC analysis

As detailed in 4.2.2

7.3.4 DSC analysis

Instrument. Mettler Toledo DSC 1 Stare System, Liquid N_2 cooled. Samples were analysed between -100°C and +100°C, heating rates of 10°C/minute were used. Samples were cut using a scalpel from the bulk, ensuring a flat surface so good thermal contact is made with the sample pan.

Sample preparation. Samples of approximately 20mg (±0.1mg) and sealed in aluminium sample pans.

7.4 Results

7.4.1 Dynamic mechanical properties (DMA)

A typical temperature scan result for propellant is shown in Figure 7-1. As the loss modulus curve is a peak with a shoulder, it is likely that two events are occurring. The linear combination of two Gaussian distribution method for de-

convolution described in 2.2, was used to determine the thermal transition temperatures.

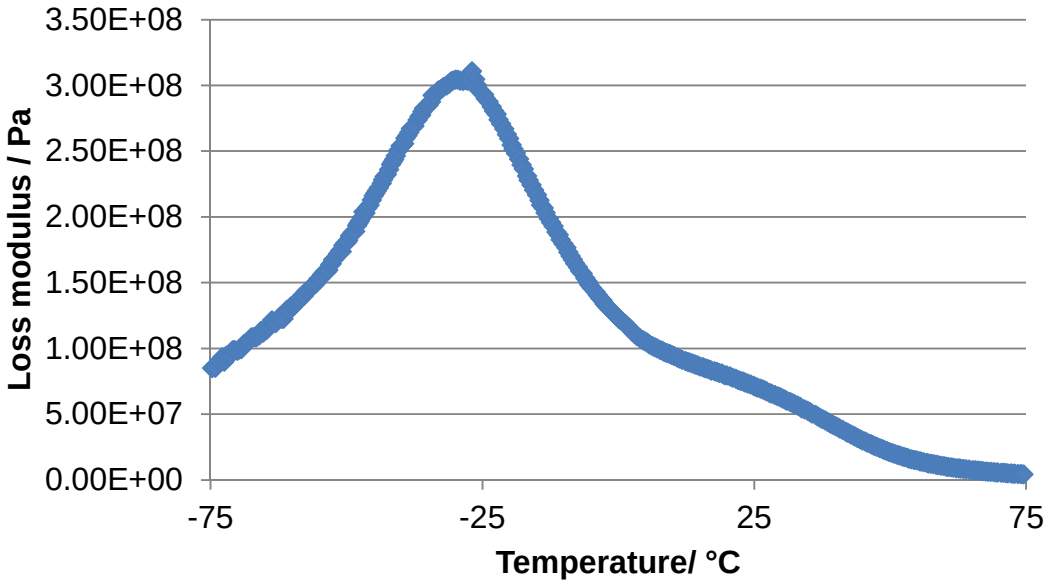

Figure 7-1 DMA loss modulus result of the sample ('Double base II') aged at 40°C for 90 days, simulating 580 days of age. Measured at 1Hz

There was no observed increase or decrease in the transition temperatures detected using this method. The full results are given in Table 7-2.

Table 7-2 Thermal transitions observed in the DMA loss modulus at 1Hz in aged and un-aged propellant samples ('Double base II')

Temperature/ °C	Ageing duration/ days	Simulated ageing duration/ days	T_β	T_α
un-aged	0	0	-28.11	16.84
40a	90	580	-31.10	15.82
40b	180	1160	-29.52	15.45
40c	240	1548	-29.20	16.60
40d	333	2148	-30.61	12.85
60a	16	937	-23.80	21.19
60b	24	1406	-28.32	18.30
60c	44	2579	-29.96	14.00
60d	50	2931	-21.21	23.85

The Gaussian deconvolution method used, uses the whole data set when determining a curve of best fit. It is therefore possible that fluctuations in data at the extremes of the data set influence the peak determination, this explains the fluctuation observed between repeats. This effect was minimised by excluding data below -50°C from the curve fitting. However applying exclusion rules and other limitations on Matlab's curve fitting introduces the exact operator bias and inconsistency that this method was conceived to eliminate.

There is no trend in change of complex modulus values measured at -50, 0 or 50°C over the course of the ageing program. The values are given in Table 7-3. The comparatively broad fluctuation observed in the measurements at -50°C is likely due to very large changes in complex modulus associated with the α transition, which occurs in this region over a temperature range which extends to below -50°C.

Table 7-3 Complex modulus values of propellant samples ('Double base II') after accelerated thermal ageing at 40°C. Complex modulus values measured at 1Hz at -50,0,50°C / Pa

Sample	Age /days	Simulated age/days	-50°C	0°C	50°C
Un-aged	0	0	3.53E+09	8.36E+08	4.37E+07
40a	90	580	3.50E+09	8.22E+08	7.00E+07
40b	180	1160	3.14E+09	8.36E+08	7.93E+07
40c	240	1548	3.30E+09	8.21E+08	7.34E+07
40d	333	2148	3.57E+09	9.56E+08	8.66E+07

7.4.2 Stabiliser analysis (HPLC)

The stabiliser concentration in the propellant samples decreased throughout the accelerated thermal ageing, Table 7-4. The rate of stabiliser consumption was higher at higher temperatures. The consumption of stabiliser is linked to the denitration of the nitrocellulose. The stabiliser consumption measured here was used to determine why thermal transition temperatures measured using DSC decreased.

Table 7-4 Stabiliser consumption throughout the accelerated thermal ageing of the propellant samples ('Double base II')

Sample and ageing temperature/ °C	Ageing time/ days	Average stabiliser concentration	2x Standard deviation
Un-aged	0	2	0.03
40a	90	1.99	0.04
40b	180	1.95	0.03
40c	240	1.92	0
40d	333	1.88	0.02
50a	41	1.94	0
50b	70	1.87	0.02
50c	88	1.84	0.01
50d	101	1.8	0.01
60a	16	1.83	0.03
60b	24	1.71	0.07
60c	44	1.53	0.03
60d	50	1.55	0

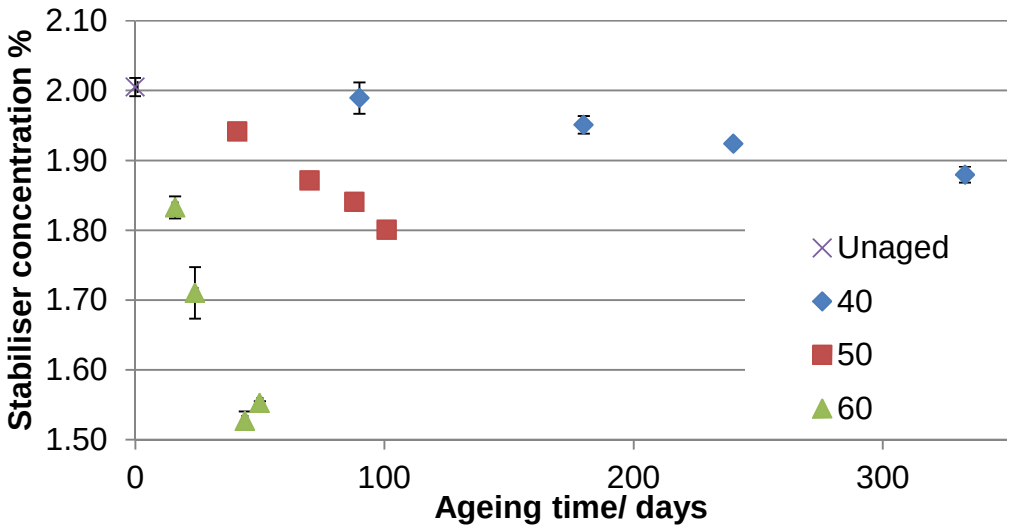

Figure 7-2 Average stabiliser depletion during accelerated thermal ageing. Error bar shows 2x standard deviation ('Double base II')

7.4.3 GPC analysis results

The weight average molecular weight, number average molecular weight and the polydispersity decreased throughout the ageing program. The data is shown in Table 7-6.

Calculation of the scission factor (S) equation (8-1) was used in section 4.3.1 to evaluate whether chain scission has occurred. Scission factors were calculated for the decreases in number average molecular weight that occurred during the accelerated thermal ageing at each temperature. The values are shown in Table 7-5

Table 7-5 Chain scission factors for aged samples of propellant ('Double base II')

Ageing temperature/ °C	Ageing time/ days	Scission factor (S)
40	333	1.25
50	101	1.27
60	50	1.11

The chain scission factors indicate the average number of chain scissions per molecule, in this case slightly greater than 1 in each sample. A value of 5 or higher would be considered a strong indicator that chain scission is occurring (43). It is concluded that chain scission has not been significant in these cases.

Denitration is known to occur in nitrocellulose (2), the observed consumption of stabiliser during the course of the accelerated thermal ageing undertaken in this study, indicates that denitration had occurred Table 7-4. Gel permeation chromatography separates polymer chains based on their hydrodynamic volume or size. Denitration of nitrocellulose will reduce the hydrodynamic volume as the alcohol groups which replace the nitrates are less bulky. This is the likely explanation for the decreases observed in the weight and number average molecular masses.

Table 7-6 GPC analysis of aged propellant ('Double base II'), indicating percentage change in molecular weight and polydispersity

Sample	Age/days	Mn %	Mw %	Polydispersity %
Un-aged	0	100	100	100
40a	90	89.22	87.91	98.53
40b	180	90.28	88.69	98.24
40c	240	88.91	86.97	97.81
40d	333	79.65	77.69	97.53
Un-aged	0	100	100	100
50a	41	94.96	94.86	99.9
50b	70	91	90.56	99.51
50c	88	91.43	90.27	98.73
50d	101	78.63	76.59	97.4
Un-aged	0	100	100	100
60a	16	90.83	84.87	93.43
60b	24	87.77	79.86	90.98
60c	44	90.63	83.62	92.26
60d	50	88.71	80.05	90.23

7.4.4 Thermal Transitions Analysis (DSC)

The DSC results indicate a decrease in the T_g of approximately 3°C over the course of the ageing program, Table 7-7, Figure 7-6. Denitration can influence the properties of the material in a more than one way:

Denitration leads to increased intermolecular bonding between chains, which would act to increase glass transition temperature, as polymer chains are held more tightly together and more energy is required for movement.

It is also likely that denitration of cellulose allows easier rotation of the chain backbone. As the comparatively bulky nitrate groups are replaced with hydroxyl groups Figure 7-3, Figure 7-4, Figure 7-5. I believe that this reduced the

activation energy of the rotation between trans and gauche rotational positions, and the free volume required for the rotation as the size of the molecule is reduced (Figure 7-3, Figure 7-4, Figure 7-5). This factor may reduce glass transition temperature, as chains become more flexible at lower temperature. This principal is discussed in 3.1.1, where polyethylene, polystyrene and poly(9-vinylcarbazole) are examples.

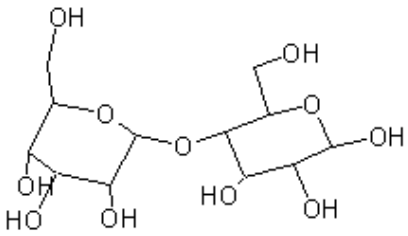

Figure 7-3 Two cellulose monomer units

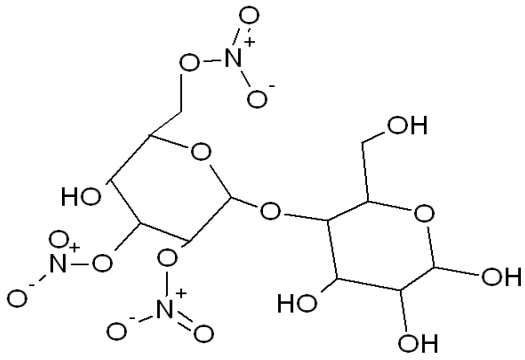

Figure 7-4 Two cellulose monomer units, one nitrated

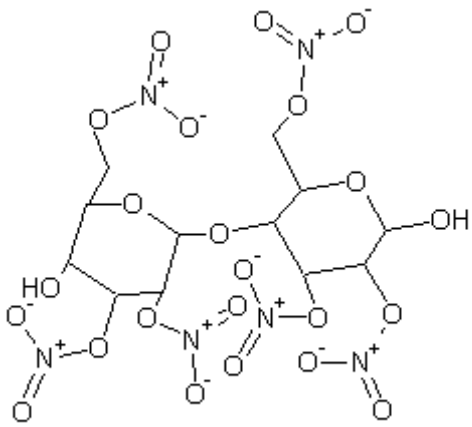

Figure 7-5 Two nitrocellulose monomer units

As chain scission reduces polymer length, the energy required for the chains to move will too decrease, and so the glass transition will be reduced. Though the scission factors calculated indicate that chain scission has not been significant, it may have still have a contributed to the observed reduction in T_g temperature.

It is known that the denitration of the cellulose is not a random process. The mono-nitrated units are first denitrated, then followed by the dinitrated and trinitrated (49). I believe that the first denitration which leave some denitrated cellulose units are the cause of the initial large shift in glass transition observed. As they allow greater rotation in the polymer backbone, due to the reduction in energy required for movement.

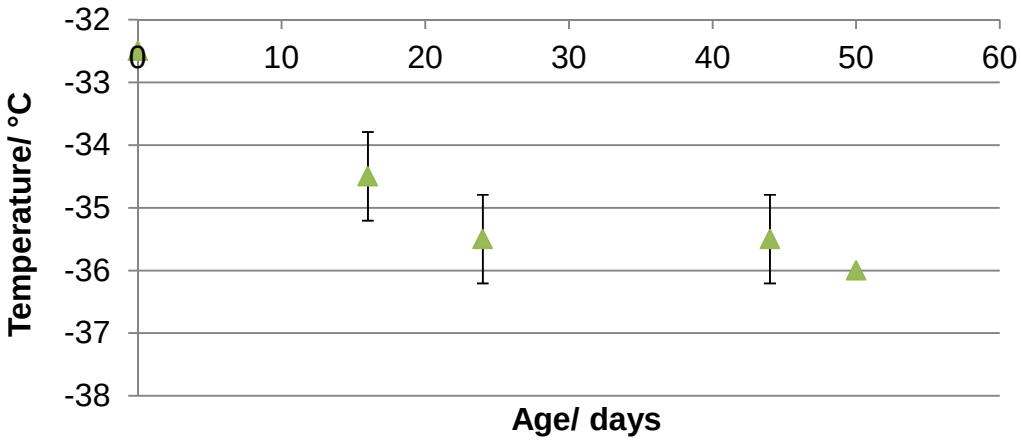

Figure 7-6 The glass transition of propellant aged at 60°C measured by DSC, plotted against the duration of ageing, the sample indicated as aged for 0 days including an un-aged sample ('Double base II').

Table 7-7 The glass transition of aged and un aged propellants ('Double base II') measured by DSC

Sample	Ageing time/ days	Analysis 1	Analysis 2	Average
Un-aged	0	-33	-32	-32.5
40a	90	-34	-34	-34
40b	180	-34	-35	-34.5
40c	240	-34	-36	-35
40d	333	-35	-35	-35
50a	41	-34	-35	-34.5
50b	70	-34	-35	-34.5
50c	88	-36	-35	-35.5
50d	101	-36	-35	-35.5
60a	16	-34	-35	-34.5
60b	24	-35	-36	-35.5
60c	44	-35	-36	-35.5
60d	50	-36	-36	-36

7.5 Discussion

A determination of which technique is most suitable for investigating whether a propellant is fit for service depends on the anticipated mode of failure of the propellant.

When a loss of energy caused by denitration of nitrocellulose is the cause of a propellant failing to perform. HPLC and DSC may be useful, as the energy of the propellant is linked to the level of nitration. The consumption of stabiliser caused by the denitration will provide an indirect method for monitoring this. DSC analysis could be used to decompose the material and quantify the energy content. The level of nitration required for a propellant to perform its function will depend on the exact composition and application.

If the concentration of the stabiliser is the limiting factor then the HPLC would be an appropriate technique as it can quantify the stabiliser concentration directly.

The thermal operating range of the propellant material may be influenced by a change in the glass transition temperature. In this analysis a lowering of glass transition temperature was observed as a function of ageing, the change was attributed to a combination of chain scission reducing the energy required for chains to move past one another, and denitration increasing the flexibility of the chains by reducing the activation energy of chain rotation, though these attributions were not proven they are reported in literature (2). It was considered that denitration can have the opposite effect, as it can lead to increased intermolecular bonding. The influence of denitration may be vary depending on the concentration of plasticisers. It is possible that under different ageing conditions the glass transition might be increased, this would reduce the thermal operating range of the propellant.

The DMA data tells us about the thermal transitions and how the hardness varies with temperature. This enables calculation of how the propellant will deform under the forces it will experience in its life. It allows a vast amount of

data to be collected from a single sample. The technique does not determine the maximum stress of the propellant as it doesn't destructively test the material. Destructive tensile and compression testing could be used to determine the failure stress of the propellant. This would be useful for predicting when a propellant would fail.

The accelerated thermal ageing undertaken did not lead to changes in the dynamic mechanical properties. As thermal changes were observed by DSC and chemical changes by chromatographic methods, it is thought that if a longer period of accelerated thermal ageing were to be completed, similar changes in the dynamic mechanical properties would be observed. Such changes have been reported in literature (32) (33). In these cases the accelerated thermal ageing trial carried out was more aggressive involving higher temperatures. These high temperatures were not used in the present study, it was thought that such high temperatures would lead to decomposition of the propellant that would be unrepresentative of that which occurs at ambient conditions over long periods of time.

It is possible that a propellant grain would crack as a result of the forces experienced during firing. The grain geometry will determine how the forces act on the grain. If a propellant is burning from a central conduit to surface compressive forces will act in the direction of the burning reaction, the propellant will also be stressed in tension around the circumference of the conduit. Destructive tension and compression mechanical tests could be used to determine the breaking stress of the material. It would be useful to understand how these vary as a function of ageing. As conduit design influences the distribution of forces during firing, it will influence the acceptable variation in mechanical properties.

7.6 Conclusions

An extruded double base propellant was subjected to an accelerated thermal ageing trial. The trial carried out at 40,50 and 60°C simulated natural ageing at 25°C for up to 8 years.

The concentration of stabiliser in the propellant composition decreased throughout the ageing trial. The glass transition temperature, as measured by DSC decreased from ~32.5°C to ~35.5°C. This shift was attributed to the shortening of polymer chains and initial denitration, though this was not proven. The DMA did not measure variation in the propellant, it is thought that if more significant ageing had taken place then changes to the thermal transition temperatures such as those observed using differential scanning calorimetery would have been detected. I would expect that chain scission reactions which are reported to occur in nitrocellulose would act to soften the propellant, reducing the hardness. This is because the energy required for movement of chain sections would be reduced. The denitration of nitrocellulose may have a more complex influence on the hardness as an increase in intermolecular bonding would occur, which would harden the polymer. It is possible that reduced bond rotation energy would accompany denitration and act to reduce hardness.

It is recommended that further work include a more extensive period of accelerated thermal ageing, so that more significant variation in material properties can occur. Such an ageing program would allow an understanding of how changes in the molecular weight of the nitrocellulose influence the mechanical properties. This should include destructive mechanical testing of samples so that a prediction of when a propellant will fail in service based on molecular weight data may be made, as such mechanical failure of propellants has been reported (17).

8 RESULTS: STABILISER EXTRACTION

This chapter reviews and assesses the effectiveness of different stabiliser extraction methods used to measure the concentration of stabilisers in nitrocellulose based propellants, via high performance liquid chromatography (HPLC). The investigation revealed that the method detailed by Allied Ordinance Publication 48 edition 2 (AOP48 ed 2) provides the most efficient extraction.

The effect of both the rate of stirring, shaking and temperature on stabiliser extraction was investigated. The results indicate that stirring the solution serves to prevent a saturated solvent layer building up around the sample, it doesn't assist in physically breaking the sample up. A coefficient relating the rate of stabiliser extraction to temperature was calculated from an Arrhenius plot. It was noted that this did not represent true activation energy, as the reaction does not involve a change in intramolecular bonding.

A novel method for analysing UV-Visible spectra of solutions *in situ* was utilised, it proved to yield consistent results with relatively little operator interference. This method could be applied to a wide range of other chemical reactions/processes.

8.1 Introduction

Nitrocellulose (NC) based propellants chemically decompose over time, as this occurs the stabilisers are depleted, eventually all of the stabiliser will be consumed, at this point autocatalytic reactions occur which can lead to ignition (47). It is very important to monitor the ageing that takes place within the propellant, to prevent dangerous levels of ageing occurring (50).

Stabiliser depletion is one indication of the ageing that has occurred within a propellant. Analysis of stabiliser concentration is by HPLC. The integrity of the final result is dependent upon a complete extraction of the stabiliser from the

propellant, it is crucial that an appropriate extraction method is selected for the propellant.

There are a number of stabiliser extraction methods published in the scientific literature (5) (11) (51). This investigation compared the effectiveness of these different stabiliser extraction methods, it was determined that the AOP 48 ed 2 (5) method is the most effective. Although this method is the most effective, there are a number of variables that are not controlled or understood. Rate of shaking, stirring and the acceptable variations in ‘room temperature’ are investigated here to determine how they influence extraction of stabiliser.

The AOP 48 ed 2 method (5) details that the extraction should be carried out at room temperature, this is often understood to be 25ºC. In a non-air conditioned laboratory, the temperature could easily vary between 10-40ºC. It is therefore relevant to consider the kinetics of stabiliser extraction, to determine whether within this temperature range, the rate of extraction is significantly changed. Significant changes in extraction rate may lead to unreliable extraction procedures.

The AOP 48 ed 2 method (5) also stipulates that the solution must be shaken or stirred during extraction, but there are no specific details regarding the rate of shaking/stirring. This work analyses the extraction of stabiliser at a number of stirring rates, and assesses the underlying mechanism that is leading to the increase in stabiliser extraction rate.

As the quantification of stabiliser concentration in a sample is usually achieved with the use of time consuming and costly HPLC (high performance liquid chromatography), a faster and comparatively inexpensive method was required. The new method must be able to take a measurement from the solution without altering it, so that successive measurements can be made allowing measurement of stabiliser concentration during the extraction. The methods developed here used were based on UV-Vis spectroscopy. The stabiliser concentration was monitored by analysing the solutions absorbance 488nm

(measuring peak area), as no other propellant constituents absorbed at this frequency.

Two methods were used to monitor the extraction;

1. Samples withdrawn from bulk solution by pipet into a silica cuvette for analysis.

2. Volumetric flasks modified with a silica cuvette in the neck, allowing *in situ* UV-Vis spectroscopic measurements to be taken increasing time, efficiency and accuracy (methods are detailed in 8.5).

8.2 Analytical techniques

8.2.1 UV-Visible spectroscopy

A Zeiss, MCS 522 UV–VIS with a xenon flash lamp (Zeiss, BLX 500/4). Averages of five measurements were recorded. The base line curve was first analysed, this was a measurement of pure solvent.

8.2.2 High speed digital video

Measurements were performed using a Phantom V7 fitted with a 50mm lens.

8.2.3 HPLC

A Waters 2695 HPLC and Waters detector 996 PDA. The column, set to 30^{o}C, was an Inertsil 5 µm ODS-2, 250 x 4.6 mm (Varian Inc., Palo Alto, California, USA). The flow rate was 1 ml/min and the mobile phase 65% (acetonitrile (AcN) or methanol (MeOH))/ 35% H_2O.

8.2.4 Optical Microscopy

Images were obtained using a light Microscope, Polyvar Met with Polaroid DMC2 camera.

8.3 Propellant samples.

A range of nitrocellulose based propellant samples were analysed (Table 8-1), including: Single (Figure 8-1, Figure 8-2), double and triple base (Figure 8-3, Figure 8-4). Propellants coated with graphite and stabilised by ethylcentralite (EC), diphenylamine (DPA) and 2,nitro-diphenylamine (2,NDPA). These are detailed in Table 8-1.

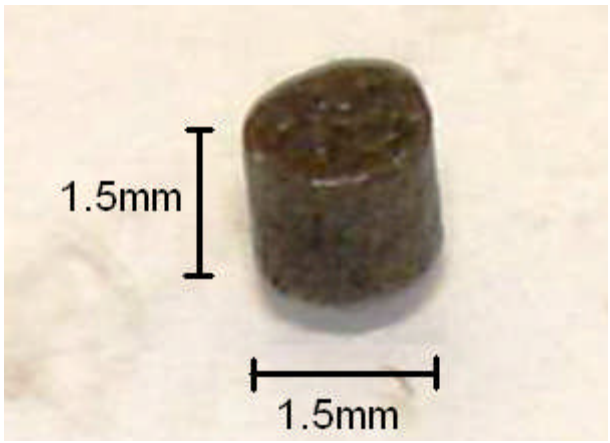

Figure 8-1 Propellant 1, Single base graphite coated gun propellant

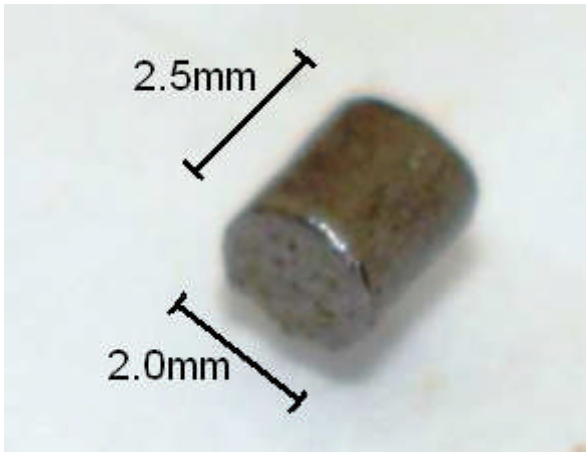

Figure 8-2 Propellant 2, Single base graphite coated gun propellant

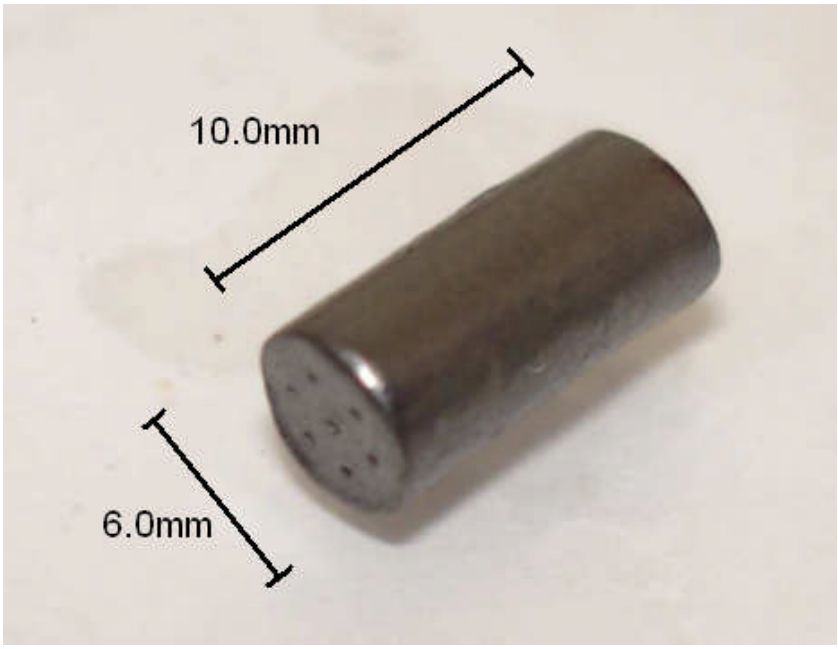

Figure 8-3 Propellant 3, Triple base graphite coated gun propellant

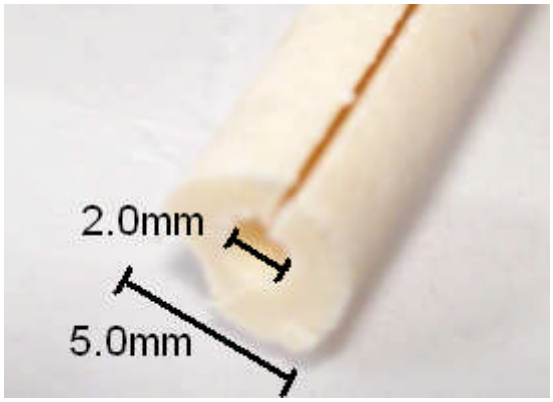

Figure 8-4 Propellant 4, Triple base non-graphite coated gun propellant

Table 8-1 Propellant samples analysed (Table 0-1)

Propellant	Type	Stabiliser	Coating	Shape and size
'Single base I' (Figure 8-1)	Single base	DPA ~2%wt	Graphite	Cylinder , 1.5 diameter, 1.5 long
'Single base I' (Figure 8-2)	Single base	DPA ~2%wt	Graphite	Cylinder , 2.0 diameter, 2.5 long 7 holes extending longitudinally throughout the grain
'Triple base I' (Figure 8-3)	Triple base	EC ~7%wt	Graphite	Cylinder, 6.0 diameter, 10.0 long 7 holed extending longitudinally throughout the grain
'Triple base I' (Figure 8-4)	Triple base	EC 2%wt	No coating	Cylinder, 5.0 diameter 2.0 conduit
'Double base II, sample G'	Double base	2-NDPA 2%wt	No coating	Sheet, 5.0 thick Sample taken from the final rolling stage of production of propellant

8.4 Stabiliser extraction methods

8.4.1 Procedure

Stabilisers were extracted using four different methods, each method was carried out using Acetonitrile and Methanol. Extractions were carried out in duplicate. The extractions were carried out on 0.5g (measured to a precision of ± 0.001g) samples of propellant. The quantity of solvent used during extraction was adjusted to maintain the concentrations detailed in the original literature.

Table 8-2 Stabiliser extraction methods

Method	Method detail
STANAG shaking (5)	The propellant and 125ml of solvent were placed into a 250ml volumetric and covered with aluminium foil to block any light from entering the solution, (to minimize any UV degradation of the propellant). The flask was then shaken for four hours (Griffin Flask Shaker- 896331), after shaking 25ml of $CaCl_2$ (2%) was added and left to stand for another hour. The $CaCl_2$ causes the NC to precipitate out of solution, helping to prevent it damaging the HPLC column.
STANAG stirring (5)	As per STANAG shaking method, using a magnetic stirrer (Bibbly B212 stirrer hotplate) in place of the shaker.
Static method (51)	The propellant and 125ml of solvent were placed into a 250ml volumetric and covered with aluminium foil and left static for 17 hours.
Ultra sonication (52)	The propellant and 20ml of solvent was placed into 100ml conical flask and ultra-sonicated (Langford LF Ultra Sonic Cleaning tank) for 30minutes. A 1ml aliquot was taken and diluted by a factor of 10. Temperature of 25°C was controlled thermostatically.

8.4.2 Results

In this investigation the two solvents (Acetonitrile and Methanol) proved equally efficient at extracting the ethylcentralite from propellants 'Triple base I/II' (Figure 8-5, Table 8-3). However this is not sufficient evidence to conclude that Methanol and Acetonitrile can be used equally effectively in all propellant samples. Methanol and Acetonitrile are similar solvents, both linear and polar, Acetonitrile has a dipole moment of 4 Daltons (D) and Methanol 1.7D (53). The higher dipole moment of Acetonitrile may increase its ability to break down intermolecular bonding in nitrocellulose. In the case of a propellant with higher nitrocellulose content, this may make an appreciable difference to the stabiliser extraction process.

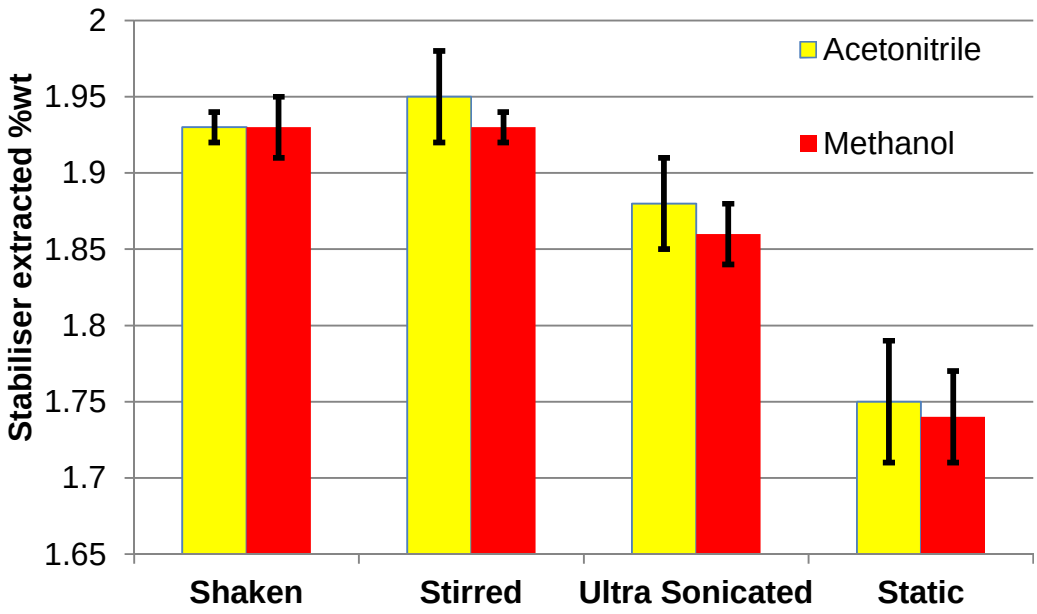

Figure 8-5 Comparison of stabiliser extraction methods for 'Triple base II' 4, error bars indicate 2x standard deviation

Table 8-3 The stabiliser % extracted from propellant samples using a variety of methods

Method and sample	Solvent	DPA % measured	Error ±
'Single base I'			
STANAG STIRRING	Ac N	0.58	0.02
STANAG SHAKING	Ac N	0.58	0.01
SOLVENT OVERNIGHT	Ac N	0.59	0.03
ULTRA SONICATE 30 MINUTES	Ac N	0.47	0.01
STANAG STIRRING	MeOH	0.59	0.06
STANAG SHAKING	MeOH	0.59	0.04
STATIC METHOD	MeOH	0.61	0.05
ULTRA SONICATE 30 MINUTES	MeOH	0.58	0.03
'Single base II'			
STANAG STIRRING	Ac N	0.74	0.04
STANAG SHAKING	Ac N	0.79	0.02
SOLVENT OVERNIGHT	Ac N	0.76	0.05
ULTRA SONICATE 30 MINUTES	Ac N		
STANAG STIRRING	MeOH	0.65	0.06
STANAG SHAKING	MeOH	0.66	0.02
STATIC METHOD	MeOH	0.90	0.00
ULTRA SONICATE 30 MINUTES	MeOH	0.58	0.04
'Triple base I'		**EC % measured**	
STANAG STIRRING	Ac N	6.99	0.04
STANAG SHAKING	Ac N	7.04	0.01
SOLVENT OVERNIGHT	Ac N	6.61	0.01
ULTRA SONICATE 30 MINUTES	Ac N	5.60	1.00
STANAG STIRRING	MeOH	6.92	0.06
STANAG SHAKING	MeOH	6.87	0.09
STATIC METHOD	MeOH	6.82	0.05
ULTRA SONICATE 30 MINUTES	MeOH	5.73	0.00
'Triple base II'			
STANAG STIRRING	Ac N	1.96	0.01
STANAG SHAKING	Ac N	1.93	0.02
SOLVENT OVERNIGHT	Ac N	1.88	0.01
ULTRA SONICATE 30 MINUTES	Ac N	1.75	0.03
STANAG STIRRING	MeOH	1.92	0.01
STANAG SHAKING	MeOH	1.95	0.04
STATIC METHOD	MeOH	1.84	0.03
ULTRA SONICATE 30 MINUTES	MeOH	1.73	0.04

The methods that yielded the highest stabiliser extraction (STANAG) involved shaking or stirring the solvent for four hours Figure 8-5, Table 8-3. This data shows that shaking and stirring significantly enhances the stabiliser extraction rate. In order for the stabiliser to dissolve into the propellant the polymer chains of nitrocellulose must move sufficiently apart so that the stabiliser can migrate into solution. The polar solvent penetrates between the NC polymer chains breaking the intermolecular bonding allowing chains to move apart and the stabilizer to escape the NC matrix. The shaking/stirring of the solution increases the effectiveness of the solvent in the process.

There is little information given in AOP 48 (ed2) regarding how vigorously the flasks should be shaken or stirred. This seems unusual given the apparent importance of the process.

The extraction of stabilisers using ultra sonication proved poor in all cases (Figure 8-5). Ultra sonication has been reported to enhance the rate in solid phase extractions (54). The ultra-sonication did not provide a complete extraction in 30 minutes. It is believed that the extraction rate is affected by the formation of a boundary layer of saturated solution surrounding the propellant sample, this theory is fully discussed in section 8.5.5. The time period could be extended, however it is considered likely that the ultra-sonication could lead to degradation of the stabiliser and invalidation of results. Ultra-sonication causes cavitation bubbles to occur, when these collapse temperatures of several thousand degrees Celsius and extreme pressures occur locally (54) . These conditions have been reported to lead to radical reactions. It would be ill advised to continue with this method until the effect of ultra-sonication has been investigated with these types of sample.

The graphite coating on samples ‘Single base I/II’ (Figure 8-6) varied in thickness by up to 0.135mm, conversely the graphite coating on 3 was very consistent.

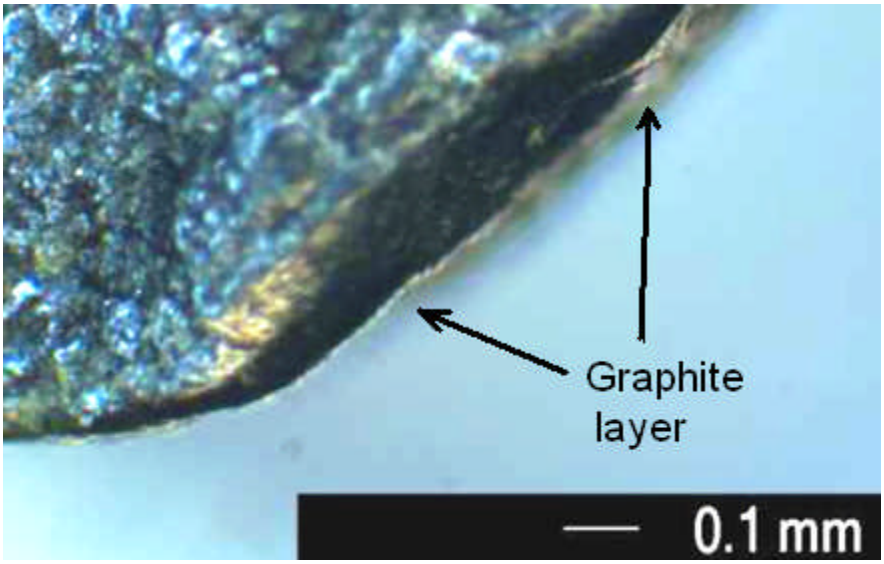

Figure 8-6 Light microscope image of 'Single base II'

A grain of propellant completely covered in a thin coat of graphite could have >20wt% more nitrocellulose than a grain of the same size with a thick coat, calculated by taking 2gcm^{-3} as the density for graphite and 1.6gcm^{-3} as the density for nitrocellulose. It is unlikely that one sample would contain purely grains with a thin coating and the other contain grains with a thick coating, however these variations do explain the high relative standard variation reported for stabiliser extraction from 'Single base I/II' (±5-10%).

The presence of a graphite layer on the propellant will inhibit the diffusion of the stabiliser in to solution. It is likely that stabiliser extraction from a graphite coated propellant sample would take longer compared to a comparable non coated sample. This serves as a second explanation for the inconsistent results obtained from 'Single base I/II' where samples were coated with an uneven graphite layer. As a consequence of the poor reproducibility of the results for 'Single base I/II', they were not used to determine which method is the most effective.

8.5 Investigating the effect of shaking and stirring

8.5.1 Investigating the effect of shaking rate (Sample ‘Single base II’), procedure

A sample of ‘Single base II’ (0.5g) was precisely weighed out (to an accuracy of 0.001g) and transferred into 250ml volumetric flask. Methanol (125ml) was added to the volumetric flask. The flask was wrapped in aluminium foil, to prevent UV degradation of the stabiliser. The stabiliser was extracted over 6 hours. Six of these flasks were prepared. Two flasks were subjected to shaking (IKA KS 501 digital shaker) at 300rpm, two at 150rpm and two flasks were not shaken. At approximately 30 minute intervals, a 1ml sample was removed from the volumetric flask and filtered using nylon syringe filters (0.2μm pore diameter) in to UV spectrometry cuvettes. Filtering removes NC from solution as it absorbs across the visible region and decreases peak resolution. The UV spectrum was recorded. The sample was then returned to the initial bulk solution via pipette. The total quantity of solution lost during this process was recorded, ensuring it didn’t exceed 1ml.

DPA absorbs UV radiation at 220, 254 and 320nm. Unfortunately the absorption maximum of nitrocellulose is in the same region as DPA making it impossible to distinguish DPA from nitrocellulose. As the nitrated DPA daughter products have a nitro group attached to phenyl group of DPA, the energy of the absorbance is lower (55), thus the nitro derivatives absorb at 350-450nm (Figure 8-8), for this reason the extraction rate of stabiliser was monitored by the extraction of N-DPA. This was confirmed experimentally by analysing standard 100ppm solutions of 2-NDPA and 2,4- dinitrodyphenylamine (2,4-DNDPA). This is based upon the assumption that the DPA and nitrated derivatives have similar extraction efficiencies.

8.5.2 Investigating the effect of stirring rate (Sample ‘Double base II’), procedure

The stabiliser extraction method detailed in AOP 48 ed 2 (5) was followed, with a reduced mass. Propellant samples (0.1g ±0.01) were cut into 1mm cubes. Solvent (acetonitrile 50ml) was pipetted into the ‘UV volumetric flasks’ the reference spectra were then measured. A magnetic stirrer bar (10mm length x 5mm diameter) was added, the flask was then placed on the stirrer hotplate. The speed of the stirrer bar was set and monitored periodically using high speed video photography to ensure it remained constant. Flasks were wrapped in aluminium foil to prevent further reaction of the stabiliser, as stipulated by AOP 48 ed 2 (5). Temperature was maintained at 25°C, monitored using thermometer. The experiment was started by the addition of the propellant sample.

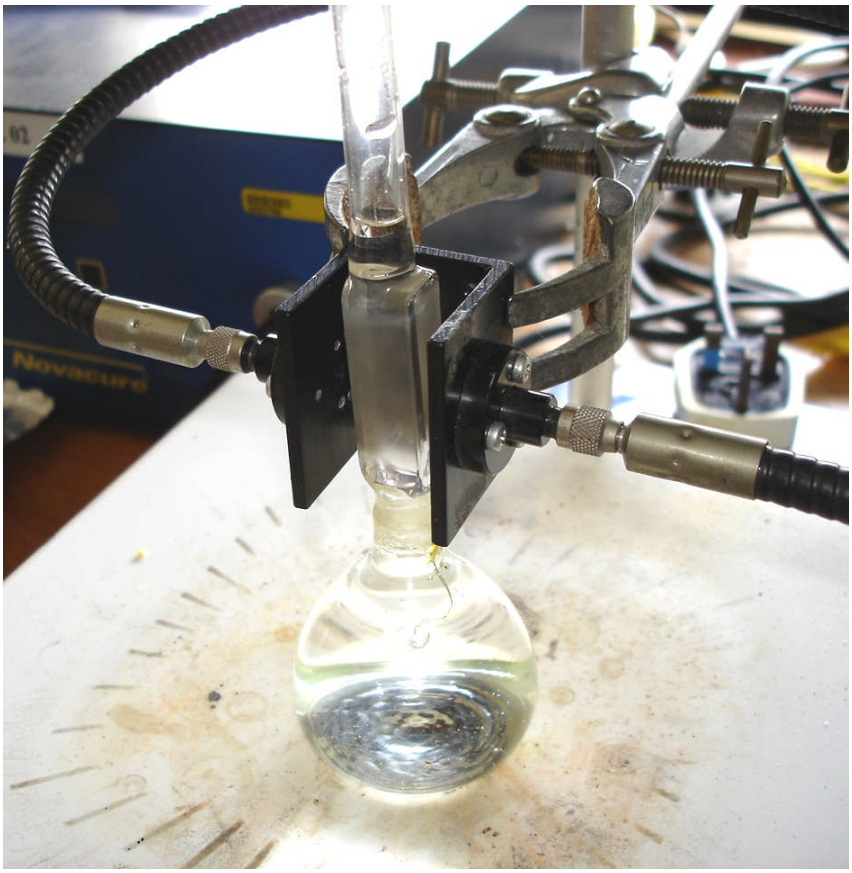

Figure 8-7 Modified volumetric flask with silica cuvette

The extractions were carried out at a number of different stirring rates; 1500, 700 and 350 rpm (±5%). Analysis was carried out in duplicate.

8.5.3 Results, Effect of shaking

The results indicate that the rate of stabiliser extraction was initially high and decreases over time, eventually reaching zero when the stabiliser was completely extracted, represented in Figure 8-9 by a plateau. The time taken to reach a plateau is indicative of the time taken for complete extraction. The time taken was ~85 minutes shorter for samples shaken than for samples not shaken.

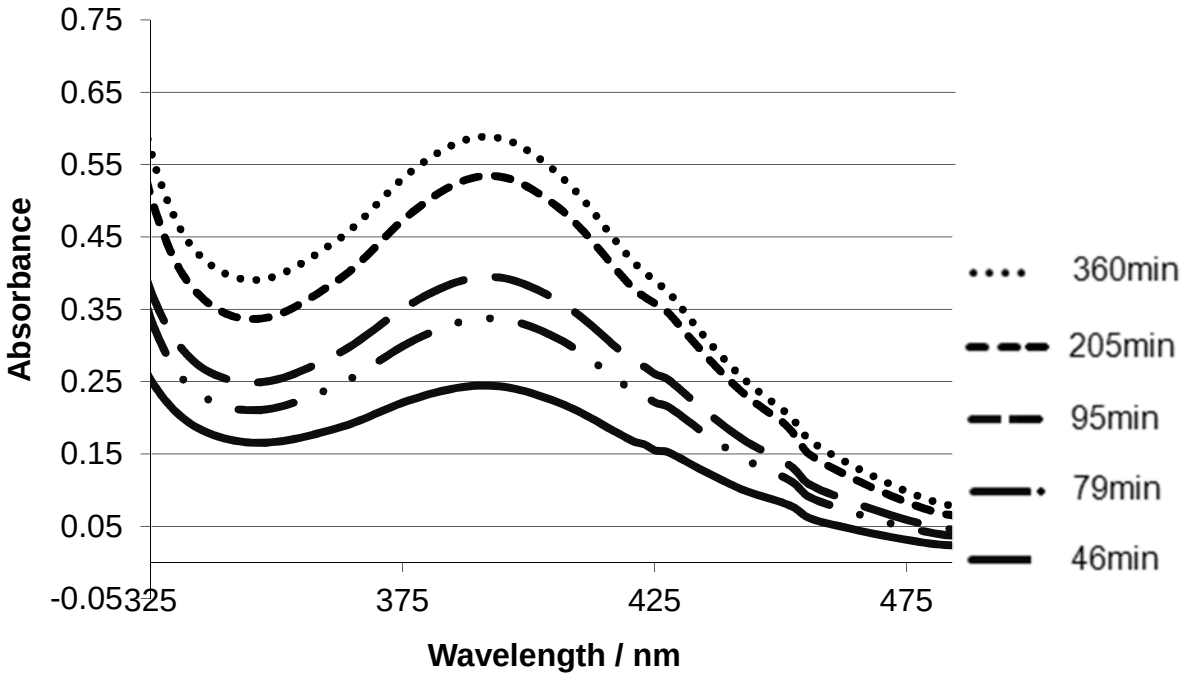

Figure 8-8 The UV-Visible spectra of a sample shaken at 300rpm measured periodically over 6 hours

Shaking the solution at 150 and 300 rpm reduced the time taken for the stabiliser to be extracted by approximately 30%. There was no difference observed between shaking at 150rpm and 300rpm (Figure 8-9).

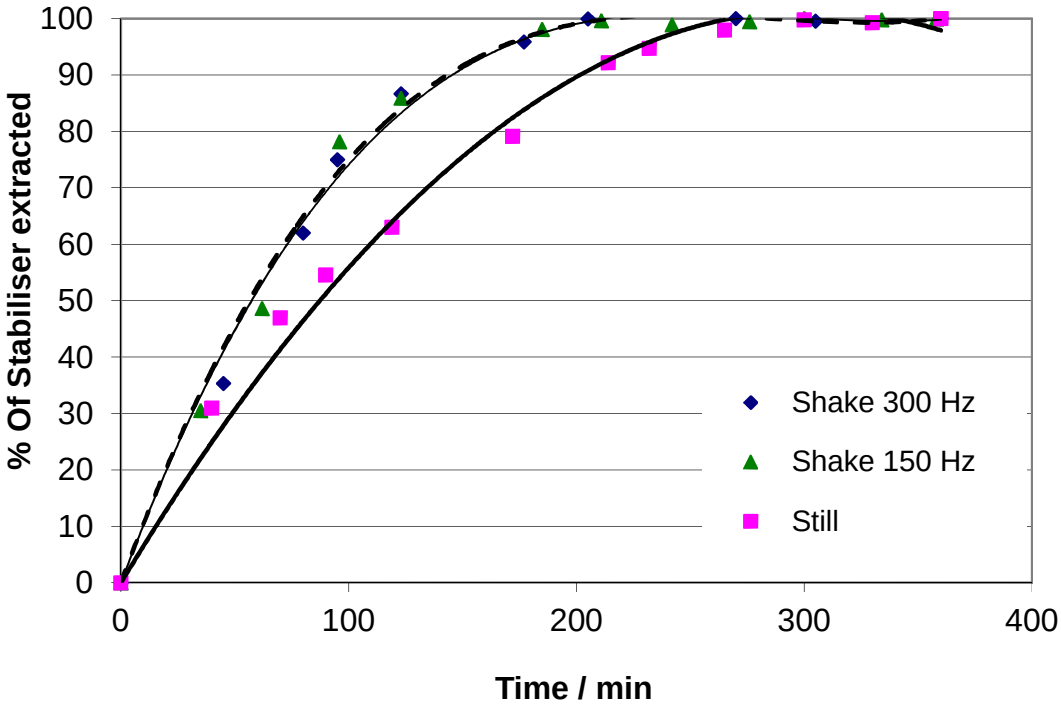

Figure 8-9 Extraction of stabiliser from propellant at different shaking rates ('Single base II')

8.5.4 Results Effect of shaking

The result Figure 8-10, show there was no difference in the time taken for the stabiliser to be completely extracted at either 1500 or 700rpm stirring rate. These were 30% faster than the extraction at 350rpm and 80% faster than stabiliser extracted from a static solution. These findings are consistent with those previously reported **(40)**, where the extraction rate was found to be identical for samples shaken at 300 and 150 rpm, which was ~66% faster than a static extraction.

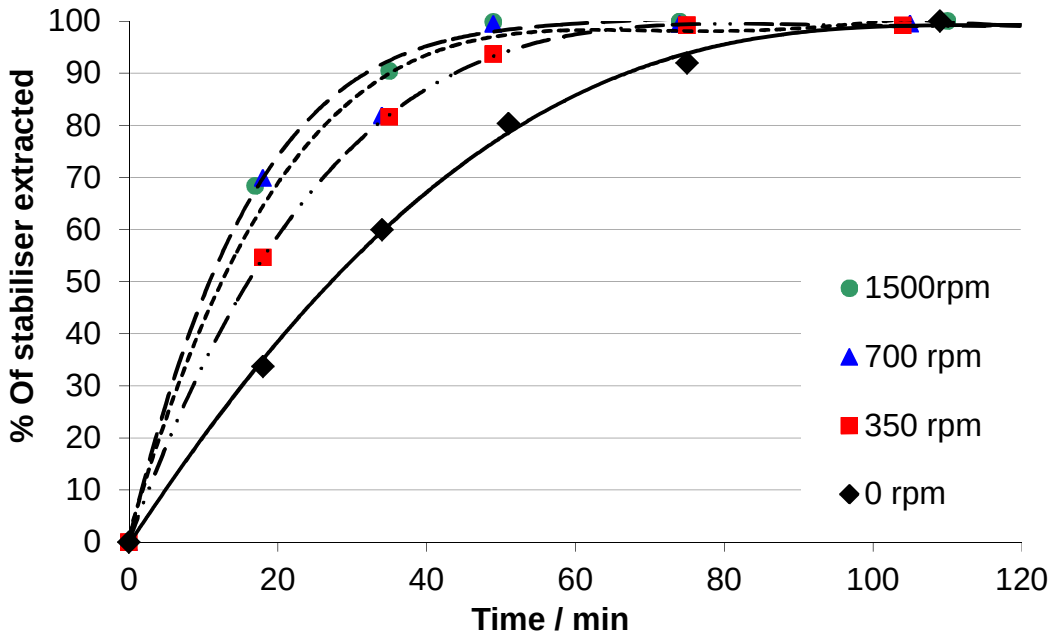

Figure 8-10 Extraction of stabiliser from sample at different stirring rates

8.5.5 Discussion, Effect of shaking and stirring

These observations suggest that the agitation of the solvent principally acts to prevent areas of saturated solvent building up around the propellant. In this case only a modest movement of solution would be required to disrupt and boundary layers formation, yielding near maximum extraction rate, and that higher stirring rates beyond this point would not lead to faster extraction. If the movement of the solution acted to physically break apart the propellant, increasing surface area and rate of extraction, then the rate of extraction would continue to be increased by increasing stirring rate. This was not observed in this research. Stirring may prove to be even more important when extracting stabiliser from graphite coated propellants, as the graphite layer will inhibit the diffusion of the stabiliser. The action of stirring would be two fold, to increase the rate of graphite dissolution and then to prevent a boundary layer forming.

8.6 Investigating the effect of temperature (Sample ‘Double base II’)

8.6.1 Procedure

The stabiliser extraction method detailed in AOP 48 ed 2 (5) was followed, with a reduced mass. Propellant samples (0.25g ±0.01) were cut into 2x5x5mm cuboids. Solvent (acetonitrile 50ml) was pipetted into the ‘UV volumetric flasks’ and the reference spectra were then measured. A magnetic stirrer bar (10mm length x 5mm diameter) was added, the flask was then placed on the stirrer hotplate, the speed of the stirrer bar was set to 700rpm and monitored periodically using high speed video photography, flasks were then wrapped in aluminium foil to prevent further reaction of the stabiliser, as stipulated by AOP 48 ed 2 (5). The experiment was started with the addition of the propellant sample. Temperatures of 10, 25 and 40°C were analysed.

The UV-Visible spectra were measured every 30 minutes over a period of 7 hours to monitor the extraction of the stabiliser. Analysis was carried out in triplicate.

8.6.2 Results, the effect of temperature

Analysis was carried out at a range of temperatures (10, 25, 40°C). The results indicated the rate of extraction varied significantly over this temperature range. The diffusion/extraction of stabiliser from the propellant into solution was monitored by analysing the evolution of the peak between 485nm, in the UV-Visible spectra.

A plot of ln stabiliser concentration versus time yielded a straight line. The rate constant (k) was calculated from equation (8-1). The reaction was found to follow first order kinetics, this was consistent with the findings of Tompa (56) where a double base propellant was dissolved in a number of organic solvents was studied. The concentration of solvent was very high with respect to the propellant, we assume that the solvent concentration doesn't change

significantly throughout the reaction. The reaction may therefore be following pseudo first order kinetics and in fact be second order overall.

$$\ln[A] = -kt + \ln[A_0] \quad \textbf{(8-1)}$$

[A] = Concentration of stabiliser

[A_o] = Initial concentration of stabiliser

k = Rate constant

t = Time

Analysis were carried out in triplicate at each temperature, Table 8-4 shows the rate constants measured.

Table 8-4 The rate constants and averages calculated at a range of temperatures.

Temperature, °C	Average rate constant, s^{-1}	2x Std dev
40	0.03	0.0013
25	0.019	0.0025
10	0.014	0.0004

An Arrhenius plot of the average rate constants for each temperature is plotted in Figure 8-11. The Arrhenius parameters calculated from the data are detailed in Table 8-5.

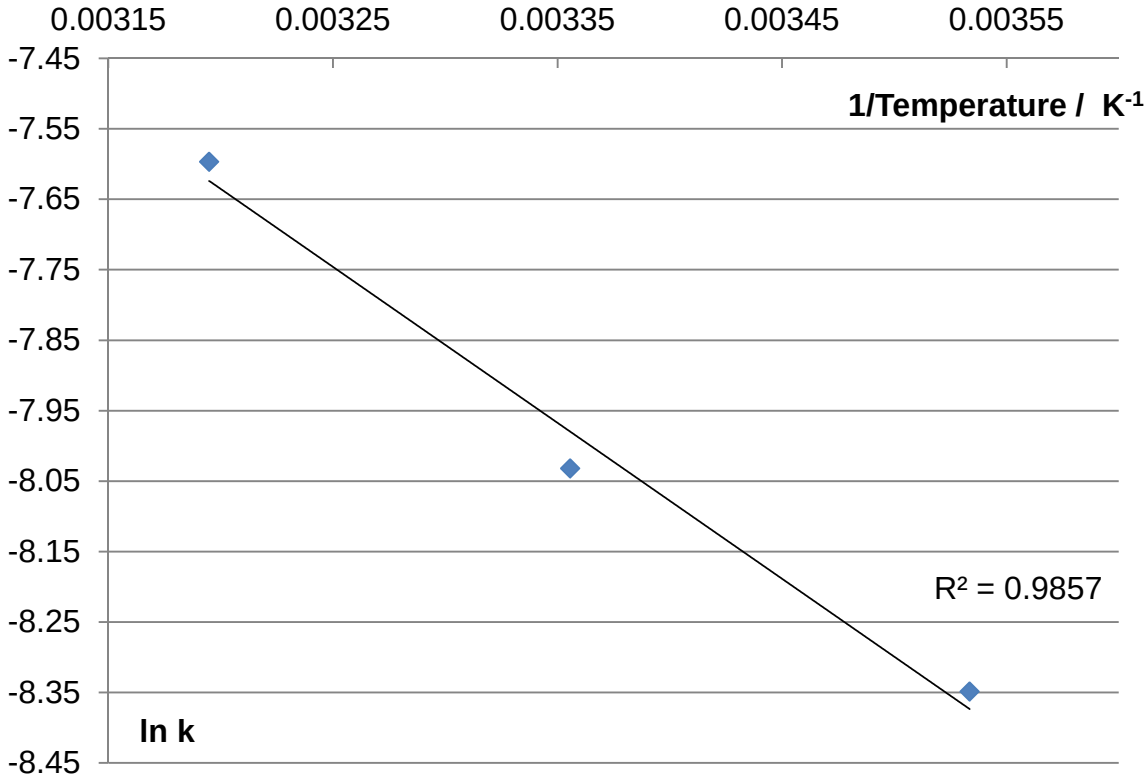

Figure 8-11 Arrhenius plot of average rate constants measured versus temperature.

Table 8-5 Arrhenius parameters calculated from kinetics data.

Arrhenius parameter	Value
Activation energy, Ea	18 $kJmol^{-1}$
Pre exponential factor, A	-0.5512

Only a small amount of stirring was required to disrupt the boundary layer of saturated solution surrounding the sample, it is therefore likely that the 'activation energy' measured is a coefficient that relates temperature to the diffusion rate of the stabiliser from the nitrocellulose.

Fick's first law of diffusion dictates that the rate of diffusion is equal to the concentration gradient multiplied by a constant equation (8-2), the terms are defined in Table 8-6. In this case the substance of interest is a stabiliser, if solvent can be considered to be in excess, then the concentration of stabiliser in

the sample is the only one effecting the rate of extraction. This supports the kinetic observations that the reaction follows first order kinetics.

$$J = -D\frac{\partial \phi}{\partial x} \qquad \textbf{(8-2)}$$

Table 8-6: The definitions and units of the terms in Fick's law

Term with units	Definition
$J = \frac{mole}{m^2 s}$	J is the diffusion flux. A measure of the rate of flow of a substance.
$D = \frac{m^2}{s}$	D is the is the diffusion coefficient.
$\frac{\partial \phi}{\partial x} = \frac{mole/m^3}{m}$	Φ is the concentration of the substance. x is the position along the diffusion length of the measurement.

The measurements carried out in this research are in fact a measure of the diffusion flux (J) equation 2, from the units of J it is clear that the rate of reaction is dependent upon the physical dimensions of the sample. If we assume the dimensions of the propellant remain constant, the rate constant for the reaction will be proportional to J.

The relationship between the diffusion flux (J) and the rate constant (k) mean that k values are specific to the size, shape, composition of the material and the solvent used. The 'activation energy' value calculated from this analysis is a coefficient which is related to the rate constant to the temperature. This value is

independent of sample measurement, and could be used to determine extraction times for other sample sizes.

8.7 Conclusions

The most effective stabiliser extraction methods are those involving shaking or stirring of the extraction solution, they proved equally efficient at extracting stabiliser. Although this research found no difference using Methanol or Acetonitrile, the data collected here is not sufficient to conclude that they are always equally effective, as the data discussed only represents two types of triple based propellant. As the stabiliser is polar it may be expected that Acetonitrile would be a more effective solvent, as it has a higher dipole moment.

Ultra sonicating a sample for 30 minutes does not provide an effective extraction technique. It was considered that ultra-sonication could induce additional chemical changes in the sample. This method could be used for preliminary investigation to determine the stabiliser type, or to produce a sample that could be used to determine optimum HPLC conditions and mobile phase to achieve separation of peaks.

It is concluded that shaking/stirring prevents a boundary layer of saturated solution forming around the propellant that would otherwise isolate the propellant from the solvent, and reduce the rate of diffusion.

The temperature dependence of the extraction was determined, an ‘activation energy’ of 18 $kJmol^{-1}$ was calculated, although the value isn’t a true activation energy as this process is one of dissolution and diffusion. The time taken for complete stabiliser extraction at 40°C was half of the time taken at 10°C. Therefore it is recommended that the room temperature should be monitored, and if temperature falls below 25°C, extraction methods and times adjusted accordingly.

This research used a novel method for analysing the stabiliser extraction rate by measuring UV-Vis spectra of a solution *in situ,* using modified volumetric flasks. The method comparatively speeds the process of extraction and increases

accuracy. The results were repeatable and were used to calculate kinetic parameters for the reaction. This method could be applied to analyse the rate of a number of other chemical reactions/processes. The method doesn't suffer from some of the potential difficulties encountered with fibre optic probes, such as incompatibility of solvent and the coating on the fibre optics. As the solution remains in the flask, treatments such as stirring or shaking, the temperature variation can be monitored *in situ*, a distinct advantage when considering the kinetics of fast reactions. With the application of appropriate spectrometry software, the process could be easily automated. This method does have limitations: It required the manufacture of bespoke glass wear, which itself limits the extractions to 50ml, this reduces the accuracy as measurement errors would be more significant. The method is incompatible with the AOP 48 shaking method as the flask is full of solvent leaving no air space for movement of solvent during shaking.

This research does indicate that the method set out be AOP 48 needs to be amended, as 4 hours is not sufficient in all cases.

Further work may look at identifying UV-visible frequencies at which other stabilisers could be detected. It would be advantageous to adapt this method for use with a fibre optic probe, this would allow for full scale extractions.

9 THESIS OUTCOMES

9.1 Thesis objectives

This thesis was concerned with understanding the manufacturing and storage of extruded double base propellants.

It set out to determine how, physical, chemical and thermal properties of the propellant change throughout production, and to evaluate the homogeneity of the final extruded product. The findings could be useful to develop future manufacturing methods.

The thesis investigated how the properties of the propellant would change during years in storage, with a specific interest in evaluating published methods of stabiliser analysis, and if and how physical and thermal properties change as a result of chemical decomposition reactions.

These areas of research were investigated over the course of five experimental chapters.

9.2 Chemical and physical effects of manufacture on extruded double base propellants

The production process for extruded double base propellants was studied in chapter 4, it involves mixing of constituents, followed by rolling and reworking stages before the final extrusion.

Analysis of propellant samples using gel permeation chromatography measured decreases in weight average molecular weight throughout the production process. This is consistent with published work studying the effect of extrusion on polymers where molecular weight changes have been reported. The reduction in weight average molecular weight was attributed to denitration of nitrocellulose. This is a process widely reported to occur due to ageing, and it was thought that the high temperatures and pressures experienced during the production processing, provided the energy for the reaction to occur. This is an

important finding. It is known that denitration occurs in nitrocellulose (2). Chapter 7 measured changes in glass transition temperature believed to be due in part to the denitration, which occurred during accelerated thermal ageing of propellant samples. It may be possible to reduce the pressures used during the production, this could reduce the forces acting on the propellant and consequently may reduce the extent of which denitration reactions take place. This is an area that should be considered for further research as reducing the decomposition processes that occur during manufacture could be a way of extending the service life of the propellant.

Differential scanning calorimetery analysis indicated that the nitroglycerine is distributed more evenly throughout the propellant during the rolling and reworking stage of the propellant production. This is a very important finding as the nitroglycerine is highly energetic, and therefore the ballistic properties of the propellant will be dependent upon the distribution of nitroglycerine. It was considered that the more even distribution of other propellant constituents such as the stabiliser or ballistic modifiers may also occur during the rolling and reworking stages of production, rather than at the initial incorporation stage. Further work in this area should consider how and when the stabilisers are distributed during production of the propellant, as the long term stability of the propellant will be dependent on the even distribution of the stabiliser.

The disruption of the crystalline structure of cellulose during propellant production was investigated using X-ray diffraction. Analysis of a sample taken from an early stage of production and a sample of the extruded product, indicated that changes are occurring, though it was not possible to quantify these . Further work would be useful to quantify the changes, as it is possible that the effective distribution of the nitroglycerine, stabiliser and any other constituents can only occur after disruption of the crystalline regions.

9.3 The effect of the extrusion process on the propellant

The homogeneity of the final extruded product was investigated in chapter 5. It was considered that decomposition occurring during extrusion may be higher at

the edges where the propellant comes into contact with the extrusion die, than in the centre.

The weight average and number average molecular weights and polydispersity measurements indicate no change between samples of a propellant grain. This result does not contradict conclusions in the previous chapter, as it is possible that changes have occurred during extrusion such as those measured in the previous chapter, and reported in the literature (36) (35). Any changes affect the propellant equally across the grain. The sample representing the surface was taken from the surface to a depth of 5mm. It is possible that variation is still present, and that it occurs to a shallower depth from the surface, and in the case of a 5mm thick sample the variation is masked by the majority of material that represents the bulk. Future research may consider samples taken in 1mm increments. This would offer more representative data.

Measurements of the mechanical properties were made by dynamic mechanical analysis and micro-hardness. The dynamic mechanical analysis measurements did not show changes between samples, this is consistent with the gel permeation chromatography data. If variation does occur at the surface one would not expect to be able to measure it with the dynamic mechanical analyser, as the sample size required is too large to represent the surface. Mechanical data collected by nano-indentation in future research may allow a measurement of changes occurring near the edge of the sample. However it may be subject to the same limitations as the micro-hardness measurements where the sample mounting clay supported the sample and gave falsely high hardness measurements.

The research did not measure variation across the grain of the propellant, however does not rule out that it may occur. This area of research should be continued, as it is possible that if the outside layer of propellant is harder and more brittle, it could be a source of cracks which may propagate during firing. A hardening may result from denitration which was reported to occur during extrusion.

9.4 Application of dynamic mechanical analysis for analysing nitrocellulose based materials

In chapter 6, time temperature superposition (TTS) of frequency scan data found that it superpositioned well. This is an important conclusion as TTS does not always work well on semi crystalline polymers. Though the manufacturing steps seek to disrupt the crystalline structure, is was considered possible that some crystal structure could remain, and that TTS may not be a useful method. As TTS allows prediction of how a material may behave at frequencies higher than directly measureable using the DMA, future work should consider any high frequency loads a propellant will be subjected to in service, for example during transport, when carried on an aircraft or during firing. Then TTS could be used to predict material properties at these frequencies.

Analysis of creep test data (chapter 6) indicated that creep testing of propellants may be a useful tool to predict the deformation of a propellant grain under its own weight during storage. This will be of particular importance when considering propellant grains with conduits as they may be weaker, making them more vulnerable to changes. Samples of aged and un-aged propellant were analysed but no significant differences were observed between the two. This is a very positive result as the ageing simulated 8 years of ageing. It was considered that the increase in intermolecular bonding that is observed as a result of denitration would increase the viscous component of the materials behaviour as it would further restrict chain movement. Conversely the influence of chain scission would have the opposite influence, as shorter chains can more easily move past one another. As these two processes have competing influences it is unsurprising that it is difficult to identify changes in properties. Future work in this area should test samples which have been aged more extensively. It is important to determine how much ageing can take place before changes are observed in the creep properties. It would also be useful to measure the changes in molecular weight that accompany any change in mechanical properties, so that a relationship between the two can be understood.

9.5 Ageing trial of extruded double base propellant

Prediction of how propellant samples will change during storage at ambient temperature over a time period of years was investigated in chapter 7. Samples had been subjected to accelerated thermal ageing at elevated temperatures. The aged samples were then analysed with a number of analytical techniques to determine how decomposition processes had changed the propellants properties.

The stabiliser concentration was quantified using high performance liquid chromatography. The stabilisers are consumed by the nitrate groups liberated by the denitration decomposition reactions. The consumption of the stabiliser can therefore be used as guide to the extent of the denitration of the nitrocellulose. A decrease of 0.5, 0.2 and 0.1 %wt stabiliser was observed in the samples aged at 60, 50 and 40°C and from this data it was concluded that denitration had occurred. This conclusion was used when considering the causes for the changes in thermal properties.

The weight average and number average molecular weight of the nitrocellulose were measured using gel permeation chromatography, reductions in both were observed, which indicated both chain scission and denitration.

It is important to understand the influences of the chemical changes measured on the mechanical and thermal properties of these decomposition reactions, as this may become the service life limiting factor. Variations in properties were not observed in dynamic mechanical analysis measurements, though the method used for deconvolution of peaks using Gaussian curve fitting proved successful.

A decrease in the glass transition temperature was detected using differential scanning calorimetery. This was attributed to the increased ease of bond rotation caused by denitration, and the chain scission reducing polymer chain length. It was considered that future work involving a more extensive accelerated thermal ageing trial would be needed to draw firm conclusions.

9.6 Stabiliser extraction

The process of stabiliser extraction was analysed in chapter 8. The ageing that has occurred in nitrocellulose based propellants is often analysed by quantifying the stabiliser concentration using high performance liquid chromatography (HPLC).

There have been a number of stabiliser extraction methods for HPLC analysis published. These methods were compared and the method set out in AOP 48 ed2 was found to be the most reliable.

It was demonstrated that methanol can be used as an extraction solvent as effectively as acetonitrile, in the case of the two triple base propellants analysed. This is a significant result as methanol is significantly cheaper than acetonitrile. It is necessary in future work to repeat this work using a wider range of propellants including both single and double base to verify that methanol is still as effective, as the higher nitrocellulose content in single base propellants may reduce the rate of dissolution, a difference between extraction rates between MeOH and AcN may be observed.

The influence of the rate of shaking and stirring the solution on stabiliser extraction was studied. The results found a significant increase in extraction rate between static solutions and those with slow stirring or shaking. At higher rates of shaking and stirring the stabiliser extraction rate became constant. It is concluded that shaking/stirring prevents a boundary layer of saturated solution forming around the propellant that would otherwise isolate the propellant from the solvent, and reduce the rate of diffusion. This is an important conclusion as it means that the rate of stirring or shaking does not have to be monitored closely during extraction processes.

The extraction process temperature dependence was investigated, as it is possible for a laboratory to fluctuate in temperature, possibly between 10 and 40°C. An ‘activation energy’ of 18 $kJmol^{-1}$ was calculated, although the value is not a true activation energy as this process is one of dissolution and diffusion. It

was observed that the time taken for complete stabiliser extraction at 40°C was half of the time taken at 10°C. Therefore a recommendation that the room temperature should be monitored, and if temperature falls below 25°C, extraction methods and times adjusted accordingly was made.

REFERENCES

1. *Cellulose fibre morphology and its potential effects on nitrocellulose manufacturing and performance.* **M.Paquet.** Shrivenham : 4th Nitrocellulose workshop, 2010.

2. **T.Urbanski.** *Chemistry and Technology Of Explosives.* Warsaw : Pergamon Press, 1964.

3. *Cellulose: The structure slowly unravels.* **A.C.O'Sullivan.** 1997, Cellulose, Vol. 4, pp. 173-207.

4. *Hydrolytic decomposition of esters of nitric acid. Part 1, general experimental techniques, alkaline hydrolysis and neutral solvolysis of methyl, ethyl isopropyl and tert-butyl nitrates in aquous alcohol.* **J.W.Baker, D.M.Eastley.** 1952, Journal Of The Chemical Society, Vol. 1, pp. 1190-1192.

5. **NATO.** *Allied Ordinance Publication 48 Edition 2: Explosives, nitrocellulose based propellants, stability test procedures and requirements using stabiliser depletion.* s.l. : NATO, 2008.

6. *A desorption electrospray ionization mass spectrometry study of aging products of diphenylamine stabiliser in double base propellants.* **A.Venter, D.R.Ifa, G.Cooks.** 2006, Propellants Explosives and Pyrotechnics, Vol. 6, pp. 472-476.

7. **J.Elsby.** *The development of a time temperature indicator for rockets. PhD Thesis.* Shrivenham : Cranfield University, 2000.

8. **Ministry Of Defence.** *Joint Service Publication.* UK : MOD(PE), 1998. 333.

9. *Determination of the nitrogen content of nitrocellulose from smokeless gunpowders and collodions by alkaline hydrolysis and ion chromatography.* **M.Lopez-Lopez, J.M.R.Alegre, C.Garcia-Ruiz, M.Torre.** 2011, Analytica Chimica Acta, Vol. 685, pp. 196-203.

10. *Use of UV-visible spectroscopyto monitor nitrocellulose degradation in thin films.* **M.Moniruzzaman, J.M.Bellerby.** 2008, Polymer Degradation and Stability, Vol. 93, pp. 1067-1072.

11. *Stabizer reactions in cast double base rocket peopellant. Part 8: Characteriastion of propellant gasing properties during simulated ageing.* **M.H.Sammour.** 1996, Propellants Explosives and Pyrotechnics, Vol. 17, pp. 196-201.

12. *Kinetic modelling of the stabiliser consumption and of the consecutive products of the stabiliser in a gun propellant.* **M.A.Bohn, N.Eisenreich.** 1997, Propellants Explosives and Pyrotechnics, Vol. 22, pp. 125-136.

13. **NATO.** *STANAG 4540 Procedure for dynamic mechanical analysis (DMA) and determination of glass transition temperature.* s.l. : NATO, 2008.

14. **P.Gabbott.** *Principals and applications of thermal analysis.* Oxford : Blackwell Publishing, 2008.

15. **K.P.Menard.** *Dynamic mechanical analysis a practical introduction.* London : CRC Press, 2008.

16. *The effect of ageing and annealing on the physical properties of nitrocellulose plasticised with nitroglycerine.* **R.C.Warren.** 1990, Polymer, Vol. 31, pp. 861-868.

17. *Dynamic mechanical analysis for characteriastion of a solid rocket propellant transitionin double base propellant.* **J.Pachman, J.Selesovsky.** 2005, Science and Technology Of Energeyic Materials, Vol. 66, pp. 380-383.

18. *Dynamic mechanical studies of nitrocellulose/nitroglycerine mixtures.* **F.B.Privett.** 1989, Polymer, Vol. 28, pp. 1121-1126.

19. *Ageing behavior of composite rocket propellant formulations.* **S.Cerri, M.A.Bohn, K.Menke, L.Galfetti.** Munich : Insensitive Munitions and Energetic Materials Technology Symposium (IMEMTS), 2010.

20. *Transitions and relaxations in plasticised nitrocellulose.* **R.C.Warren.** 1988, Polymer, Vol. 29, pp. 919–923.

21. *Relaxations in double base propellant.* **D.J.Townend, R.C.Warren.** 1985, Polymer, Vol. 26, pp. 79-83.

22. *Kinetics and enthalpy of nitroglycerine evaporation from double base propellants by isothermal thermogravimetry.* **S.Matecic, M.Suceska.** 2010, Thermochimica Acta, Vol. 16, pp. 5201-5102.

23. *Glass transition temperature of polymer materials measured by thermomechanical analysis.* **A.Schwartz.** 1978, Journal Of Thermal Analysis, Vol. 13, pp. 489-497.

24. *Differential thermal analysis of polymers.* **S.Strella.** 1963, Journal Of Applied Polymer Science, Vol. 7, pp. 569-579.

25. **U.W.Gedde.** *Polymer Physics.* London : Springer, 1995.

26. **R.A.Pethrick, T.Amornsakchai, A.M.North.** *Introduction to molecular motion in polymers.* Dunbeath : Whittles Publishing, 2011.

27. **R.Steinberger.** *The Chemistry Of Propellants.* Oxford : Pergamon Press, 1959.

28. *Transitions and relaxations in plasticised nitrocellulose.* **R.C.Warren.** s.l. : Polymer, 1988, Vol. 29, pp. 919-923.

29. *Mechanical and dielectric relaxation in cellulose esters.* **R.W.Seymour, S.Weinhold, S.K.Haynes.** 1978, Journal Of Macromolecular Science, Vol. 3, pp. 337-353.

30. *Mechanical loss processes in polysacharides.* **S.A.Bradley, S.H.Carr.** 1986, Journal Of Polymer Science, Vol. 14, pp. 111-124.

31. *Study of mechanical properties of naturally aged double base rocket propellants.* **S.Matecic, M.Suceka.** 2010, Central European Journal of Energetic Materials, Vol. 7, pp. 47-60.

32. *Artificial ageing of double base rocket propellant effect on dynamic mechanical properties.* **S.Matecic, M.Suceka.** 2009, Journal Of Thermal Analysis and Calorimetery, Vol. 96, pp. 523-529.

33. *Use of dynamic mechanical measurements to determine the ageing behavior of solid propellants.* **M.Husband.** 1992, Propellants Explosives and Pyrotechnics, Vol. 17, pp. 196-201.

34. *Polypropylene chain scission and molecular weight changes in multipul extrusion.* **V.A.Gonzalez-Gonzalez, G.Neira-Velazquez, J.L.Angulo-Sanchez,.** 1998, Polymer Degradation and Stability, Vol. 60, pp. 33-42.

35. *Influence of the repeated extrusion on the degradation of polyethylene, structural changes in low density polyethylene.* **J.Dostal, V.Kasparkova, M.Zatloukal, J.Muras, L.Simek.** 2008, European Polymer Journal, Vol. 44, pp. 2652-2658.

36. *Thermal analysis as a quality tool for assessing the influence of thermo-methanical degradation on recycled poly(ethylene terepthalate).* **J.D.Badia, F.Vilaplana, S.Karlsson, A.Ribes-Greus.** 2009, Polymer Testing, Vol. 28, pp. 169-175.

37. *Measurement of the relaxation transition of nitrocellulose based gunpowder.* **W.P.C.de.Klerk, G.Herder.** 2006, Journal of Thermal Analysis and Calorimetery, Vol. 85, pp. 169-172.

38. **A.Davanas.** *Solid rocket propulsion technology.* Oxford : Pergamon Press, 1993.

39. **S.Fordham.** *High explosives and propellants second edition.* Oxford : Pergamon Press, 1980.

40. *Assessment of propellant stabiliser extraction methods.* **J.Tucker, P.P.Gill, N.Mai, J.Hand.** Karlsruhe : 41st International Conference of ICT, 2010.

41. *Effect of manufacturing processes on nitrocellulose in extruded double base propellant.* **J.Tucker, P.P.Gill, N.Mai, J.Hand.** Karlshruhe : 41st International Conference of ICT, 2010.

42. *Whole life assessment of nitrocellulose in double base rocket propellants.* **J.M.Bellerby, P.Deacon, C.Baker, N.Mai.** Karlsruhe : 41st International Conference of ICT, 2010.

43. *Mechanism and molar mass modelfor thermal oxidation of linear ethyenebutene copolymers.* **C.Sarmoria, E.Valles, O.Chiantore, S.Tripodi,.** 2001, Polymer, Vol. 43, pp. 3981-3986.

44. *The effect of ageing and annealing on the physical properties of nitrocellulose plasticised with nitroglycerine.* **R.C.Warren.** s.l. : Polymer, 1990, Vol. 31, pp. 861-868.

45. *Mechanical analysis on rocket propellants.* **G.Herder, F.P.Weterings, W.P.C.Klerk.** 2003, Journal Of Thermal Analysis and Calorimetery, Vol. 72, pp. 921-929.

46. **D.R.Askeland.** *The Science and Engineering of Materials. Third S.I.Edition.* Cheltenham : Nelson thornes, 2001.

47. *Chemical compatibility and shelf life of explosives.* **B.Vogelsanger.** 2004, Chimia, Vol. 58, pp. 401-408.

48. **N.Kubota.** *Propellants and Explosives.* Hoboken : Wiley-VCH, 2002.

49. *Inhomogeneity in the molecular structure of NC.* **V.I.Kovalenko.** 1995, Russian Chemical Review, Vol. 8, pp. 752-766.

50. **A.Wilkinson.** *The threat from explosive events in amunition stores.* Explosive Capabilities Limited, 2009. Edition 2010/03.

51. *Analysis of 2-nitrodiphenylamine and its major derivatives in double and triple base propellants.* **I.Kansas, D.Robertson.** 1994, Propellants, Explosives and pyrotechnics, Vol. 19, pp. 171-173.

52. **M.H.Sammour.** *Reactions of stabilisers and ballistic modifiers during simulated ageing of double base propellants: PhD Thesis.* Shrivenham : Cranfield University, 1992.

53. **I.M.Smallwood.** *Handbook of organic solvent properties.* Amsterdam : Elsevier, 1996.

54. **J.L.Capelo-Martinez.** *Ultrasound in chemistry.* Weinheim : Wiley-VCH, 2009.

55. **P.Atkins, J.De.Paula.** *Physical Chemistry.* Oxford : Oxford University Press, 2006.

56. *A TG study of the solvolytic breakdown of a crosslinked double base propellant.* **A.S.Tompa.** 1983, Thermochemica Acta, Vol. 62, pp. 9-20.

57. **J.Akhavan.** *The Chemistry Of Explosives.* Cambridge : Royal Society Of Chemistry, 2004.

58. **Perkin Elmer.** www.perkinelmer.co.uk. [Online] 16 03 2011. http://las.perkinelmer.co.uk/Catalog/ProductinfoPage.htm?ProductID=N5330100.

59. **J.Reid.** *Nitrocellulose studies. MSc Thesis.* Shrivenham : Cranfield University, 2005.

60. *Results of the multi-national study about STANAG 4620/AOP-48 edition 2 (new NATO standard for the assessment of chemical stabiility and safe storage life of propellants using stabiliser depletion.* **B.Vogelsanger.** Karlsruhe : 37th International Conference of ICT, 2006.

61. *STANAG 4178 ed 2, testing of nitrocellulose.* **P.Folly, B.Vogelsanger, R.Sopranetti,** Shrivenham : 4th Nitrocellulose Workshop, Cranfield University, 2010.

62. *Comparison of the uniaxial tensile modulus and dynamic shear storage modulus of a filled hydroxyl-terminated polybutadiene and gap propellant.* **J.S.Duncan, P.Brousseau,** 1996, Journal of Materials Science, Vol. 31, pp. 1275-1284.

63. *Determination of dipyenylamine and its mono-derivatives in single-base gun propellants during ageing by high performance liquid chromatographydaughter products.* **L.Jelisavac, M.Filipovic.** 2002, Chromatographia, Vol. 55, pp. 239-241.

64. *Determination of chemical and mechanical properties of double base propellants during ageing.* **F.Volk, M.A.Bohn, G.Wunsch.** 1987, Propellants Explosives and Pyrotechnics, Vol. 12, pp. 81-87.

65. *Effect of crystallinity on ageing behavior of nitrocellulose.* **Moniruzzamam, M.** Shrivenham : 4th Nitrocellulose workshop. 2010.

66. **J.G.Stark, H.G.Wallace.** *Chemistry data book 2nd edition in SI units.* Stoughton : Hodder Murray, 1970.

67. **S.Leary.** *Principals of Instrumental Analysis 4th Edition.* Philadelphia : Saunders College Publishing, 1992.

68. **J.Clayden, N.Greeves, S.Warren, P.Wothers.** *Organic Chemistry.* Oxford : Oxford University Press, 2001.

69. *Study of the daughter products of akardite.* **L.Lussier, E.Bergeron, H.Gagnon.** 2006, Propellants Explosives and Pyrotechnics, Vol. 31, pp. 253-262.

70. *Assessment of factors effecting stabiliser extraction from nitrocellulose based propellants.* **J.Hand, J.Tucker P.P.Gill.** Pardubice : New Trends in Research of Energetic Materials Conferance, 2011.

10 APPENDICES

Appendix A Cellulose

A.1 Structure of cellulose

Cellulose polymers are composed from beta-D-Glucopyranose rings, these rings are bonded in the 1 and 4 positions only, this leads to a linear polymer with no branching. Beta-D-Glucopyranose is the specific name for the type of glucose that forms the cellulose structure. Glucose can take a number of both linear and cyclic forms. The beta refers to the hydroxyl group on carbon 1, in the Beta form this group is planar to the molecule, in the alpha form the group is axial. as shown in Figure 10-1.

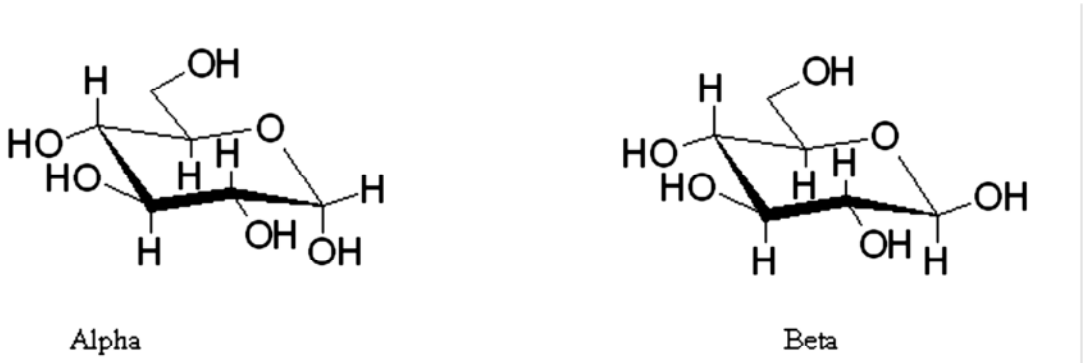

Figure 10-1 The alphas and beta forms of D-Glucopyranose rings

The cellulose strands lye parallel with hydrogen bonding between forming a fibril. The fibrils lye in a crossed manner in the plant material, it is both the length of the polymer chains and the ordered structure that gives the material its strength.

A.2 Sources of cellulose

Cellulose is a naturally occurring polymer, it is found in high concentrations in the cell walls in plants. The two main sources of cellulose for industry are; wood and cotton plants. The typical polymer length in wood is 10,000 monomer units, in cotton plants typically 15,000 (3). The cotton source has been recognized as the superior source for use in propellants (2).

A.3 The first uses of nitrocellulose

As early as 1833 scientists simultaneously worked on the nitration of starch, cotton and paper (2). Not until 1865 when the detonation properties were sufficiently understood could it be used commercially. The problem was that nitrocellulose is too easy to ignite in its dry state, thus accidents were common. The solution was to store the nitrocellulose wet, then to use a primary explosive to detonate a small quantity of dry nitrocellulose, this would act as a booster and detonate the wet nitrocellulose.

A.4 Nitroglycerine

Nitroglycerine was first synthesised in 1846, however it was in 1863 that Immanuel Nobel developed a process and built a manufacturing plant. In the early days of its use, nitroglycerine plants were built very close to the site of intended use, as transportation of liquid nitroglycerine “tended to generate loss of life and property” (57) . Nitroglycerine is a primary explosive, it is commonly used in combination with nitrocellulose to produce double based propellant, it increases the energy content of the propellant over nitrocellulose alone. The structural formula for nitroglycerine is shown in Figure 10-2.

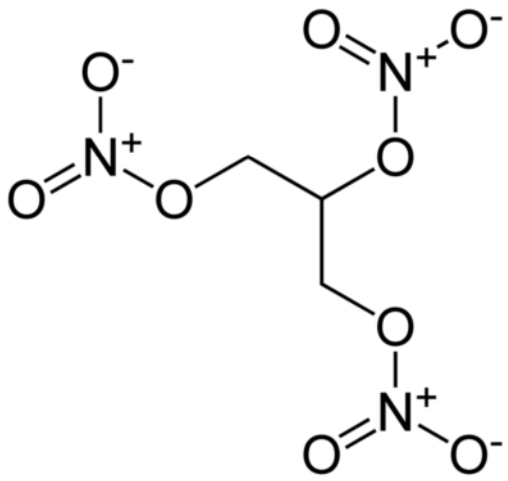

Figure 10-2 A nitroglycerine molecule

Nitroglycerine is a nitrate ester, obtained by the nitration of glycerine with a similar mixed acid nitration mixture used in the nitration of cellulose. Nitroglycerine is extremely sensitive to shock, this sensitivity has limited its use,

for example attempts to use it a high explosive shell filling proved to be unsuccessful. It is a toxic substance with a freezing point of 2-13°C, depending on purity (2). Nitroglycerine is clear and colourless in its pure form. The commercially produced product is a yellow or a pale yellow brown, this is dependent upon the purity of the raw materials and the manufacturing process. It is not very soluble on water, however, it is completely miscible in methanol, ethyl acetate, anhydrous acetic acid, benzene, toluene, xylene, phenol, nitro benzene, nitrotoluene pyridine. It can also be combined with other liquid nitrate esters (2).

Appendix B Reaction mechanisms

B.1 Decomposition of nitrate esters

B.1.1 Nucleophilic substitution

Nucleophilic substitution with water as nucleophile. SN1,Figure 10-3

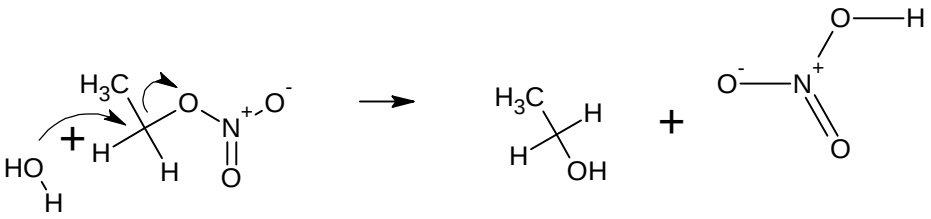

Figure 10-3 SN1

Nucleophilic substitution with hydroxide ion, SN2, Figure 10-4

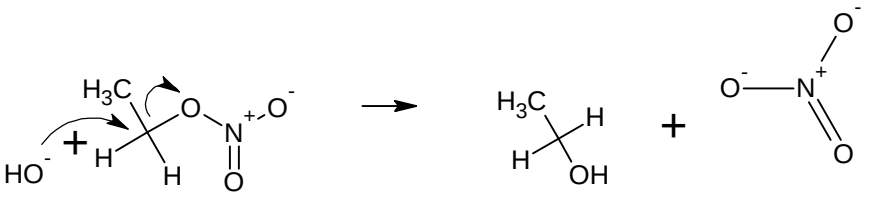

Figure 10-4 SN2

B.1.2 Elimination

Elimination of a beta hydrogen with hydroxide, E2, Figure 10-5

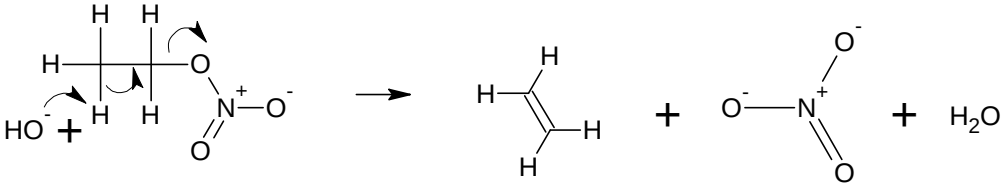

Figure 10-5 E2

Elimination of an α hydrogen with a hydroxide leading to the formation of a carbonyl.

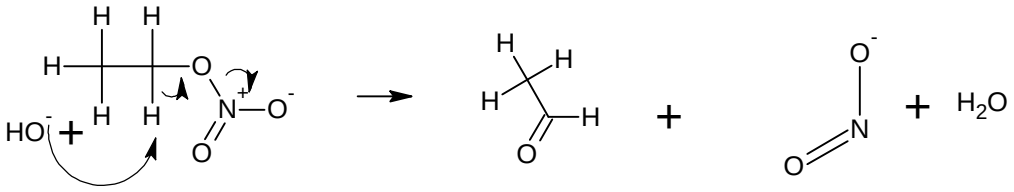

Figure 10-6 Eco2

B.1.3 Acid hydrolysis

Acid hydrolysis of the nitrate ester bond leads to formation of an alcohol group on hydrocarbon chain.

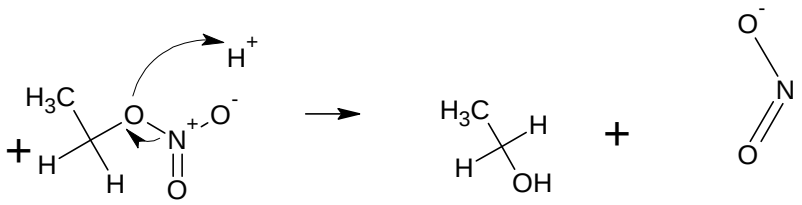

Figure 10-7 Acid hydrolysis

B.1.4 Nitration of cellulose

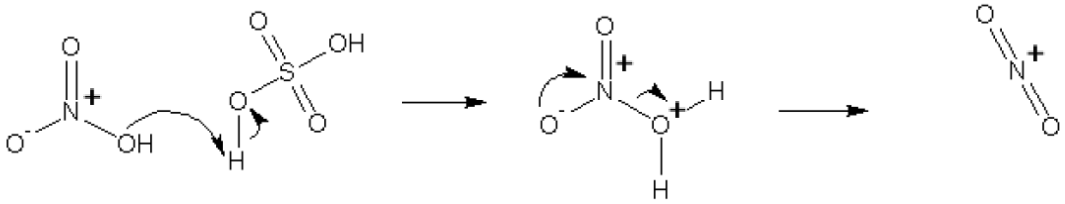

Figure 10-8 Nitration mixture, formation of reactive NO^+

Appendix C Mathematical formulae

C.1 Testing geometry factors

Geometry	Factor (j)
3-Point bend	$k = \frac{z\frac{y^3}{v^3}}{2}$
Single cantilever bend	$k = z\frac{y^3}{v^3}$
Dual Cantilever bend	$k = z\frac{y^3}{v^3}.2$
Tension and compression	$k = \frac{zy}{v}$

The free length v, in a clamped bending refers to the distance between the static sample clamp and the drive shaft clamp. In a 3-point bend it refers to the distance between the static clamp and the drive shaft contact point, this will be half the distance between the two static clamps. The y refers to the samples thickness. The z refers to the samples width.

C.2 Stress and strain equations for dynamic mechanical analysis

C.2.1 In a purely elastic material

$$\sigma(t) = \sigma_{max}\sin(\omega t) \quad \textbf{(10-1)}$$

$$\sigma = E\varepsilon \quad \textbf{(10-2)}$$

$$\varepsilon = \sigma/E \quad \textbf{(10-3)}$$

$$\varepsilon(t) = \frac{\sigma_{max}\sin(\omega t)}{E} \quad \textbf{(10-4)}$$

$$\varepsilon(t) = \varepsilon_{max}\sin(\omega t) \quad \textbf{(10-5)}$$

C.2.2 In a purely viscous material

Calculating strain in a stress control analysis

$$\sigma(t) = \sigma_{max}\sin(\omega t) \quad \textbf{(10-6)}$$

$$\sigma = \eta\frac{\delta\varepsilon}{\delta t} \quad \textbf{(10-7)}$$

$$\eta\frac{\delta\varepsilon}{\delta t} = \sigma_{max}\sin(\omega t) \quad \textbf{(10-8)}$$

$$\frac{\sigma_{max}}{\eta}\int \sin\omega t\, dt = \int d\varepsilon \quad \textbf{(10-9)}$$

Calculating stress in a strain control analysis

$$\varepsilon(t) = \varepsilon_{max}\sin(\omega t) \quad \textbf{(10-10)}$$

$$\sigma = \eta\frac{\delta\varepsilon}{\delta t} \quad \textbf{(10-11)}$$

$$\frac{\delta\varepsilon}{\delta t} = \varepsilon_{max}\cos(\omega t) \quad \textbf{(10-12)}$$

$$\frac{\delta\varepsilon}{\delta t} = \varepsilon_{max}\sin(\omega t) + \frac{\pi}{2} \quad \textbf{(10-13)}$$

$$\sigma = \eta\,\varepsilon_{max}\sin(\omega t) + \frac{\pi}{2} \quad \textbf{(10-14)}$$

Appendix D Chemical and physical effects of manufacture on extruded double base propellant

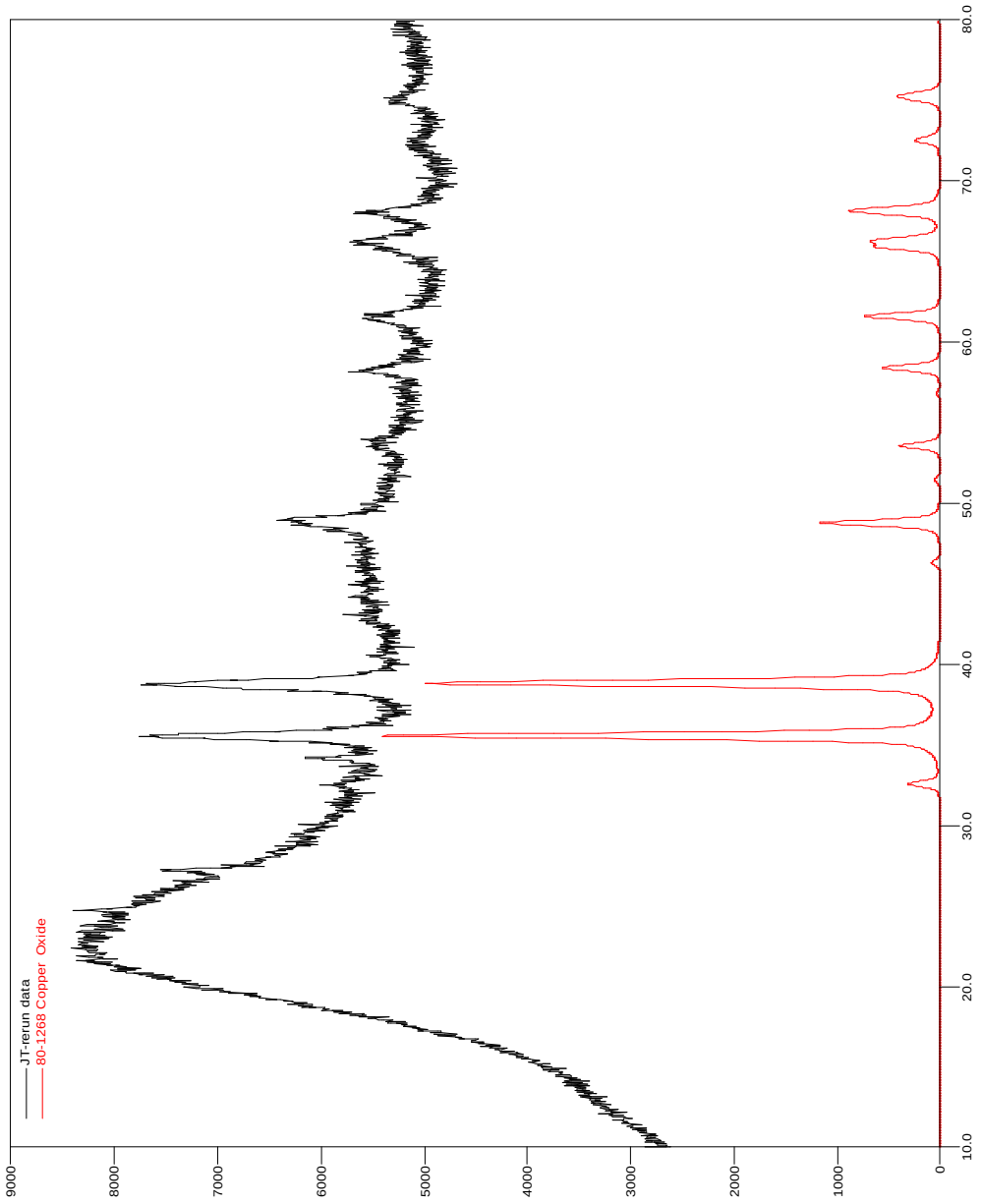

Figure 10-9 X-ray diffraction of 'Double base II' (above) shown with CuO diffraction pattern (below)

Appendix E Application of DMA for analysing nitrocellulose based materials

E.1 Time temperature superposition results

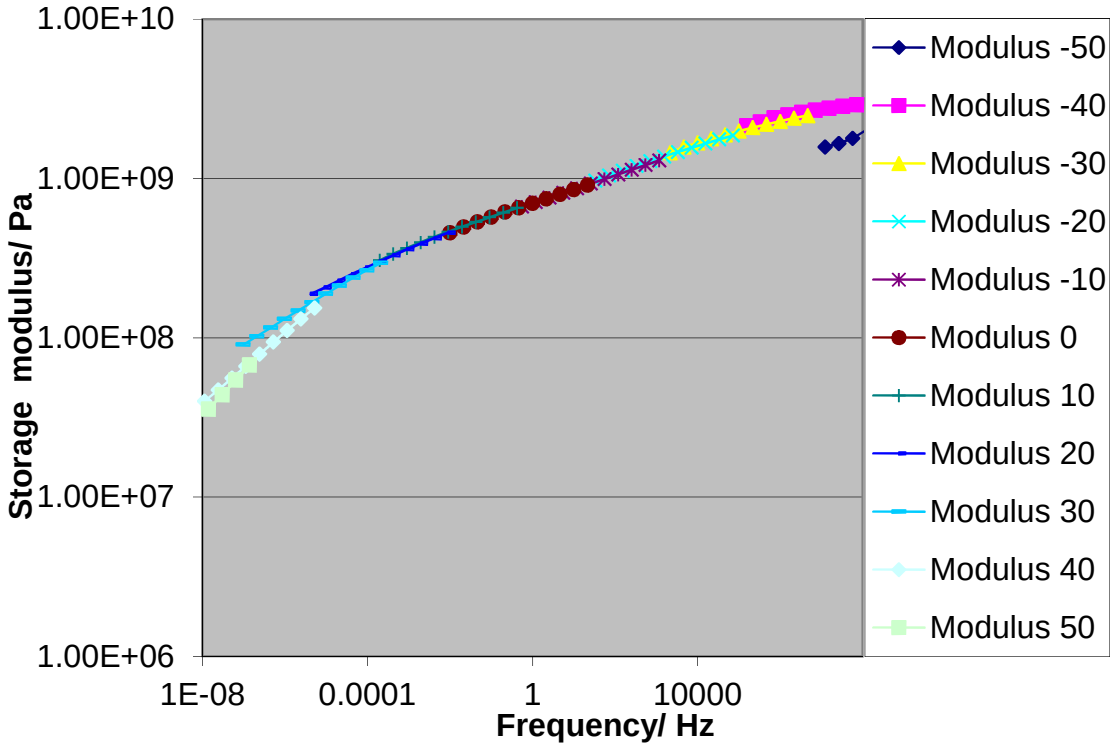

Figure 10-10 TTS storage modulus data unaged mechanite 19 propellant

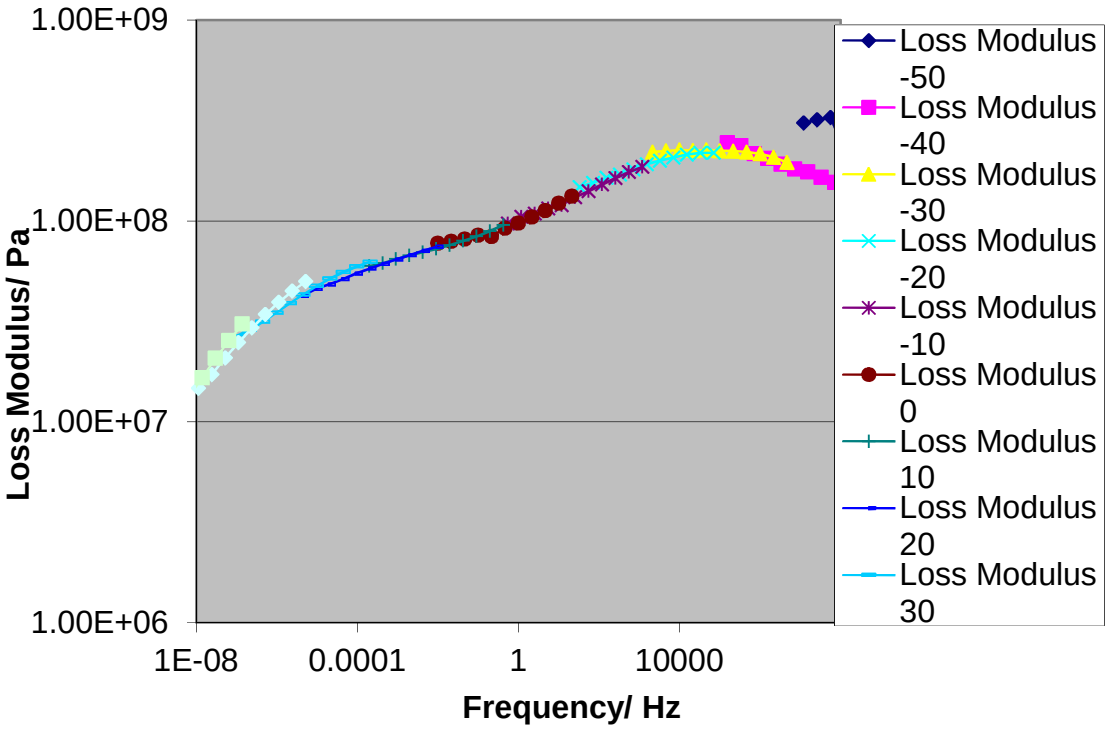

Figure 10-11 TTS loss modulus data unaged mechanite 19 propellant

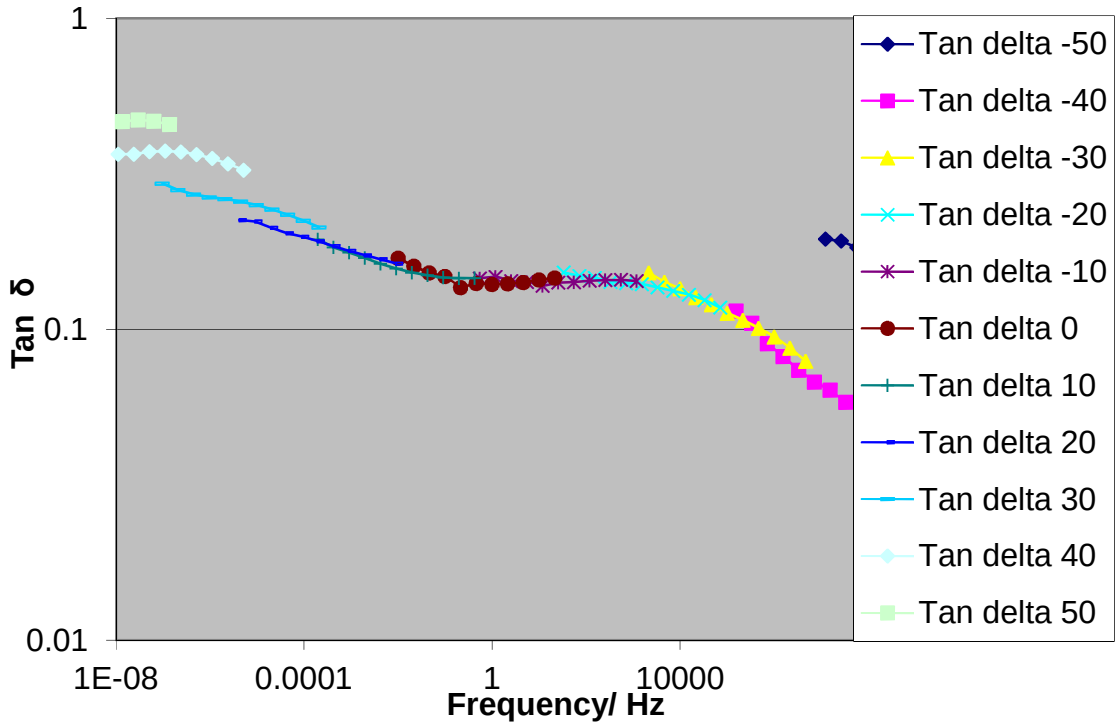

Figure 10-12 TTS tanδ data unaged mechanite 19 propellant

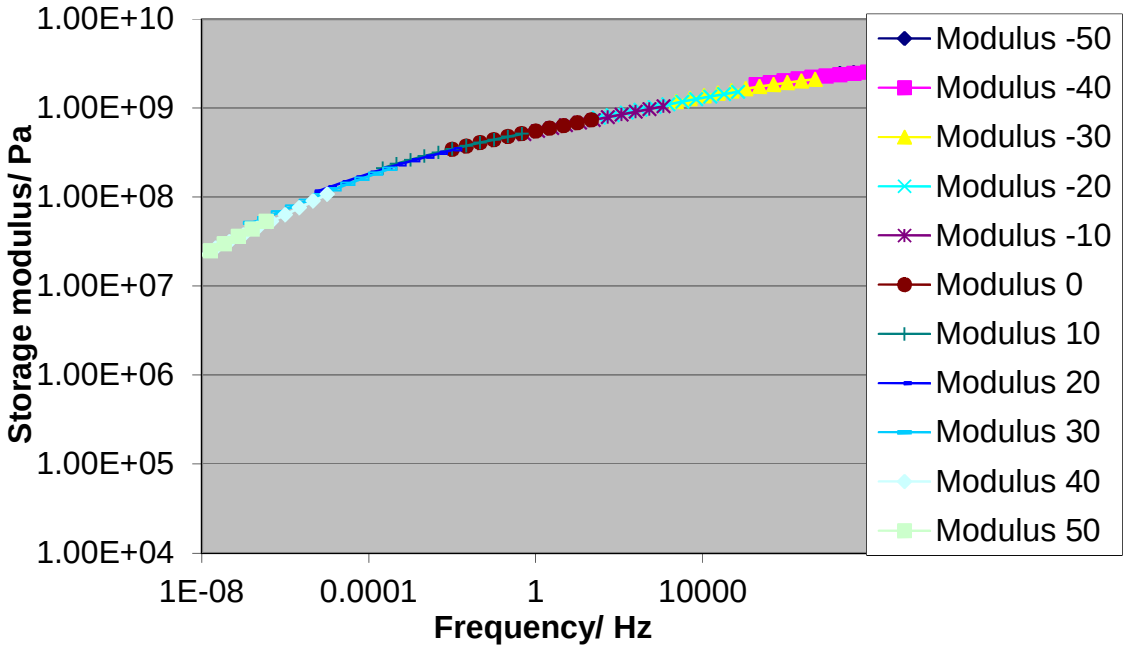

Figure 10-13 TTS storage modulus data aged at 60°C mechanite 19 propellant

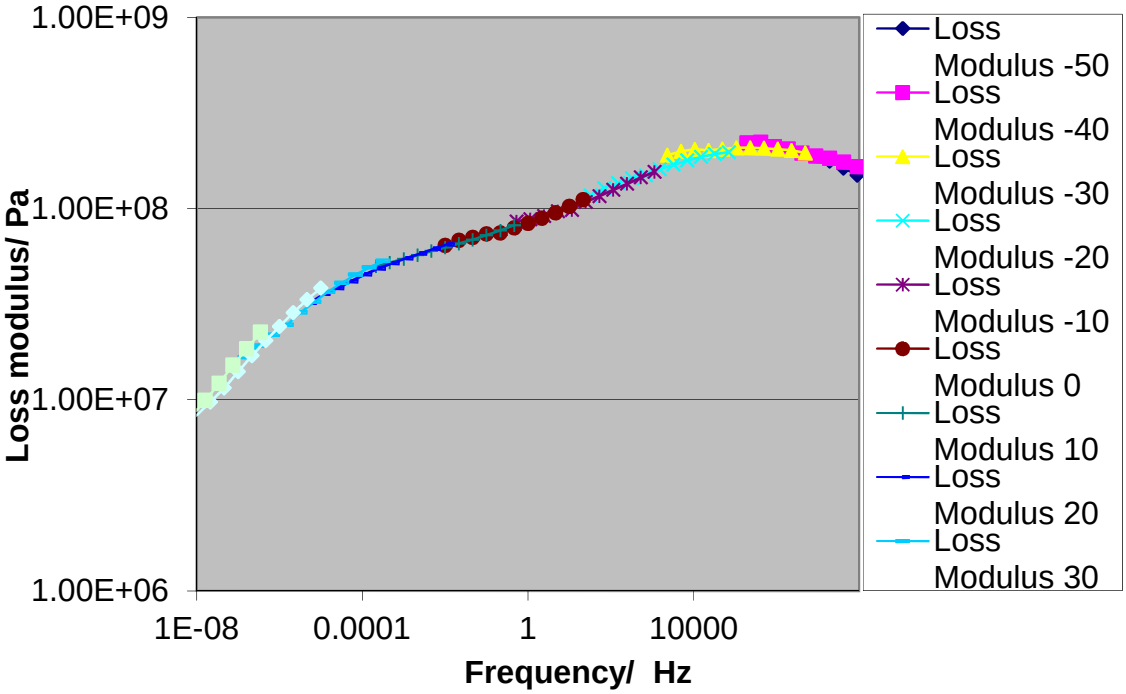

Figure 10-14 TTS loss modulus data aged at 60°C mechanite 19 propallent

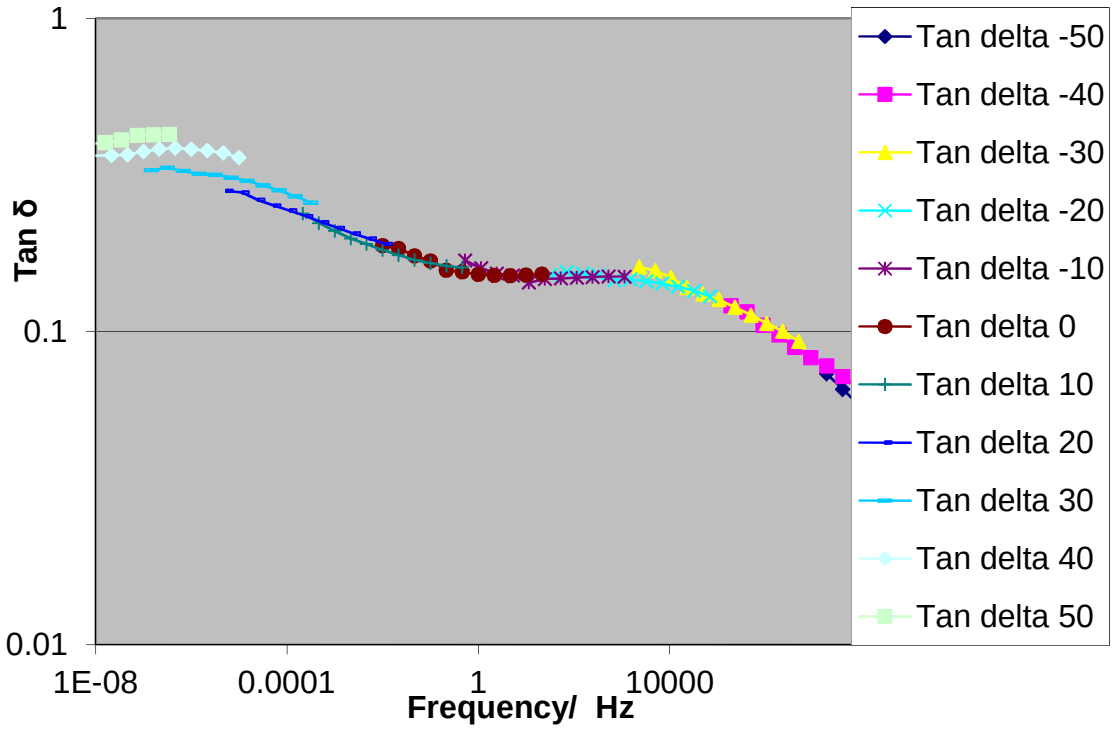

Figure 10-15 TTS tanδ data aged at 60°C mechanite 19 propellant

Table 10-1 WLF equation constants for TTS determined by the DMA software. Mechanite 19 samples

Constants	Unaged	Aged at 60°C
T_0	0	0
C_1	165.45	97.08
C_2	960.24	572.99

E.2 Creep experiments

E.2.1 Maxwell model

$$\varepsilon(t) = \frac{\sigma_0}{E} + (\frac{\sigma_0}{\eta})_t \quad \textbf{(10-15)}$$

E.2.2 Voigt model

$$\varepsilon(t) = \frac{\sigma_0}{E} + [1 - \exp(\frac{-E}{\eta})_t] \quad \textbf{(10-16)}$$

E.2.3 Four element model

$$\varepsilon(t) = \frac{\sigma_0}{E_1} + (\frac{\sigma_0}{\eta_1})_t + \frac{\sigma_0}{E_2} + [1 - \exp(\frac{-E_2}{\eta_2})_t] \quad \textbf{(10-17)}$$

E.2.4 Determining the linear viscoelastic region for creep analysis of propellant.

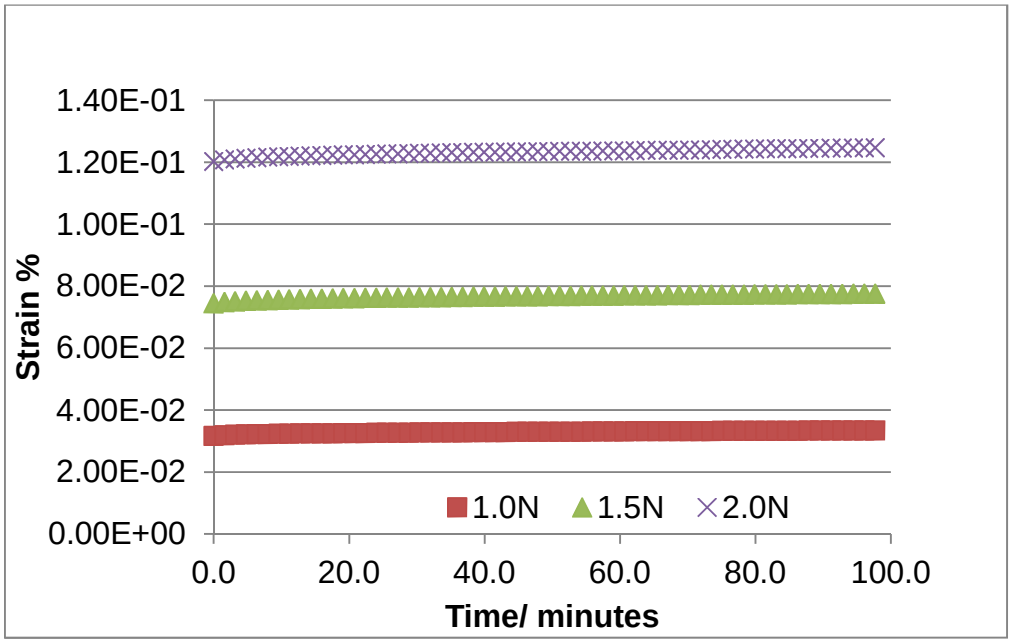

Figure 10-16 A series of creep experiments carried out at a range of forces at 0°C

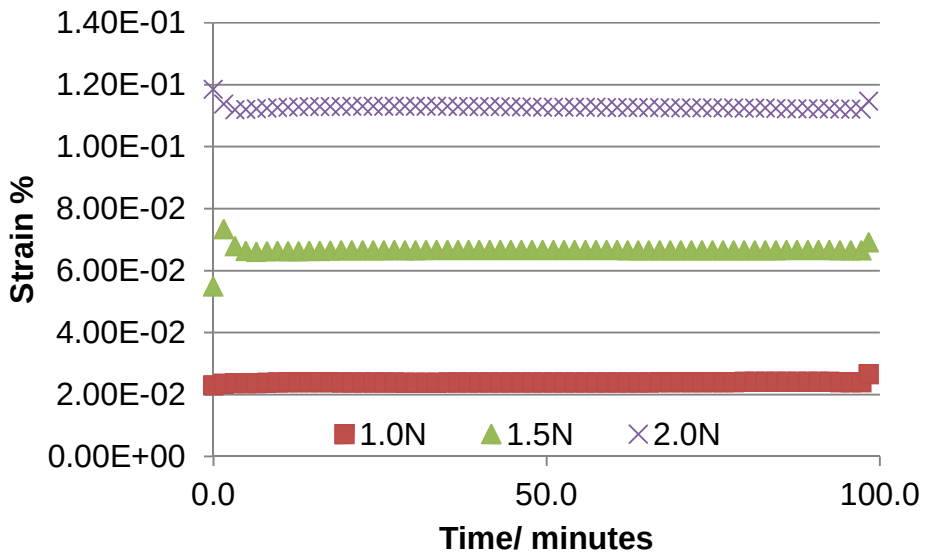

Figure 10-17 A series of creep experiments carried out at a range of forces at -50°C

E.2.5 Propellant creep tests of aged and unaged samples

Propellant samples, both aged and unaged were analysed between -50 and 50°C, at 10°C intervals for 100 minutes at each temperature, using a 2N load

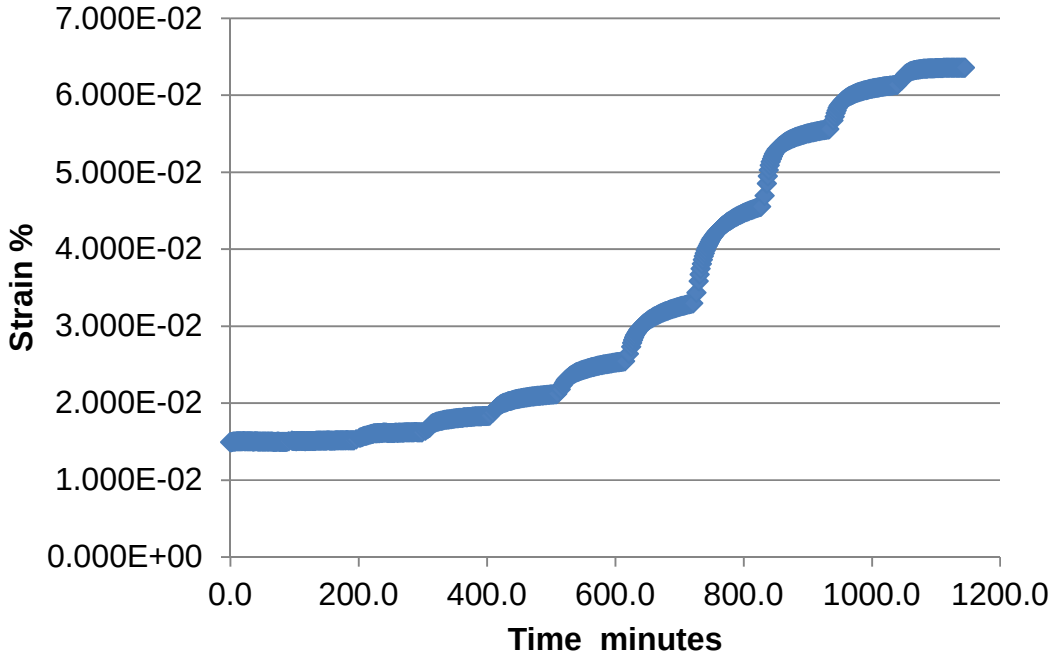

Figure 10-18 Unaged mechanite 19 creep analysis at temperatures between -50 and 50 in 10°C intervals

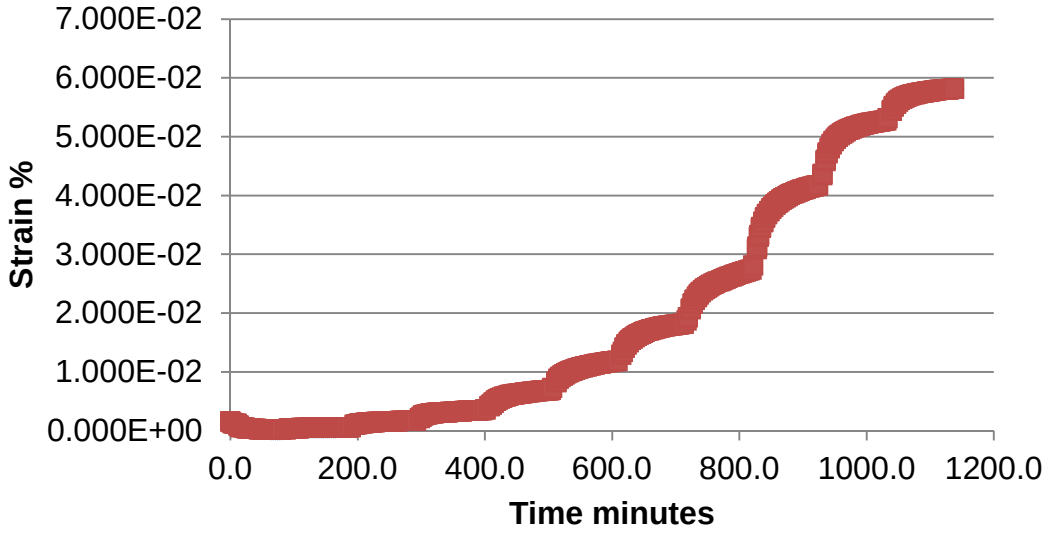

Figure 10-19 Mechanite aged at 40°C , creep analysis at temperatures between -50 and 50 in 10°C intervals

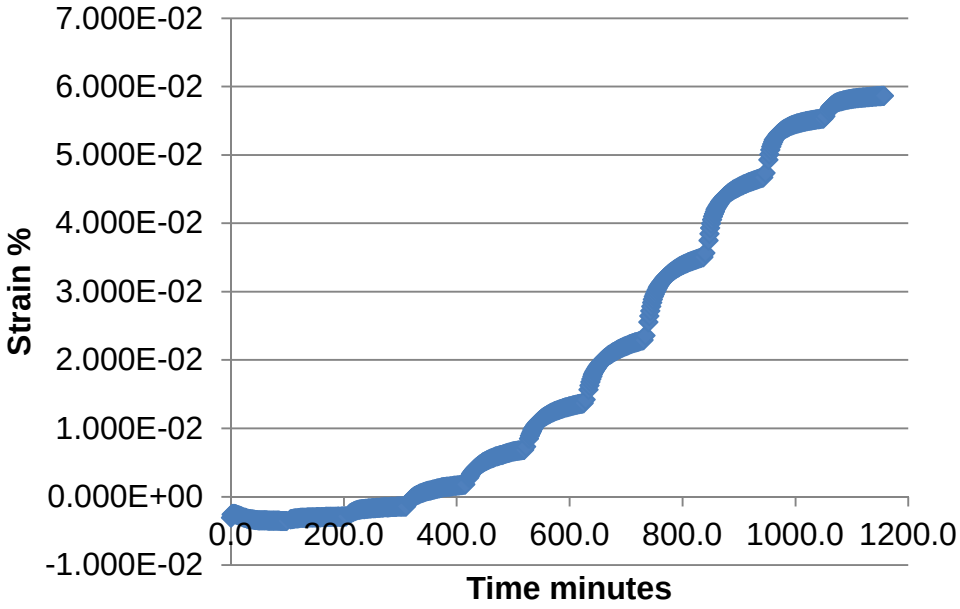

Figure 10-20 Mechanite 19 aged at 50°C, creep analysis at temperatures between -50 and 50 in 10°C intervals

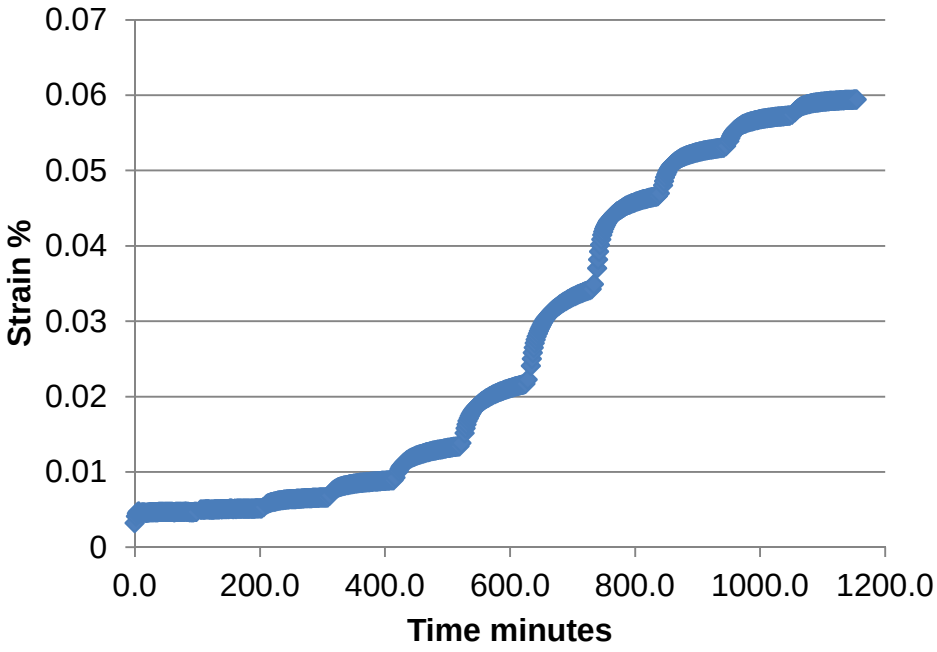

Figure 10-21 Mechanite 19 aged at 60°C, creep analysis at temperatures between -50 and 50 in 10°C intervals

Table 10-2 η1 values measured over a range of temperatures

Creep test temperature/ °C	Unaged	40°C days	50°C days	60°C days
-30.0	4.550E+11	8.630E+11	5.539E+11	6.391E+11
-20.0	2.200E+11	4.359E+11	2.002E+11	3.089E+11
-10.0	2.295E+11	2.293E+11	1.140E+11	1.445E+11
0.0	1.526E+11	1.402E+11	1.005E+11	8.482E+10
10.0	9.147E+10	1.567E+11	7.022E+10	5.748E+10
20.0	6.441E+10	6.840E+10	6.649E+10	9.373E+10
30.0	1.234E+11	7.430E+10	6.612E+10	1.511E+11
40.0	2.207E+11	1.310E+11	1.425E+11	2.251E+11
50.0	1.202E+12	2.312E+11	2.970E+11	4.660E+11

Appendix F Artificial thermal ageing of double base propellant

Artificial ageing of double based propellants can be carried in a number of ways. AOP48 (Allied Ordinance Publication) (5) describes a single temperature ageing procedure and a multi-temperature ageing procedure. Simply a higher temperature is used to increase the rate of chemical reactions. The rate constants of most reactions increase as the temperature is increased (55). It is found that for most reactions a plot of lnk versus 1/T gives a straight line, this is defined by the Arrhenius equation. The rate constant will also be higher for reactions with lower activation energies. The pre exponential factor is related to number of collisions that could lead to a chemical reaction. Single temperature ageing procedures are most commonly used for the analysis of generally well known propellants and stabilisers (5) multi temperature ageing procedures are more commonly used when the stabiliser is new, they can also be used to determine a more accurate storage life prediction. Single temperature ageing procedures can be carried out at a number of temperatures typically from 50°C to 90°C. The ageing temperatures and corresponding time required to simulate 10 years at 25 °C are listed,

Table 10-3 Time taken to simulate 10 years of ageing at 25°C

Temperature °C	Ageing time days	Temperature °C	Ageing time days
50	301	70	34.8
55	191	75	19.0
60	123	80	10.6
65	64.4	85	5.98
65.5	60.9	90	3.43

$tm = t25.\exp\left(\frac{Ea}{RTm}\right) - C$	**(10-18)**

tm = Time taken for 10 years of ageing at 25°C

t25 = 25 years of ageing in seconds

Ea = Activation energy

R = Gas constant

Tm = Temperature of ageing

C = Collision factor

Table 10-4 Arrhenius parameters for decomposition reactions

	Hydrolysis	Thermolysis
Ea	80	120
C	32.27	46.71

At temperatures greater than 60°C the rate of ageing is dramatically increased. This shift above 60°C is due to a shift from hydrolysis to thermolysis reactions. The equation used to calculate these values is, equation (10-18) (10-9)can be used to calculate the rate of reaction for the hydrolysis and during the thermolysis processes. A plot of ln Time versus 1/Temperature clearly shows the transition from one reaction dominating to the other, the blue data points represent the hydrolysis reaction that occurs below 60°C and the pink data points represent the higher temperature thermolysis reactions. It is important to note that on a traditional Arrhenius plot the gradient would be negative with the rate of reaction on the y axis. This plot has a positive gradient because the inverse of rate is plotted on y axis, the time taken for a specific amount of reaction to occur, this leads to an inversion of the gradient. It has been observed that one sample of double based propellant after heating at 90 °C for 2 days became deformed due to bubble formation (27).

.

F.1 Ageing trial of extruded double base propellant.

Table 10-5 Ageing program detailed parameters

Sample name	Ageing temperature/ °C	Duration/ days	Simulated age/ days	Simulated age/ days	Total simulated ageing
			Hydrolysis	Thermolysis	
Unaged	N/A	N/A	N/A		
40a	40	90	416	164	580
40b	40	180	832	328	1160
40c	40	240	1110	438	1548
40d	40	333	1540	608	2148
					0
50a	50	41	490	311	801
50b	50	70	837	533	1370
50c	50	88	1053	670	1723
50d	50	100	1197	760	1957
					0
60a	60	16	467	470	937
60b	60	24	700	706	1406
60c	60	44	1284	1295	2579
60d	60	50	1460	1471	2931

F.2 Gel permeation chromatography data from ageing trial

Table 10-6 GPC data in full

Age/days		Mn	Mn std dev	Mw	Mw std dev	Polydispersity	Polydispersity std dev
0	Unaged	76411	666.5104271	279620	6567.959568	3.65945	0.054846012
580	40a	68174	431.4952242	245819	1876.590347	3.60575	0.050017163
1160	40b	68983	2106.254923	247993	3107.757522	3.595	0.067409931
1548	40c	67940	175.8751622	243186	49.7545457	3.57943	0.011163749
2148	40d	60862	781.327834	217224	1353.278242	3.5691	0.021311999
0	Unaged	74543	509.2998804	259840	3023.5175	3.48579	0.064277683
801	50a	70784	454.3520953	246497	1057.359667	3.48237	0.007695949
1370	50b	67834	983.7557733	235302	658.921942	3.46879	0.040284502
1723	50c	68155	98.73674803	234558	1130.332226	3.44155	0.013099448
1957	50d	58616	261.264447	199007	809.3169128	3.3951	0.028815871
0	Unaged	71038	248.4879418	254793	2494.635497	3.58669	0.022675571
937	60a	64527	86.0561149	216235	1696.882146	3.35106	0.031028775
1406	60b	62353	616.896086	203480	1782.189783	3.26334	0.060565059
2579	60c	64382	305.2494427	213052	1441.987372	3.3092	0.006973249
2931	60d	63021	584.8992324	203961	286.0530212	3.23638	0.025259237

Table 10-7 GPC data in full expressed as percentage change

Age/days		Mn %	Mn % std dev	Mw %	Mw % std dev	Polydispersity %	Polydispersity % std sev
0	Unaged	100	0.872275119	100	2.348883701	100	1.498672834
580	40a	89	0.632931791	88	0.7634048	99	1.387087569
1160	40b	90	3.242332082	89	1.30145729	98	1.83383441
1548	40c	89	0.288972191	87	0.022904737	98	0.312787086
2148	40d	80	1.132643089	78	0.545693203	98	0.59279325
0	Unaged	100	0.683229653	100	1.163607412	100	1.843991848
801	50a	95	0.641885306	95	0.428954375	100	0.220997462
1370	50b	91	1.450239958	91	0.280032444	100	1.161341628
1723	50c	91	0.14487088	90	0.481898816	99	0.380626391
1957	50d	79	0.445722067	77	0.406677611	97	0.848748805
0	Unaged	100	0.349795802	100	0.979083215	100	0.632214412
937	60a	91	0.133364506	85	0.784739818	93	0.925939116
1406	60b	88	0.989360714	80	0.875855014	91	1.855922421
2579	60c	91	0.474122337	84	0.676824143	92	0.210723111
2931	60d	89	0.928102113	80	0.140248882	90	0.780478104

Appendix G Stabiliser extraction

Table 10-8 Average time to complete extraction of stabiliser

Rate,	Ave, 100% extraction, minutes. (2x STD DEV) /normalised			Ave, 50% extraction, minutes. (2x STD DEV)		
	Time	2xStd dev	Normalised	Time	2xStd dev	Normalised
1500 (Stirring)	50	± 3	0.56	11	± 2	0.43
700 (Stirring)	51	± 2	0.57	12	± 1	0.46
350 (Stirring)	65	± 3	0.72	15	± 2	0.57
0	90	± 4	1	26	± 3	1
300 (Shaking)	207	±2	0.71	56	± 2	0.71
150 (Shaking)	207	±3	0.71	58	± 3	0.73
0	291	±4	1	79	± 3	1